MAGNETIC ABRASIVE FINISHING OF INTERNAL SURFACES

By

VINOO THOMAS

Bachelor of Engineering

Bombay University

Bombay, India

1994

Submitted to the Faculty of the
Graduate College of the
Oklahoma State University
in partial fulfillment of
the requirements for
the Degree of
MASTER OF SCIENCE
July, 1997

MAGNETIC ABRASIVE FINISHING OF

INTERNAL SURFACES

Thesis Approved:

R Komanduri

Thesis Advisor

Dona A. Duca

Ronald L. Dougherty

Thomas C. Collins

Dean of the Graduate College

PREFACE

The creation of smooth internal surfaces has wide applications. Conventionally this is done using the process of internal grinding. There are certain disadvantages associated with internal grinding as a process, namely the comparitively large force exerted by the grinding wheel and the difficulty of making and maintaining complex shapes on the wheel . This precludes the finishing of thin walled components and complex shaped internal surfaces. Magnetic field assisted finishing (MAF) is a process which overcomes these hurdles. The major advantage of this process is the reduced forces and ability to finish complex internal shapes.

In MAF the tool is composed of a flexible brush of magnetic abrasives and iron particles under the influence of a known magnetic field. The workpiece rotates, while either the workpiece or the flexible brush is reciprocated. Material removal is effected by the relative motion of the abrasives and the workpiece.

In the present work, the objective was to develop a technique of internal finishing using conventional abrasive products in lieu of magnetic abrasives. The permanent magnet design was adopted due to its light weight construction. A systems approach involving design of equipment and process studies to determine optimum conditions was used. Using the technique pipes of 12.7 mm O.D. and 9.9 mm I.D. were finished to an Ra of 20 nanometers over a length of 25.4 mm. The work materials polished were

AS304, A272, and A6061. The times for polishing were 4, 2, and 3 minutes repectively.

The design methodology developed started with a prelimnary geometric design based on the pipe diameter. Next, FEM analysis of the magnetic field was conducted to determine the placement and shape of the magnets to be used to give maximum field intensity at the polishing zone. After this was done a force analysis was carried out to find the reciprocation amplitudes needed for the different air gaps.

Parametric tests were conducted to determine the effects of spindle speed, polishing time, abrasive type, reciprocation frequency, iron concentration in mix, and zinc sterate (solid lubricant) concentration in mix on material removal rate and surface finish. These studies establish certain optimum conditions to obtain the best results with existing setup.

The present work has demonstrated that the process of MAF of internal surfaes can be applied to different work materials.

ACKNOWLEDGEMENTS

I wish to express my sincere appreciation to my major advisor Dr. Ranga Komanduri for his guidance. My sincere appreciation extends to my other committee members Dr. Don Lucca and Dr. Ron Dougherty for agreeing to serve on my committee.

This research was funded by grants from the National Science Foundation and the MOST chair. I would like to thank Drs. Larsen Basse, J. Lee, Ming Lev, and B.M. Kramer of N.S.F. for their interest and support.

I also wish to express my gratitude to those who provided suggestions and assistance during the investigation namely, Dr. Ali Noori Khajavi, Dr, Makaram Raghunandan and Jerry Dale.

Further, I wish to thank my colleagues, Mr. Murat Cetin, Mr. Johnnie Hixson, Mr. Ming Jiang, Mr. Brian Perry, Mr. Rajesh Iyer and Ms. Mallika Kamarajugadda for all their help and suggestions.

TABLE OF CONTENTS

LIST OF FIGURES

LIST OF TABLES

NOMENCLATURE

Ra= The average surface roughness of the surface.

D= Diameter of the iron particle

X= Susceptibility of the iron particle

H= Magnetic field strength

M= Mass of the tool

a= Acceleraton of the tool

F= Force

μ_{eq}= Equivalent coefficent of friction

J= Current density

N= Number of turns of the coil

i= Current

S= Cross-sectional area of coil

B= Magnetic flux density

f= Magnetic flux

A= Normal area across gap

m_0= Relative permeability

E= Energy product of the circuit

CHAPTER 1

INTRODUCTION

There are various applications today which require smooth internal surfaces in pipes. The internal surfaces of pipes carrying gases in the semiconductor industry must be extremely smooth, as contamination by extraneous materials is to be avoided. In the food processing industry, the rough internal surfaces in pipes act as breeding grounds for bacteria. This eventually leads to contamination. A similar need would be that of cleaning piping in the chemical industry. Magnetic field assisted polishing is a process by which the internal surfaces of the pipes can be finished to a surface roughness of the order of nanometers (Ra) to meet these needs.

1.1 Principle

Magnetic field assisted polishing (MAP) is a process which employs a magnetic abrasive brush under the influence of a magnetic field provided by a permanent magnet or an electromagnet to polish surfaces. The principle applied is to use magnetic force to provide polishing pressure between a mixture of iron and abrasives, or abrasives in magnetic fluid and the workpiece. The workpiece is rotated while the mixture is reciprocated to provide a relative motion for finishing the surface.

1.2 Process Principles

Figure 1.1 shows a two-dimensional schematic view of magnetic abrasive machining. The iron-abrasive mixture supplied into the tube conglomerates at the finishing zone. This is due to the magnetic field generated by the external magnet. When the tube is rotated at high speed, the relative motion between the tube and abrasive mixture finishes the inner surface.

As shown in Fig 1.1 a non-uniform magnetic field is ordinarily generated at the finishing zone. As a result, an abrasive particle at position "A" would experience Fx and Fy. The resultant of these forces would always act in such a manner as to push the abrasives toward the polishing zone. This prevents the dispersion of the magnetic abrasive mixture.

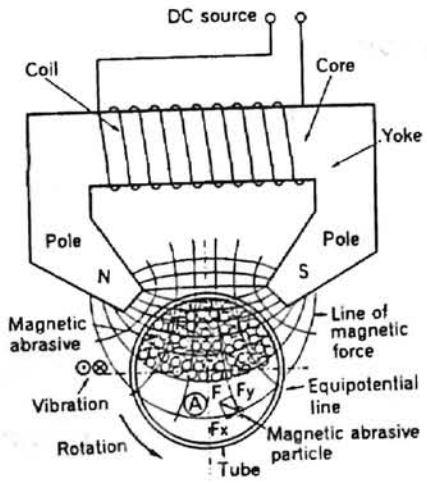

Figure 1.1 Schematic Setup of MAF (Shinmura et al., 1992)

$$Fx = kD^3XH(dH/dx)$$

$$Fy = kD^3XH(dH/dy)$$

where k= coefficient ,

D= diameter of particle,

X= susceptibility of particle,

H= magnetic field strength,

(dH/dx), (dH/dy)= gradients of magnetic field strength in the directions of equipotential lines and magnetic lines of force respectively.

The MAP process has certain merits which make it an efficient process:

i) The abrasive brush is flexible to conform to workpiece surface and hence complex surfaces can be finished.

ii) The finishing pressure can be controlled by varying the magnetic field (current in the case of an electromagnet, and air gap in the case of a permanent magnet).

iii) The finishing tool is independent of any structural members.

iv) Finishing times required to get the surface roughness down to nanometer Ra levels are short.

v) It is possible to finish small and long internal surfaces.

vi) In the case of electromagnet assemblies, automatic disposal of used abrasive and feeding new abrasive to the polishing zone is done by suitably turning the current in the coils off and on.

vii) No heat build-up in the work.

viii) No scattering of abrasives due to the magnetic field.

ix) Lesser consumption of abrasives.

1.3 Abrasives

Different abrasives used in the experiments were

- silicon carbide
- aluminum oxide
- chromium oxide

Various properties of interest for these materials are in Table 1.1. All of these abrasives are harder than the work materials used and so the polishing action is mainly by scratching.

Table 1.1 Properties of abrasives (Coes, 1971)

Material	Density	Hardness	Melting Point
	g/cc	MPa	deg C
Silicon Carbide	3.2	2500	2400
Aluminum Oxide	4.0	2100	2040
Chromium Oxide	5.2	2000-2200	2265

1.4 Problem Statement

The objective of this research has been to develop a method to finish the internal surface of tubes (9.9 mm I.D.) using the principle of magnetic abrasive finishing. All initial work by Shinmura et al. (1985) has been done with the use of magnetic abrasives. This is a special material which makes the process slightly expensive. The work done as part of this report attempts to use normal abrasives in place of the magnetic abrasives. This makes the process more cost effective. The work materials polished were stainless steel (AS 304), brass (A272), and aluminum (6061 T 6). This involved designing the equipment, building it and optimizing the process parameters. Designing the equipment involved the following three steps:

Geometric design of components.

Design of a suitable magnetic field in the polishing zone by performing a magnetic analysis using ANSYS 5.0a.

Selection of amplitude of reciprocation by performing a force analysis on the setup.

The advantage of having a flexible abrasive brush as a tool could mean that the forces available for polishing are low. This has to be corrected by providing a high magnetic field density in the polishing zone. A study to optimize the magnetic field density in the polishing zone needed to be conducted. This was accomplished by running FEM (finite element method) studies on ANSYS 5.0a. Various setups of magnets were evaluated by the magnetic field density in the polishing zone.

Another parameter of importance besides the magnetic field density in the polishing zone is the amplitude of reciprocation of the external magnet. As the flexible brush reciprocates with the external setup, the normal force and the tensile force (axial to pipe) acting on it changes. If the amplitude is too large, the pulling force on the flexible brush cannot overcome the frictional forces acting against it. If the amplitude is too small, no axial movement of the flexible brush takes place. Hence it is necessary to find a suitable amplitude of reciprocation. An analytical study was done as part of the design of the setup to determine an optimum amplitude.

In order to obtain a good surface finish, it was necessary to understand the effect of various process parameters. A series of experiments were conducted in which the effect of some of the variables in the process was ascertained. The effect of the variables was evaluated in isolation, i.e. one variable was changed each time. The variables studied were:

- abrasive type

- method of applying the abrasive
- time of polishing
- percentage of iron in the mixture
- percentage of solid lubricant in the mixture
- combined effect of rotational and reciprocation speeds

The components were built at the MAE West Lab with the existing facilities.

CHAPTER 2

LITERATURE REVIEW

Initial work in the field of magnetic abrasive assisted polishing was done in the former USSR (Konovalov et al, 1967; 1974; Baron, 1975; Sakulevich et al, 1977; 1978) led chiefly by Baron and in Bulgaria by Mekedonski (1974). These studies concentrated on finishing of external surfaces. The Japanese researchers applied the process to external and internal surfaces (Shinmura et al, 1985, 1991; 1992; 1993; 1995; Umehara et al, 1995, Part 1; 1995, Part 2). Shinmura experimented with both permanent magnets (Fig. 2.1) and electromagnets. The electromagnetic setups included ones with (Fig. 2.2) and without (Fig. 2.3) rotating magnetic fields. One disadvantage cited by Shinmura of using electromagnets is the size and weight of the equipment in order to obtain a strongly nonuniform field distribution (Shinmura et al., 1992). In comparison, permanent magnet assemblies are lighter and smaller. This means that reciprocatory motion can be given to the magnet assembly quite easily.

In addition to the use of an external magnetic field to provide finishing pressure, Shinmura describes the use of a finishing tool (Shinmura et al., 1992). This helps in making the field more nonuniform and increases the magnetic gradient in the polishing region. This increased the forces of finishing by almost four times (Fig. 2.4). The tool used was made of a permanent rubber magnet, although other types were investigated.

Complicated profiles like bent tubes (Fig. 2.5) and clean gas bombs (Fig. 2.6) were finished from an initial roughness of 7 microns R_{max} to 0.2 micron

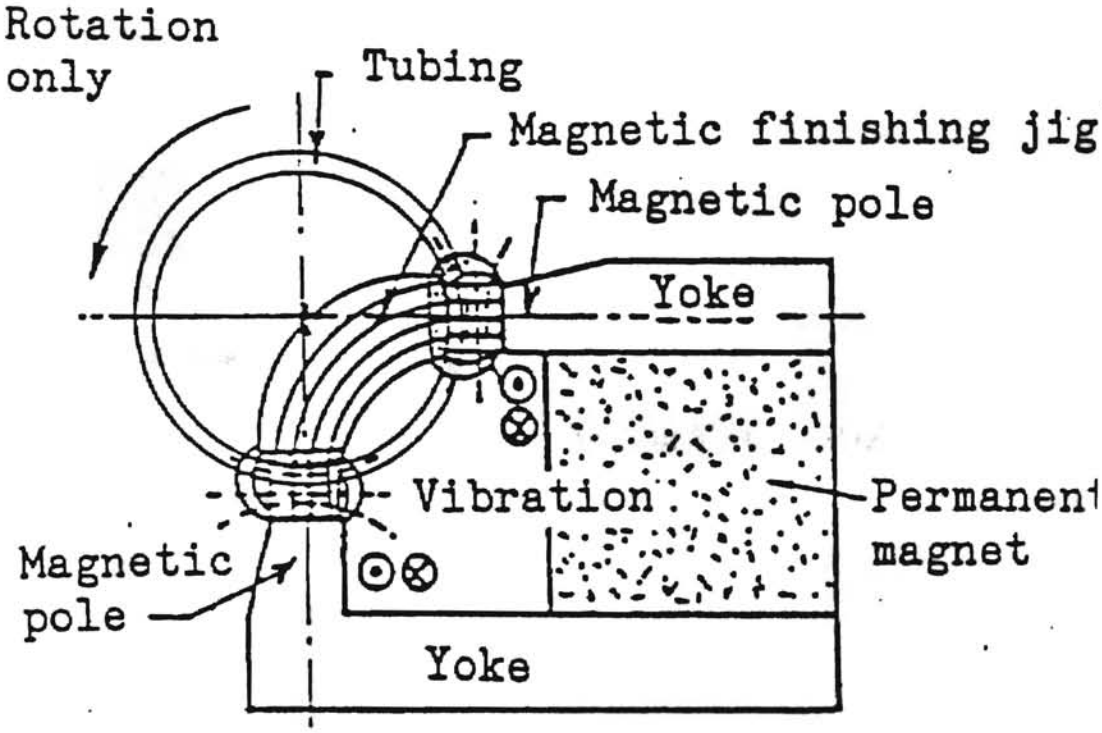

Figure 2.1 Permanent Magnet Setup (Shinmura et al., 1992)

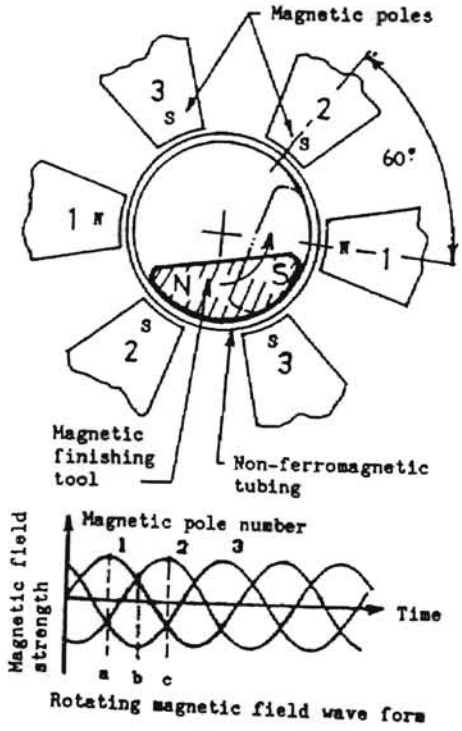

Figure 2.2 Electromagnet Setup with Rotating Magnetic Field

(Shinmura et al., 1993)

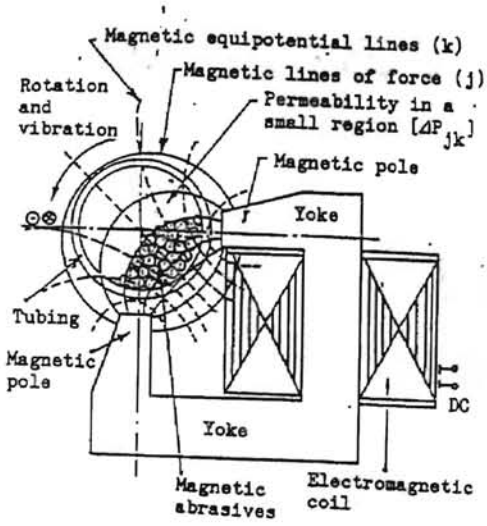

Figure 2.3 Electromagnetic Setup with Stationary Magnetic Field

(Shinmura et al., 1992)

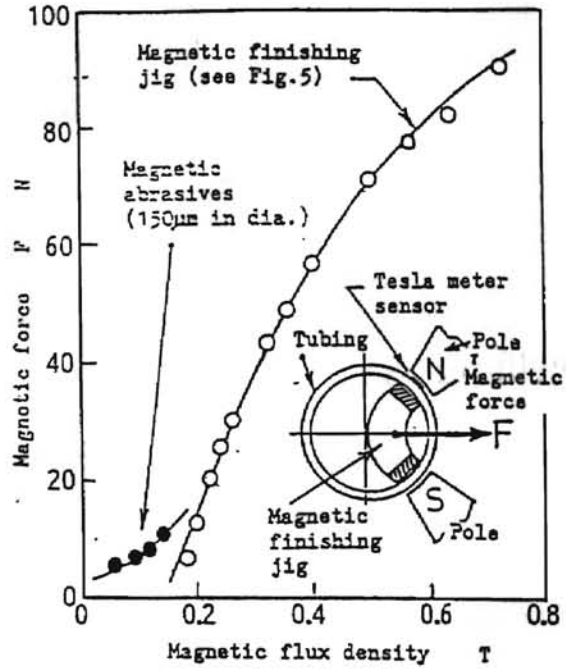

Figure 2.4 Variation of Force with and without Finishing Jig (Shinmura et al., 1992)

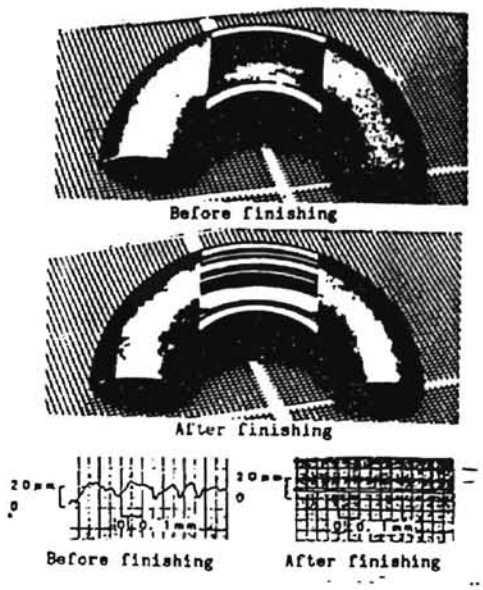

Figure 2.5 Finished Bent Tube by Internal Polishing (Shinmura et al., 1993)

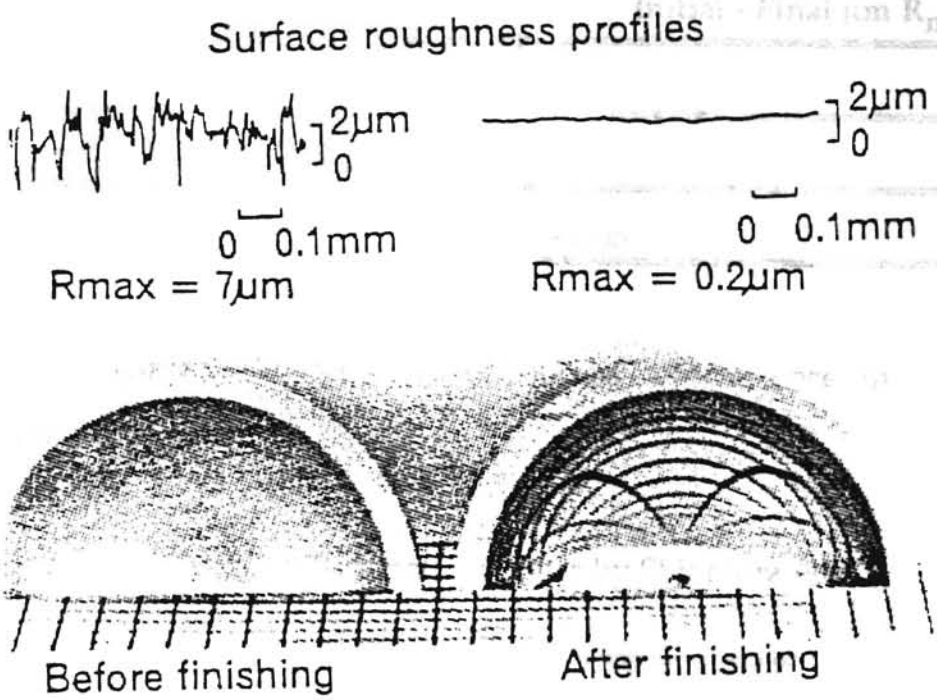

Figure 2.6 Finished Gas Bomb (Shinmura et al., 1995)

R_{max} (Shinmura et al., 1995). The results by Shinmura for polishing various workpieces are tabulated as below:

Table 1.0 Shinmura's results (1992)

Material	Initial - Final μm R_{max}
SUS304	7 - 0.2
Al	2.7 - 0.2
Brass	2 - 0.05

The major parameters of the process which were investigated by Shinmura et al. could be stated as:

Table 2.0 Parametric studies by Shinmura (1992)

Parameter	Effect on
Size of iron particles	Magnetic force
Weight percentage of iron particles in mix	Magnetic force, surface roughness of workpiece
Finishing time	Surface roughness of workpiece

The fundamental difference in Umehara's method is the use of a magnetic fluid as a medium to convert the magnetic force into finishing force. Magnetic flux densities employed in this method were comparitively lower than when using a solid mixture (0.83 Tesla for solid versus 0.038 Tesla

for the magnetic fluid method). In addition to the pressure provided by the fluid, a finishing tool was also employed to increase the removal rates. Various constructions (Figs. 2.7-2.8) of finishing tools were investigated including ZrO_2 balls (Umehara et al., 1995, Part 1) and taper type tools (Umehara et al., 1995, Part 2). The use of softer taper type tools (PVA) resulted in better a finish (Fig. 2.9). The workpieces polished were brass. Removal rates are comparitively lower than that obtained by using a solid mixture of iron and abrasive. A brass tube of less than 10 mm inner diameter was finished to 40 nanometers Ra in 90 minutes. Umehara et al. have also compiled parametric data as tabulated in Table 3.0.

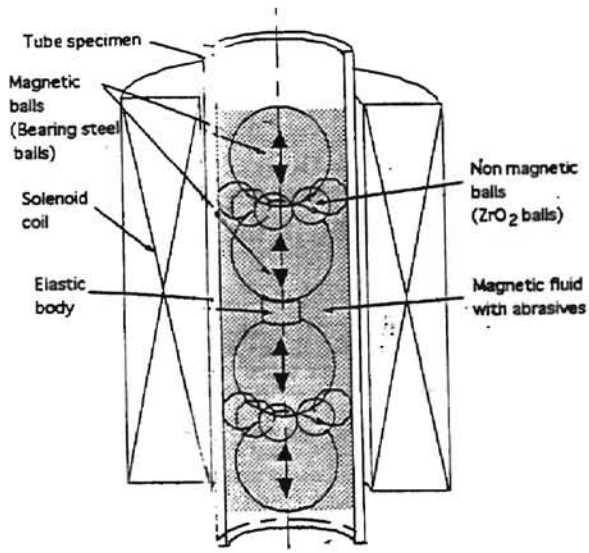

Figure 2.7 ZrO_2 Construction for Magnetic Fluid Polishing

(Umehara et al., Part 2, 1995)

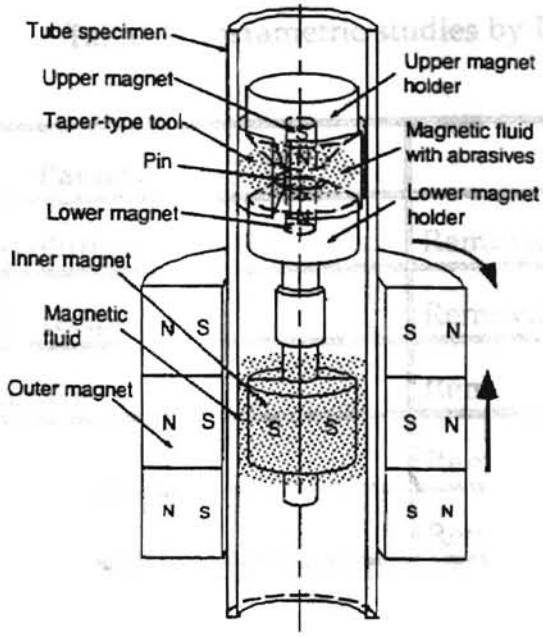

Figure 2.8 Taper Type Construction for Magnetic Fluid Polishing (Umehara et al., Part 1, 1995)

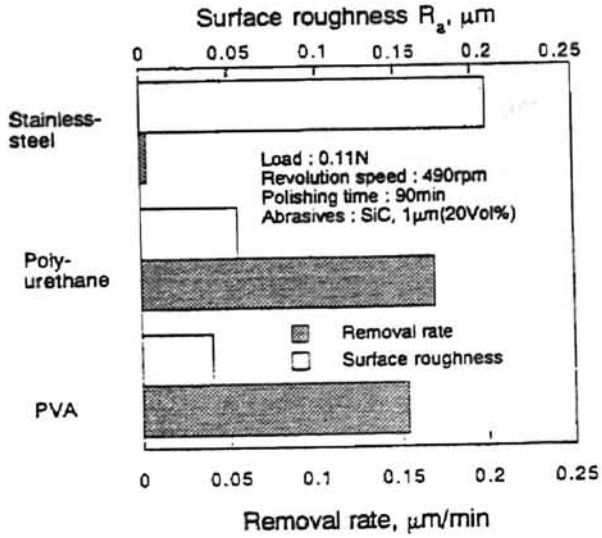

Figure 2.9 Comparison of PVA, Polystyrene, Steel Tools used in Magnetic Fluid Polishing (Umehara et al., Part 1, 1995)

Table 3.0 Parametric studies by Umehara (1995)

Parameter	Effect on
Speed of revolution	Removal rate
Frequency of reciprocation	Removal rate
Finishing time	Removal rate
Polishing stroke	Removal rate
Abrasive size	Removal rate, surface roughness

Korean researchers, namely Kim and Choi (1995), in the field have dealt with the theoretical aspects of the process. Their studies involved simulation for prediction of the surface roughness obtained by the MAP process (Kim and Choi, 1995). Another simulation study involved the prediction of polishing forces in 2 directions, namely along and across the axis of the work tube. This study also explains the condition for effective finishing to occur (Kim et al, 1995). An internal polishing system for curved workpieces which employed a rotating magnetic field (Fig. 2.10) was also designed and developed (Kim et al, 1996).

2.1 Effect of Process Parameters

The results of studies of various process parameters which were investigated by Shinmura et al. (1992) and Umehara et al. (1995) are listed below.

2.1.1 Effect of size of iron particles

The magnitude of magnetic force for different sizes of iron particles did not vary considerably (Fig. 2.11). This was explained as follows. The

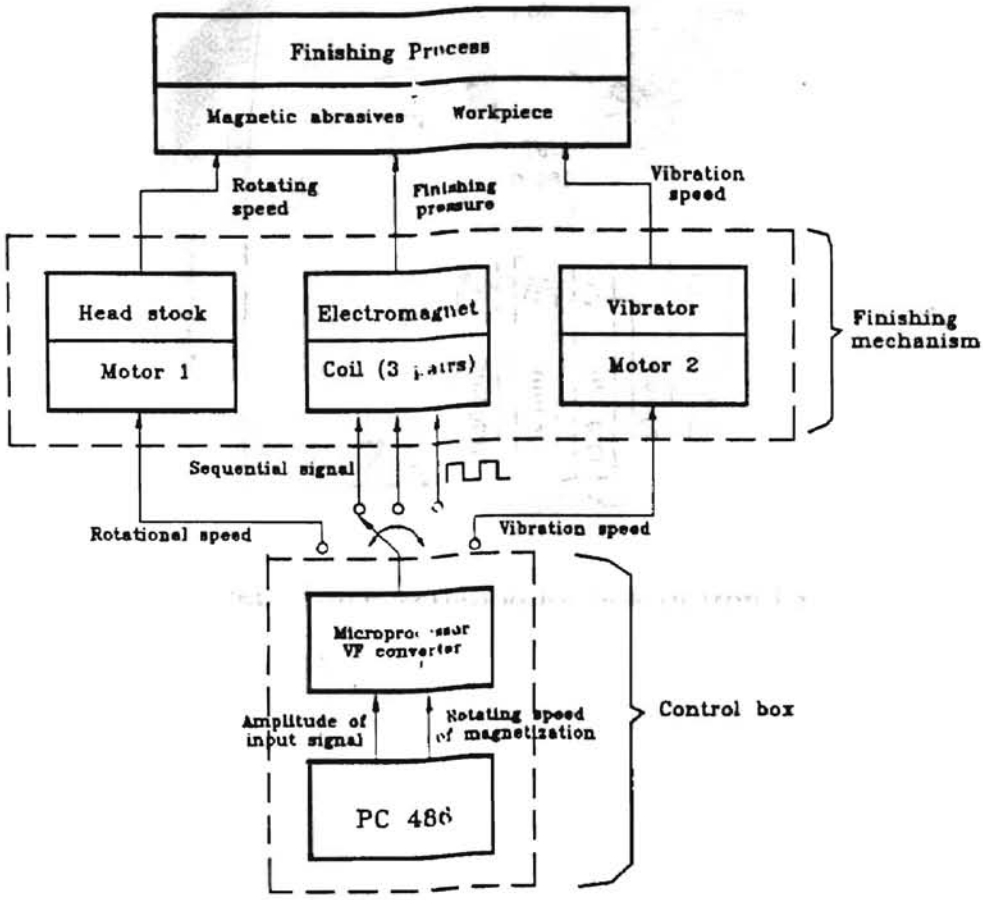

Figure 2.10 Schematic of Rotating Electromagnet Setup (Kim et al., 1995)

magnetic force acting on a particle is directly propotional to the cube of the diameter.

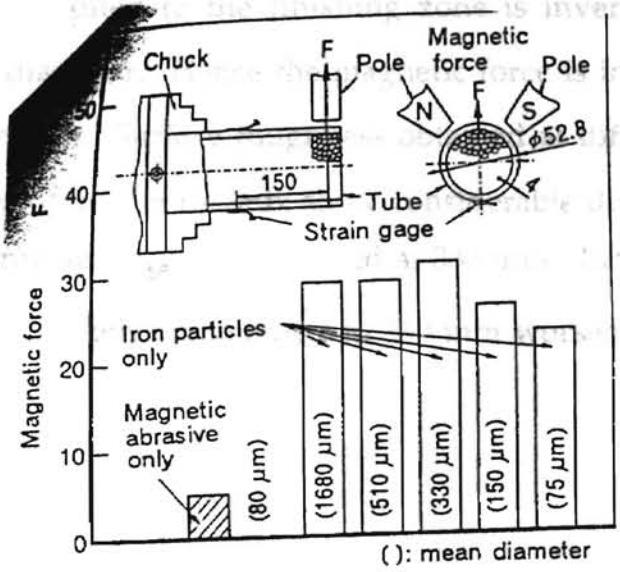

Figure 2.11 Magnetic Force Variation for Size of Iron Particles in Mix (Shinmura et al., 1995)

$$F=kD^3xH(dH/dx) \quad \text{.....(1)}$$

where F= Magnetic force

k= Coefficient

D= Diameter of particle

x= susceptibility of particle

H= Magnetic field strength

The magnitude of the resultant force of iron particles acting on the inner side of tube is obtained as a product of the number of particles and the magnitude of the magnetic force given by each particle. On the other hand, the number of particles supplied to the finishing zone is inversely proportional to the cube of the diameter. Hence the magnetic force is independent of the size of the iron particles. Surface roughness obtained at different finishing times for various sizes of iron in the mix show considerable differences (Fig. 2.12). Best results in terms of R_{max} are obtained at 330 mm. Increasing or decreasing the iron particle size when compared to 330 mm worsens the finish (Shinmura et al., 1995).

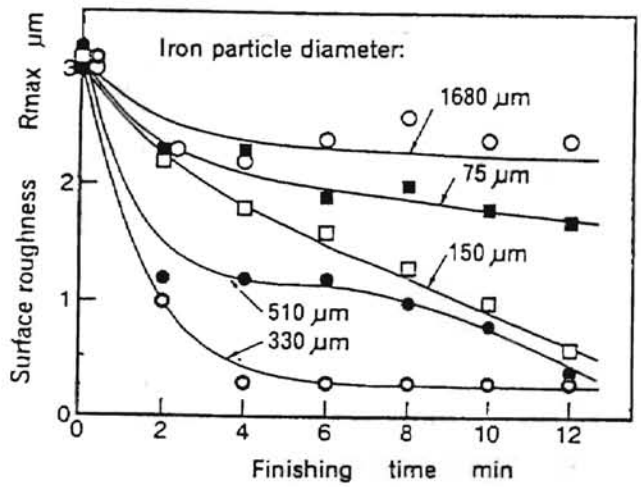

Figure 2.12 Surface Finish Variation on Work for Size of Iron Particles in Mix (Shinmura et al., 1995)

2.1.2 Effect of Weight Percentage of Iron in Mix

The magnetic forces increased linearly as the percentage of iron in the mix was increased (Fig. 2.13). This was because of the fact that the ferromagnetic content of the mix increased and so did the magnetic susceptibility of the mix.

It is observed that the finish obtained was best at 80% weight percentage of iron in the mix (Shinmura et al., 1995) as observed in Fig. 2.14. As the weight percentage of iron in the mix is increased, the number of cutting edges decreases. This means that the initial rough surface cannot be removed rapidly. On the other extreme, the magnetic forces are not enough to cause finishing.

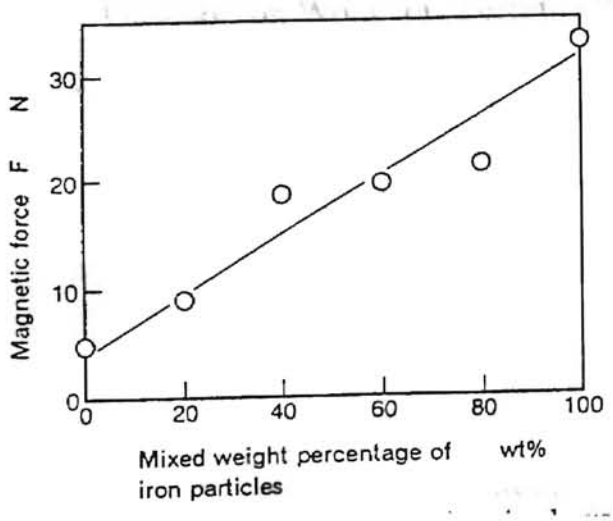

Figure 2.13 Magnetic Force Variation for Percentage of Iron Particles in the Mix (Shinmura et al., 1995)

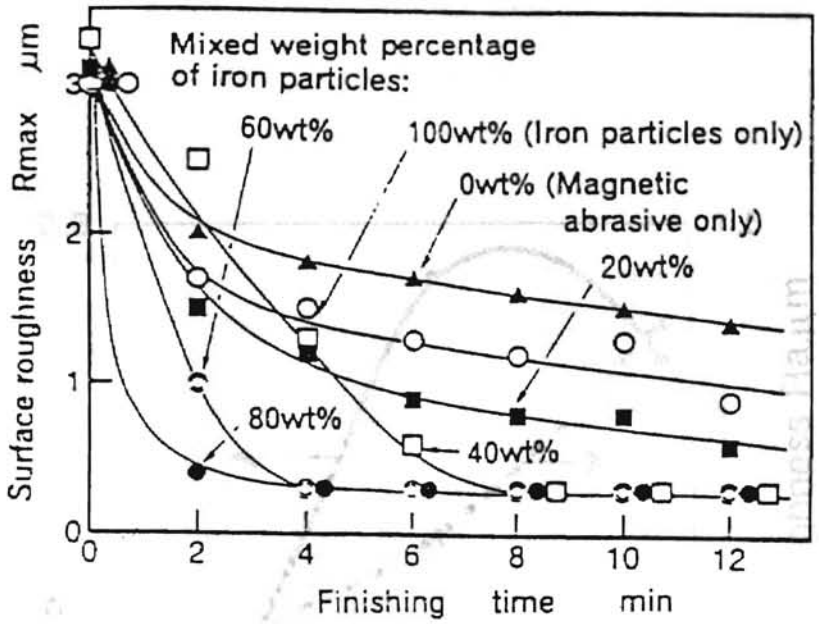

Figure 2.14 Surface Finish Variation on Work for Percentage of Iron Particles in the Mix (Shinmura et al., 1995)

2.1.3 Effect of Abrasive Size in Magnetic Fluid Method

The removal rate is observed to increase with abrasive size (Fig. 2.15). Surface finish (Ra) shows an increase (Fig. 2.16) with abrasive size (Umehara et al., 1995, Part 1).

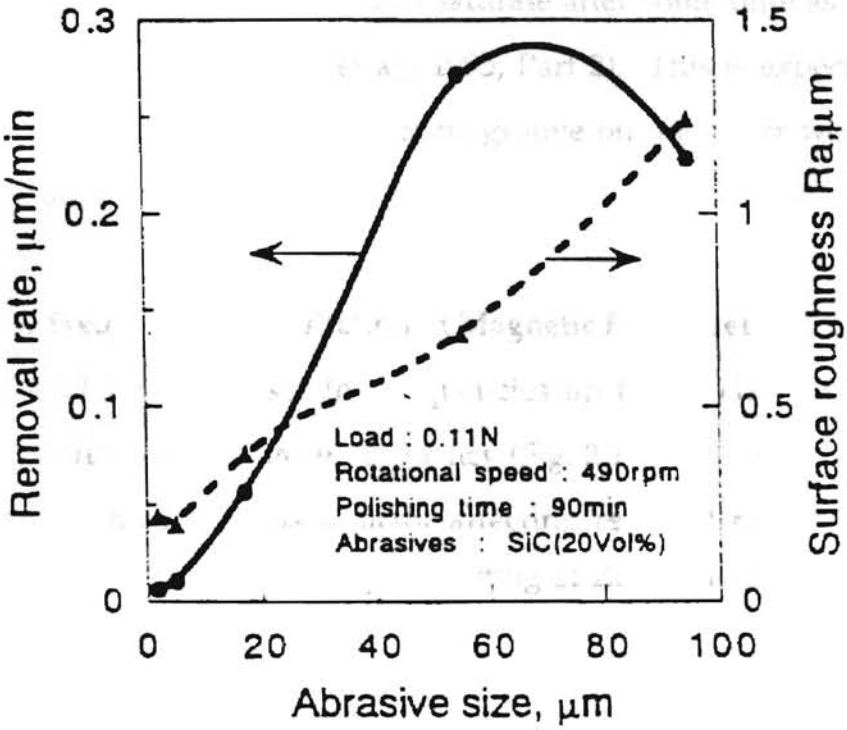

Figure 2.15 Material Removal Rate and Surface Finish Variation for Size of Abrasive (Umehara et al., Part 1, 1995)

2.1.4 Effect of Finishing Time in Magnetic Fluid Method

The removal rate drops as the finishing time is increased (Fig. 2.17). This is a sign of decreased polishing efficiency, the reason being deterioration of the abrasives after polishing action. The surface finish obtained using a given size of abrasive particle is observed to saturate after some time as in Fig. 2.18 (Shinmura et al., 1992; Umehara et al., 1995, Part 2). This is expected as each size of abrasive will make a characteristic groove on the softer work material under a set load.

2.1.5 Effect of Frequency of Oscillation in Magnetic Fluid Method

The removal rate increases for frequencies up to 2-3 Hz, but then drops rapidly for any further increase in frequency (Fig. 2.19). The effect of polishing stroke was also considered as a factor affecting removal rate. These set of experiments were done on the setup consisting of ZrO_2 and bearing steel balls (Umehara et al., 1995, Part 2).

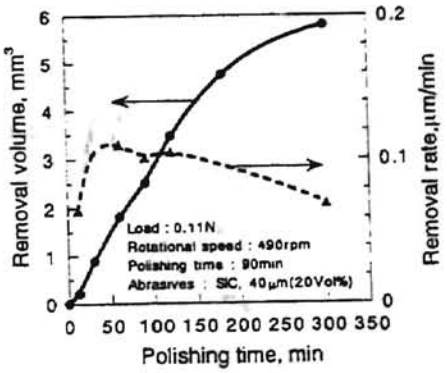

Figure 2.16 Material Removal Rate Variation for Polishing Time
(Umehara et al., Part 1, 1995)

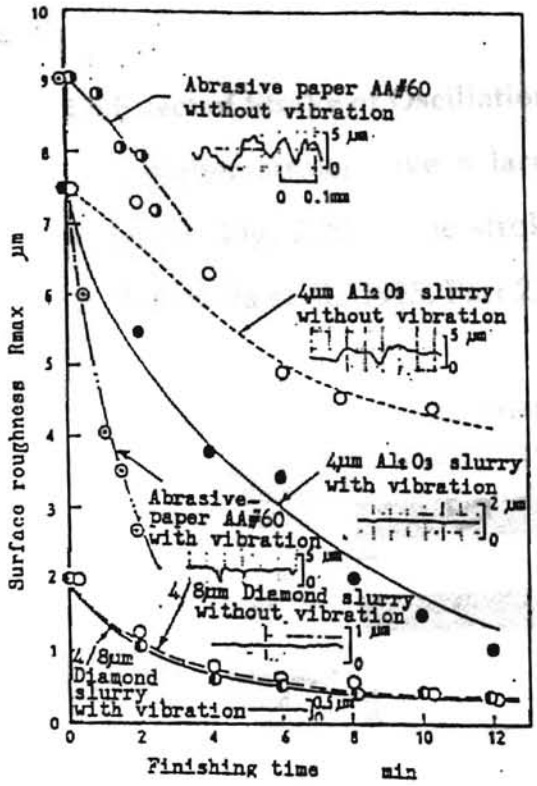

(Conditions) workpiece: stainless steel tubing (SUS304), 50.6mm in outer dia., 1mm in thickness; work revolution: 450rpm; magnetic flux density in air gap: 0.7T; clearance: 1.5mm; magnetic pole vibration : frequency=15Hz, amplitude=8mm; vibration of magnetic finishing tool: frequency=15Hz, amplitude =7.5mm; abrasives: see this figure.

Figure 2.17 Surface Finish Variation on Work for Polishing Time

(Shinmura et al., 1992)

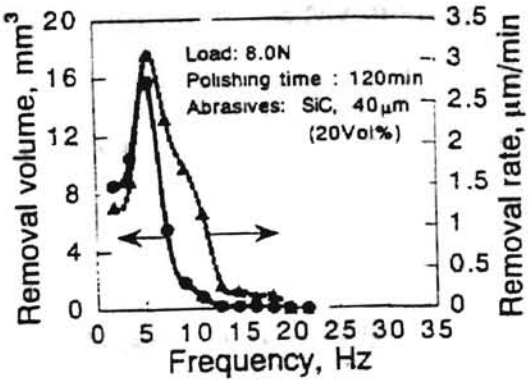

Figure 2.18 Material Removal Rate Variation for Frequency of Oscillation

(Umehara et al., Part2, 1995)

2.1.6 Effect of Stroke of Oscillation in Magnetic Fluid Method

A higher stroke gave a larger removal rate at the same frequency of oscillation (Fig. 2.20). The strokes experimented with were between 2 to 3 mm (Umehara et al., 1995, Part 2).

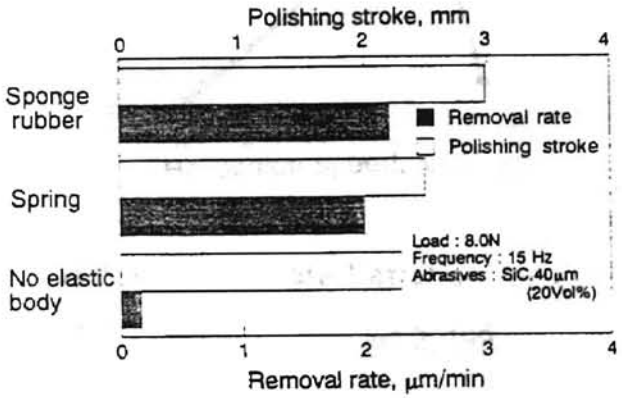

Figure 2.19 Material Removal Rate Variation for Length of Stroke (Umehara et al., Part 2, 1995)

2.1.7 Effect of Revolution Speed in Magnetic Fluid Method

Revolution speed has the effect of increasing the removal rate upto a critical speed, and then causes the removal rate to decrease (Fig. 2.21). The speeds analyzed were up to 22000 rpm, with the maximum removal rate (20 mm/min) obtained at 16000 rpm (Umehara et al., 1995, Part 2). The construction of the finishing tool in this set of experiments was in the form of ZrO_2 and bearing steel balls. A uniform surface finish could not be achieved as the balls did not move in the longitudinal direction during polishing.

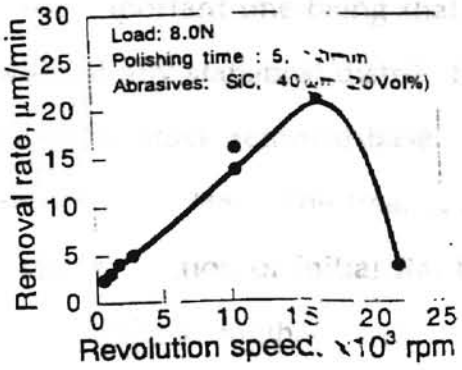

Figure 2.20 Material Removal Rate Variation for Revolution Speed of Work (Umehara et al., Part 2, 1995)

2.2 Theoretical Studies

This section details the theoretical studies conducted by Kim and Choi (1995) for magnetic field assisted polishing of internal surfaces.

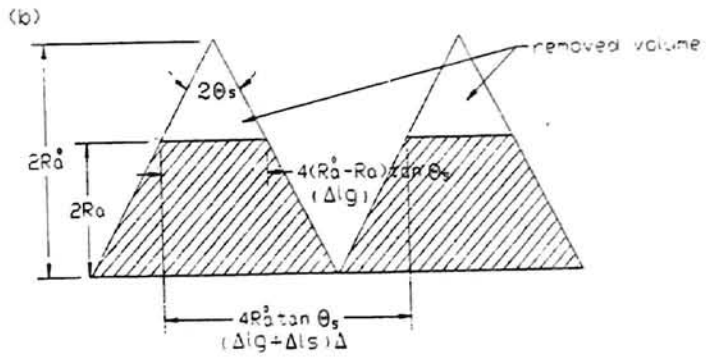

Figure 2.21 Schematic Model of Surface (Kim et al., 1995)

2.2.1 Simulation for Prediction of Surface Accuracy

In order to model the surface, certain assumptions were made by Kim and Choi (1995), the most important one being that the surface is uniform. This implies that it is without any statistical distribution of peaks and valleys as in Fig. 2.22. The model for stock removal based on microcutting mechanisms was employed (Wang et al, 1988). The final roughness was derived from an expression which was a function of initial Ra, force per grain, time, number of grains, and magnetic field strength.

The algorithm (Fig. 2.23) employed for the simulation calculates the machining pressure from the inputs of magnetic field

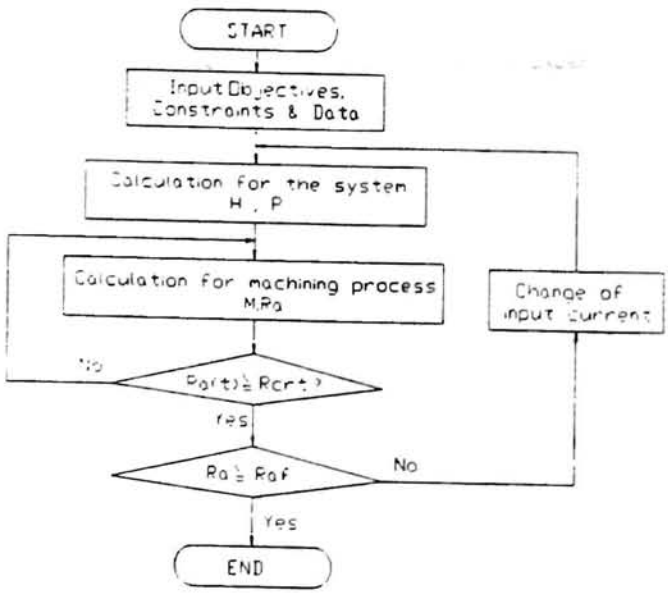

Figure 2.22 Algorithm for Surface Finish Simulation (Kim et al., 1995)

strength and permeability. The maximum machining pressure is obtained at a magnetic flux density of 1.2 T. The program calculates the final Ra and constantly compares with the critical Ra for the set machining pressure. If the Ra becomes the same as the critical Ra and the final Ra required is lower, then the magnitude of input current is decreased to lower the machining pressure. The program ends if the surface roughness reaches the objective final Ra value. The predicted values agreed closely (Fig. 2.24) with experimental values at lower magnetic flux densities than for higher magnetic flux densities (0.6 T-1.2 T).

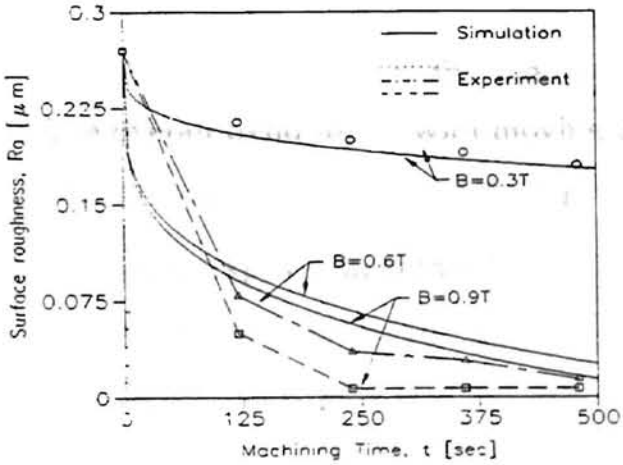

Figure 2.23 Comparison of Simulated and Experimental Surface Roughness Values (Kim et al., 1995)

2.2.2 Simulation of Forces Involved in the Process

A major assumption made by Kim and Choi (1995) for the simulation of the polishing forces is that the leakage flux is negligible. The equivalent reluctance of the circuit is calculated initially. Then the energy product of the circuit is computed and differentiated with respect to two directions to obtain the forces in those two directions. The movement of the finishing tool is represented as:

$$Ma = F_x - \mu_{eq} F_y$$

where M = mass of the tool

a = acceleration of the tool

$F_{x,y}$ = forces in the respective directions

μ_{eq} = equivalent coefficient of friction between tool and workpiece.

The simulated results of F_x (the force in the direction of the axis of workpiece) show an increase with air gap, and then a decrease after a certain value (Fig. 2.25). The overall trend for F_x with moving distance of the pole is similar to that of with air gap (Fig. 2.26). The F_y force (force in the direction normal to the axis of the workpiece) increases first and then decreases as the air gap is increased. This trend is observed for all values of moving distance of the pole other than zero. If the pole is stationary, the F_y force decreases exponentially as air gap is increased (Fig. 2.27).

Assuming coefficients of friction between the finishing tool and workpiece, it was observed that the tool moving force ($F_x - \mu_{eq} F_y$) is negative initially (Fig. 2.28) for some value of pole moving distance (this range of values of pole moving distance is termed as the dead zone). The force increases quadratically as the tool is moved.

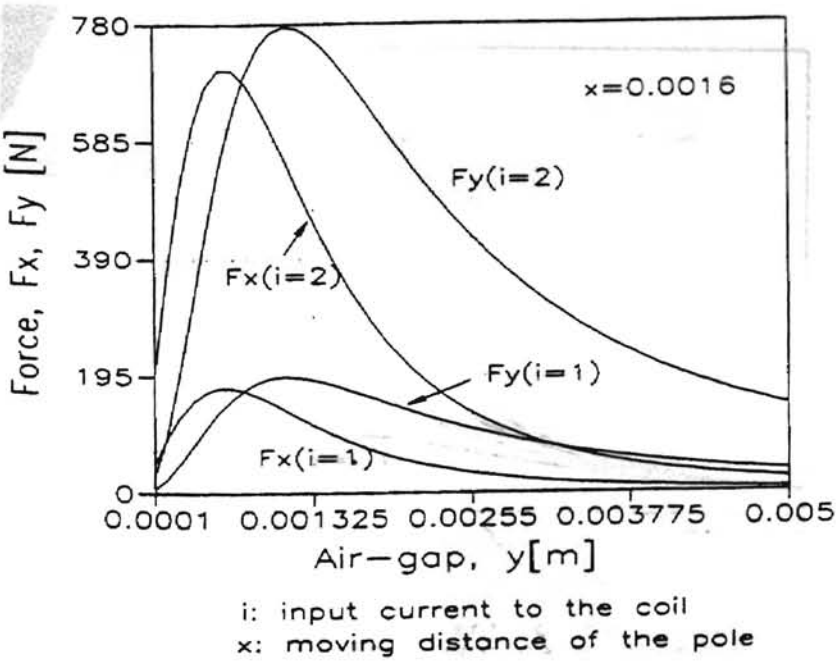

Figure 2.24 Variation of Forces with Change in Air Gap (Kim et al., 1995)

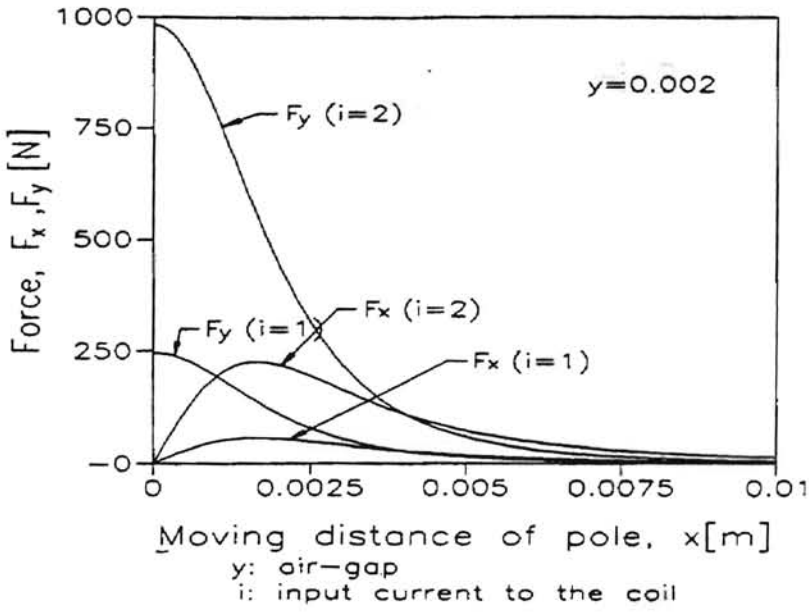

Figure 2.25 Variation of Forces with Moving Distance of Pole (Kim et al., 1995)

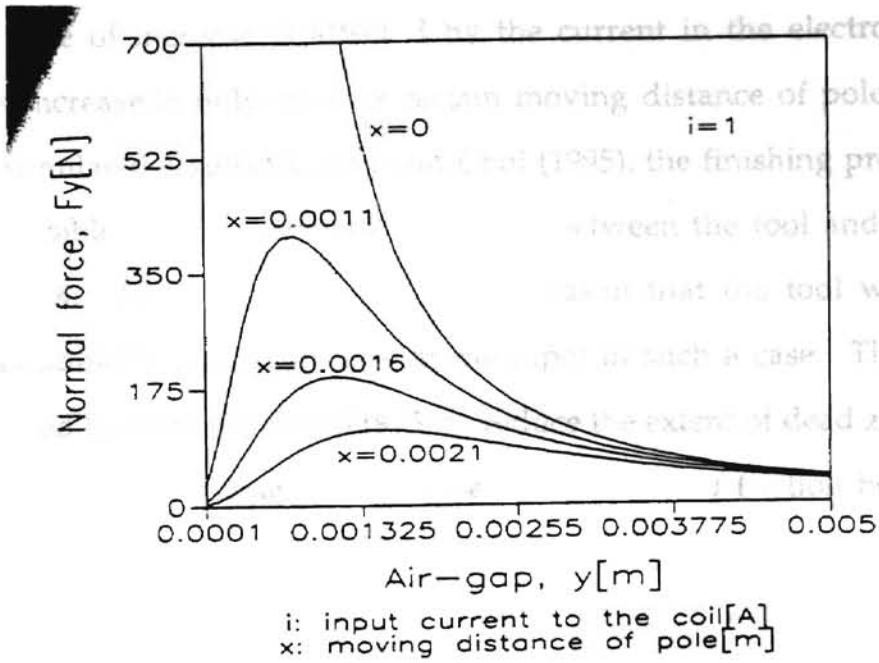

Figure 2.26 Fy Force Variation for Various Air Gaps and Moving Distances (Kim et al., 1995)

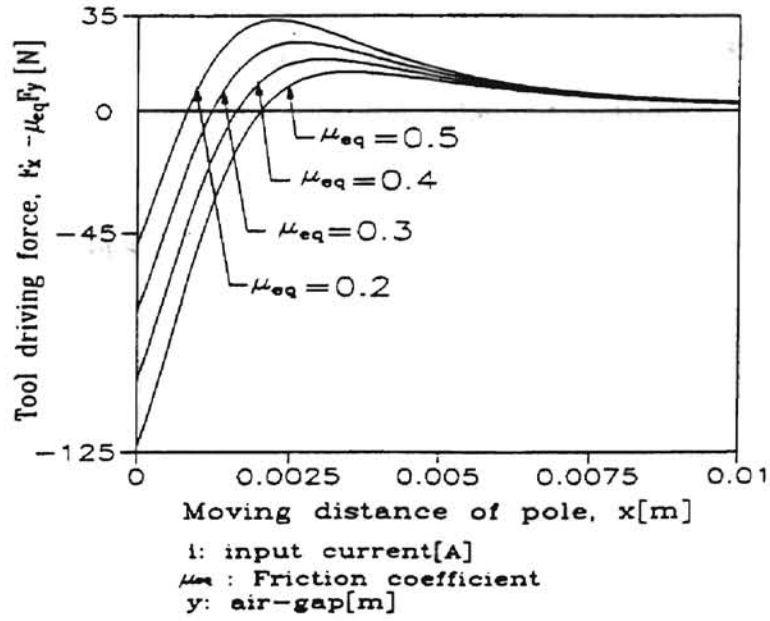

Figure 2.27 Guidance Force Variation with Dead Zone (Kim et al., 1995)

The rate of increase is affected by the current in the electromagnetic coils. This increase is only up to a certain moving distance of pole. According to the simulated results by Kim and Choi (1995), the finishing process would not be possible if the coefficient of friction between the tool and workpiece was over 0.4. This is due to the simple reason that the tool would not move longitudinally (along the axis of the pipe) in such a case. The factors which are cited by Kim and Choi (1995) to reduce the extent of dead zone are:

- reducing the equivalent coefficient of friction between tool and work
- reducing the air gap

2.2.3 Design of a System with Rotating Magnetic Field using Finite Element Method

A major issue in such a setup is the collapse of the of the magnetic brush due to gravity in the transition point from one magnetic pole to the next. Two driving modes (Fig. 2.29) to magnetize the six magnetic poles in sequence were studied using finite element methods:

- 3 step mode, which makes one revolution of the magnetic brush in 3 steps and
- 6 step mode, which makes one revolution in 6 steps

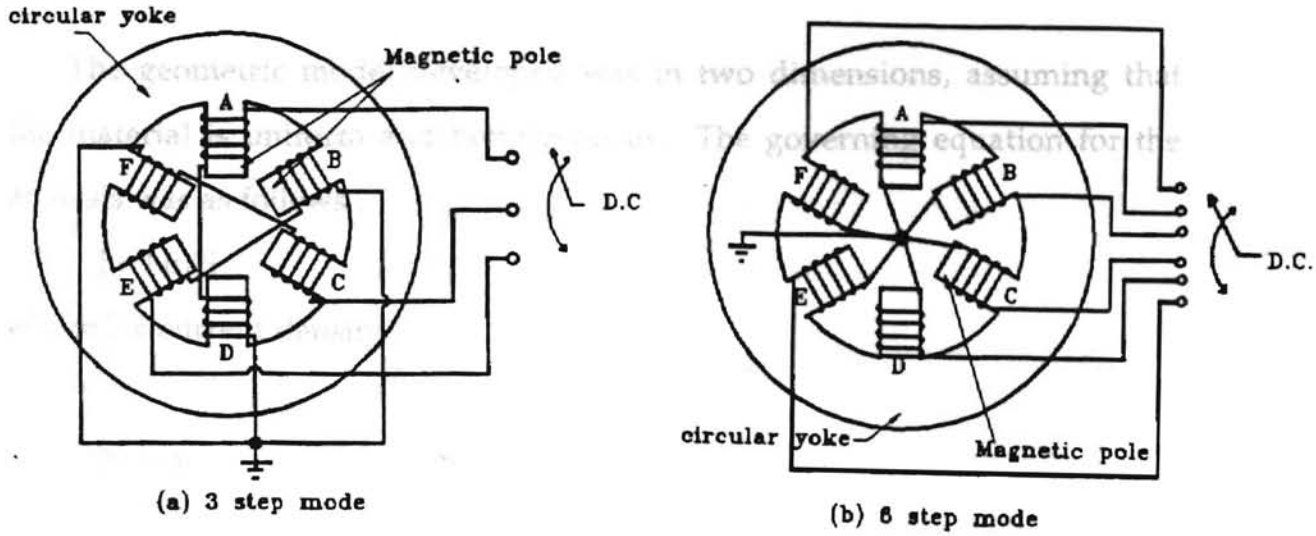

Figure 2.28 6 Step and 3 Step Modes (Kim et al., 1996)

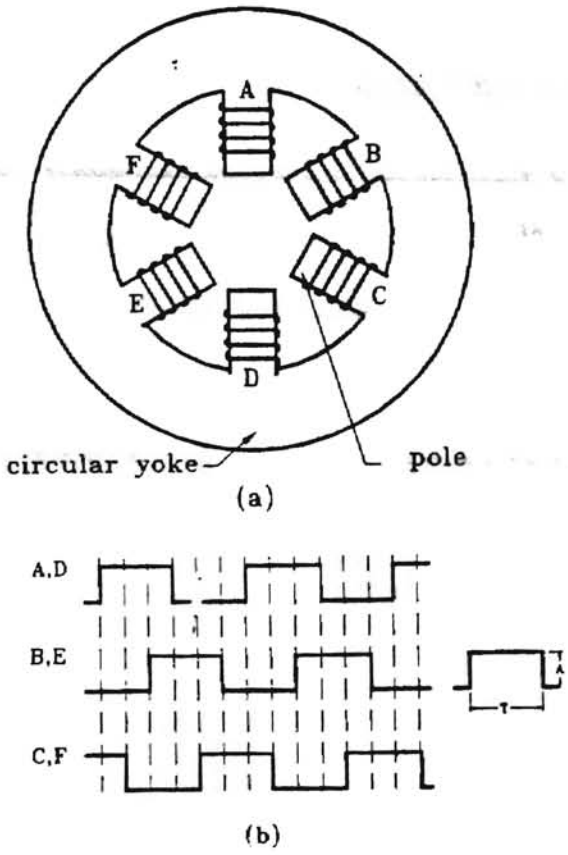

Figure 2.29 Signal to Prevent Collapse of Brush (Kim et al., 1996)

The geometric model developed was in two dimensions, assuming that the material is uniform and homogeneous. The governing equation for the analysis was as follows :

$$J = Ni/S$$

where J = current density

N = number of coil turns

i = coil current

S = cross sectional area of coil turns

The results of the analysis indicate that the 3 step mode is better as it produces a higher magnetic flux density in the working zone.

Table 4.0 Magnetic flux densities in 3 and 6 step modes

Mode	**Magnetic flux density**	
	Static	**Transition**
3 step	0.85 T	1.25 T
6 step	0.7 T	0.94 T

The collapse of the magnetic brush was avoided using (Fig. 2.30) a rectangular wave (driving voltage signal) and folded by one-third in two adjacent signals.

2.3 State of the Art Applications Employing the Process

The commercial applications of the process were studied and implemented by the Japanese researchers to a great extent (Shinmura et al., 1985). The areas of application for MAP of internal surfaces have been :

- bearing races
- sewing machine parts

The equipment for the finishing of the sewing machine parts is capable of finishing both, the external and internal surface (Figs. 2.31-2.32). There are 6 stations on a rotary table, and on each station 4 spindle heads (24 spindle heads in total) for holding the workpiece are installed. On each station, an electromagnetic and magnetic pole are installed. On the first station, loading and unloading of parts is done; then on the second and third stages, side finishing by rotating parts to both directions back and forth is done. On the fourth and fifth stations, under-face finishing is done; and on the sixth station simultaneous final finishing is done, which means the sequential controlled finishing of upper-face, under-face and side-face. As part of a feature of the equipment, it is equipped with an alarm and suspension device for accident prevention during the process.

Magnetic abrasives are used through constant circulation by using 5 automatic magnetic abrasives circulating pieces of equipment. Parts after finishing are demagnetized in a tunnel type demagnetizer, and then proceed to a washing process. The loading and unloading is performed by an operator and the total cycle time per piece is 15 seconds. The use of robots could result in full automization of the process.

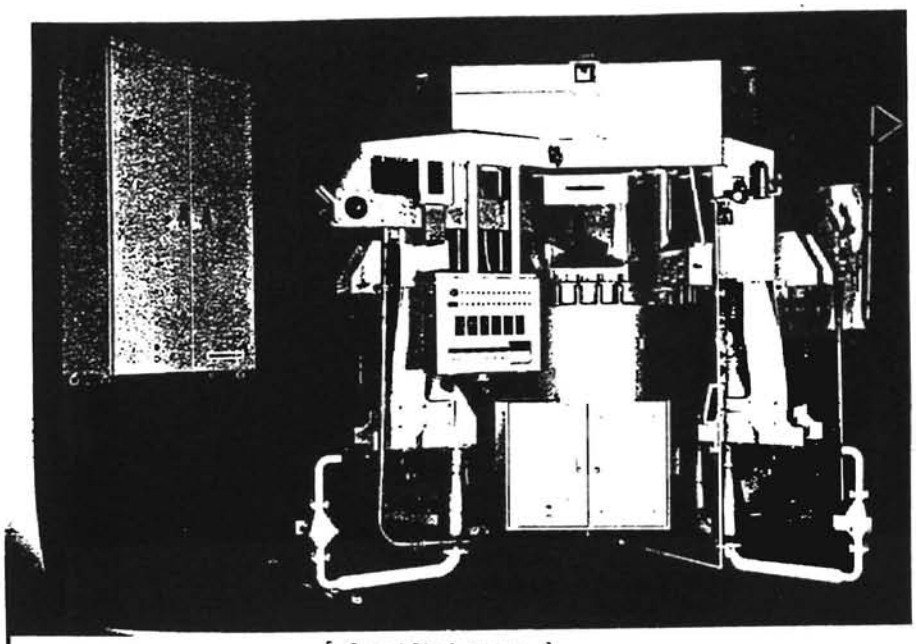

[Specified items]
Size of machine ; Height 2950
Width 3650
Depth 3150
Net weight ; 6.5 tons

Figure 2.30 Sewing Machine Parts Finisher (Shinmura et al., 1985)

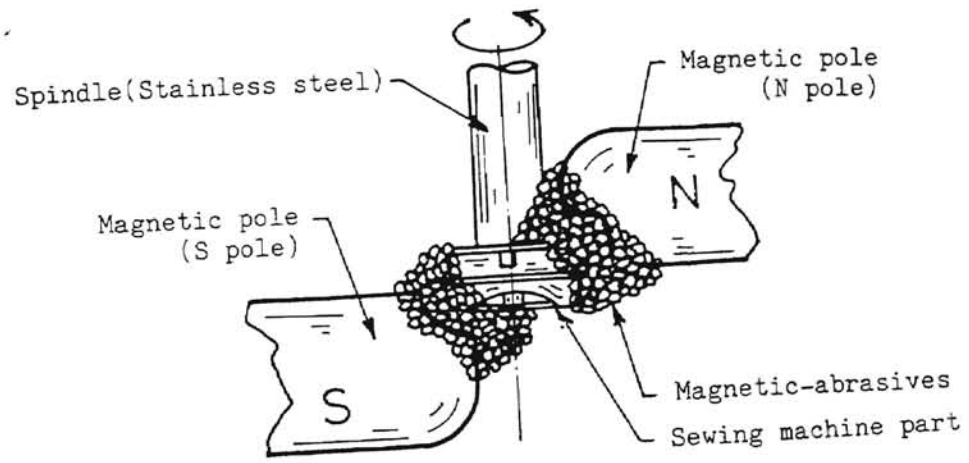

Figure 2.31 Schematic of Finishing Process of Sewing Machine Part (Shinmura et al., 1985)

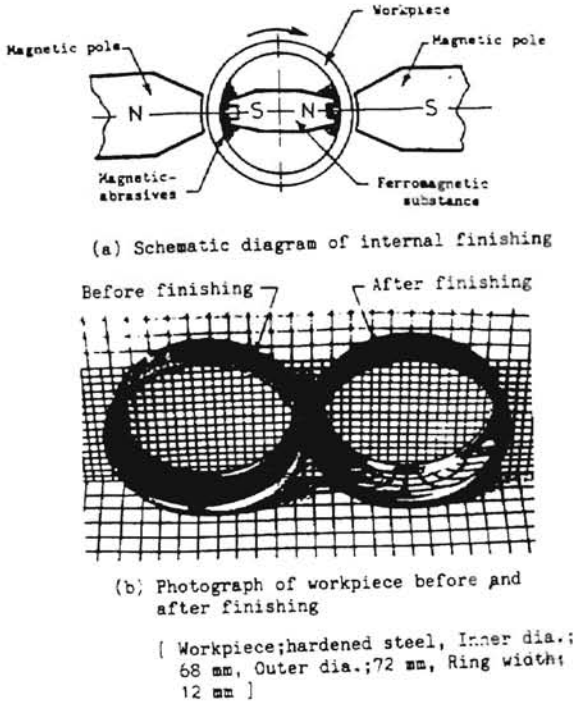

Figure 2.32 Bearing Race Finishing (Shinmura et al., 1985)

The finishing of the internal track of the outer bearing race is the other application which has been carried out commercially. The finishing tool (a ferromagnetic piece) is suspended in the inner track due to the magnetic forces exerted by 2 poles (Fig. 2.33). There is no reciprocation of the finishing tool, just rotation of the race. The total time required to finish the race from 2.0 mm R_{max} to 0.2 mm R_{max} is 1 minute.

CHAPTER 3

DESIGN OF EQUIPMENT

The primary design issues in this project were:

- Geometric design of various components
- Analysis of magnetic field (FEM)
- Analysis of forces developed during polishing

The geometric design of the components was driven by the size of the tubes to be polished. The size of the tube was fixed as one-half inch. The general flow chart details the various steps involved in the design of the equipment.

The geometric design consisted of the determination of the configuration of the magnets. Different configurations were selected and FEM analyses were conducted on all of them. The FEM analyses is described in subsection 3.1. The objective of all FEM analyses were to determine the magnetic field intensity and distribution in the polishing zone. The field had to be non-uniform and concentrated in the polishing zone, where it is most needed. The next step involved simulation of the forces in polishing. The condition for efficient polishing was investigated. This is described in subsection 3.2. Based on the results obtained, the amplitude of oscillation was determined.

3.1 Finite Element Studies

During the course of the project, it was imperative to experiment with setups that would increase the magnetic field in the polishing zone.

Employing ideas to build new setups would have taken considerable time. Finite element analysis was an efficient tool which aided in simulation of the

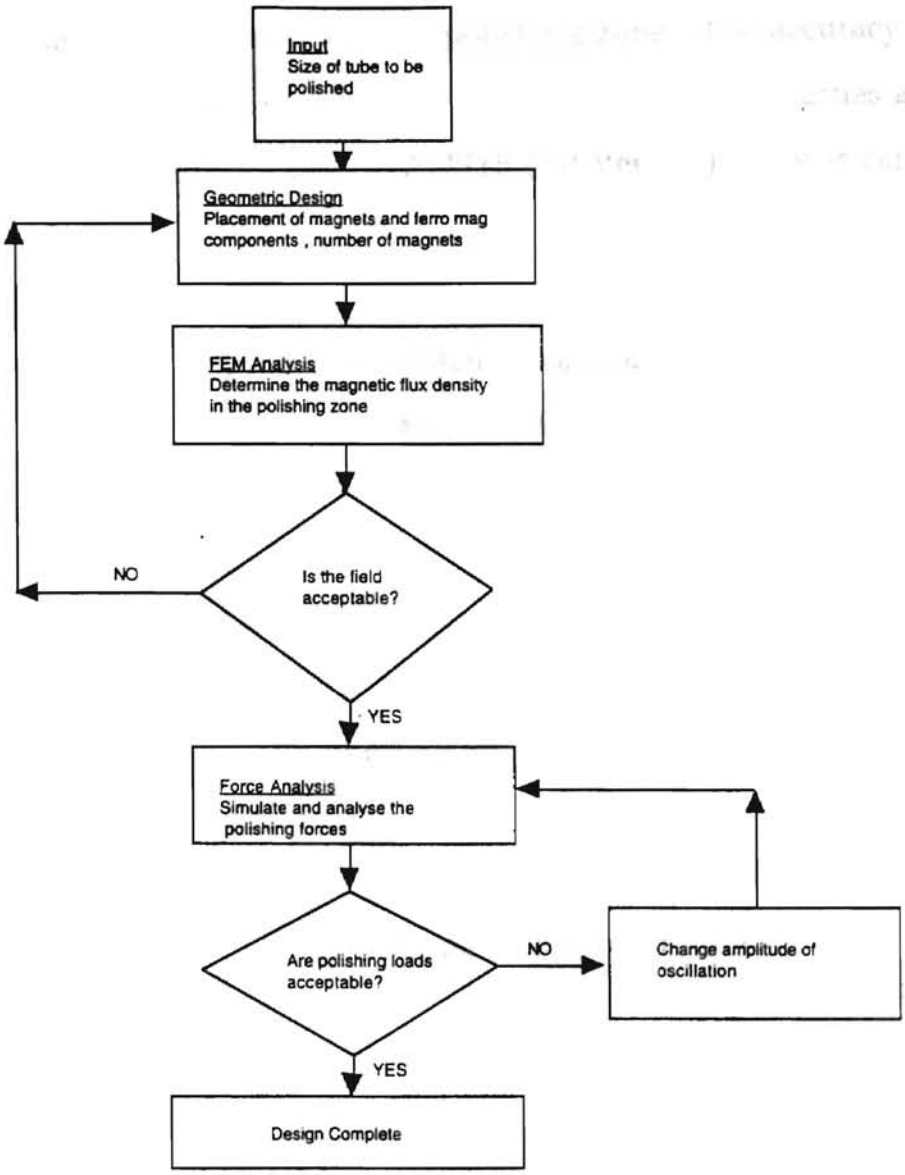

Figure 3.1 Flow Chart of Design Process Employed

visualized setup. Magnetic analysis was performed on these setups and the field in the polishing zone was determined.

The objective in all these studies was to determine ways to increase the magnetic field intensity in the polishing zone. The accuracy of the analyses depended on the input data in terms of material properties and dimensions. The procedure for a typical ANSYS (5.0 Version) analysis can be categorized into 3 steps:

1. To build a model
2. To apply loads and obtain a solution
3. To review the results

3.1.1 To Build a Model

3.1.1.1 Specifying the element types :

Magnetic abrasive finishing of a non-magnetic tube was modelled using the 2 basic elements.

1. INFIN 9 Used for boundary element type
2. PLANE 13 Used for nonmagnetic, magnetic, and air regions

3.1.1.2 Specifying material properties of various elements:

The model consisted of the following regions

- air
- nonmagnetic
- magnetic
- magnets

The material properties of air and nonmagnetic regions was input as 1. For magnetic materials the BH curve was specified using the TB commands.

3.1.1.3 Creating model geometry :

The three dimensional internal finishing apparatus was converted to two dimensional by selecting a suitable plane across the axis of the workpiece. After the model boundaries have been specified, the meshing of the model was initiated. In this procedure the size and shape of the elements could be controlled. The size of the elements at the polishing zone was much finer than elsewhere.

3.1.2 To Apply Loads and Obtain Solution

The analysis performed was static in nature with the Newton Rhapson method of solution. Two load steps were employed, with 5 iterations in the first step and 20 in the second. The number of substeps specified in each load step was 5 in the first and 1 in the second. The loads applied to the intermediate load steps were step changed. Convergence tolerance was set as 0.1% for the vector magnetic potentials.

3.1.3 To Review Results

Once the solution is obtained, the ANSYS post-processor (POST1) is used to review the results. This step can be used to view the following:

- flux lines
- contour displays of flux density, and field intensity
- vector displays of flux density, and field intensity

3.1.4 Geometric Models and Results

In order to justify the use of an internal magnet to provide pressure, an analysis was done with and without the internal magnet. The orientation of the two magnets was made in such a manner that opposite poles faced each other (Fig. 3.1). The polishing mix was represented as a conforming layer internal to the pipe. This layer was given a magnetic permeability value similar to iron. Although in reality the edges of the magnet were rounded, the rounding was hardly precise dimensionally. To assume a worst case, the edges were considered as square. The plots of magnetic flux density in the two cases evince a definite improvement with the use of internal magnet (Figs. 3.2 and 3.3).

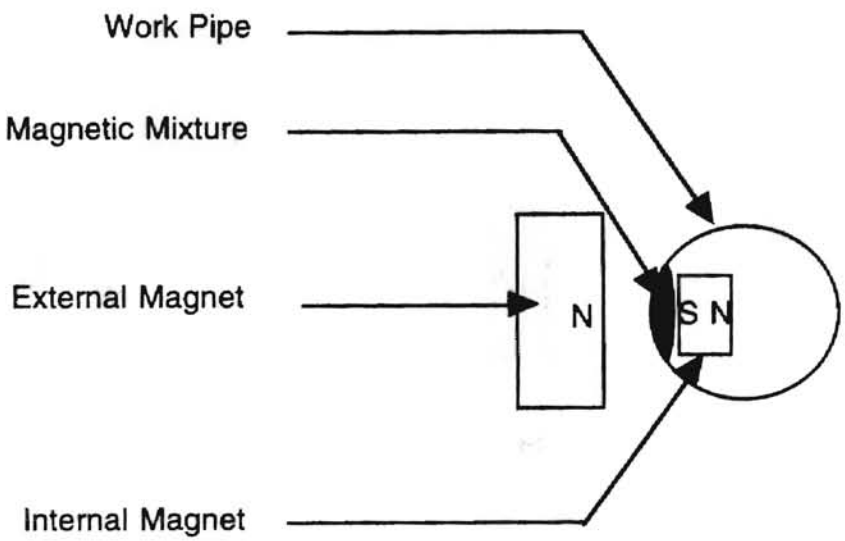

Figure 3.2 Geometric Model of Setup with Internal Magnet

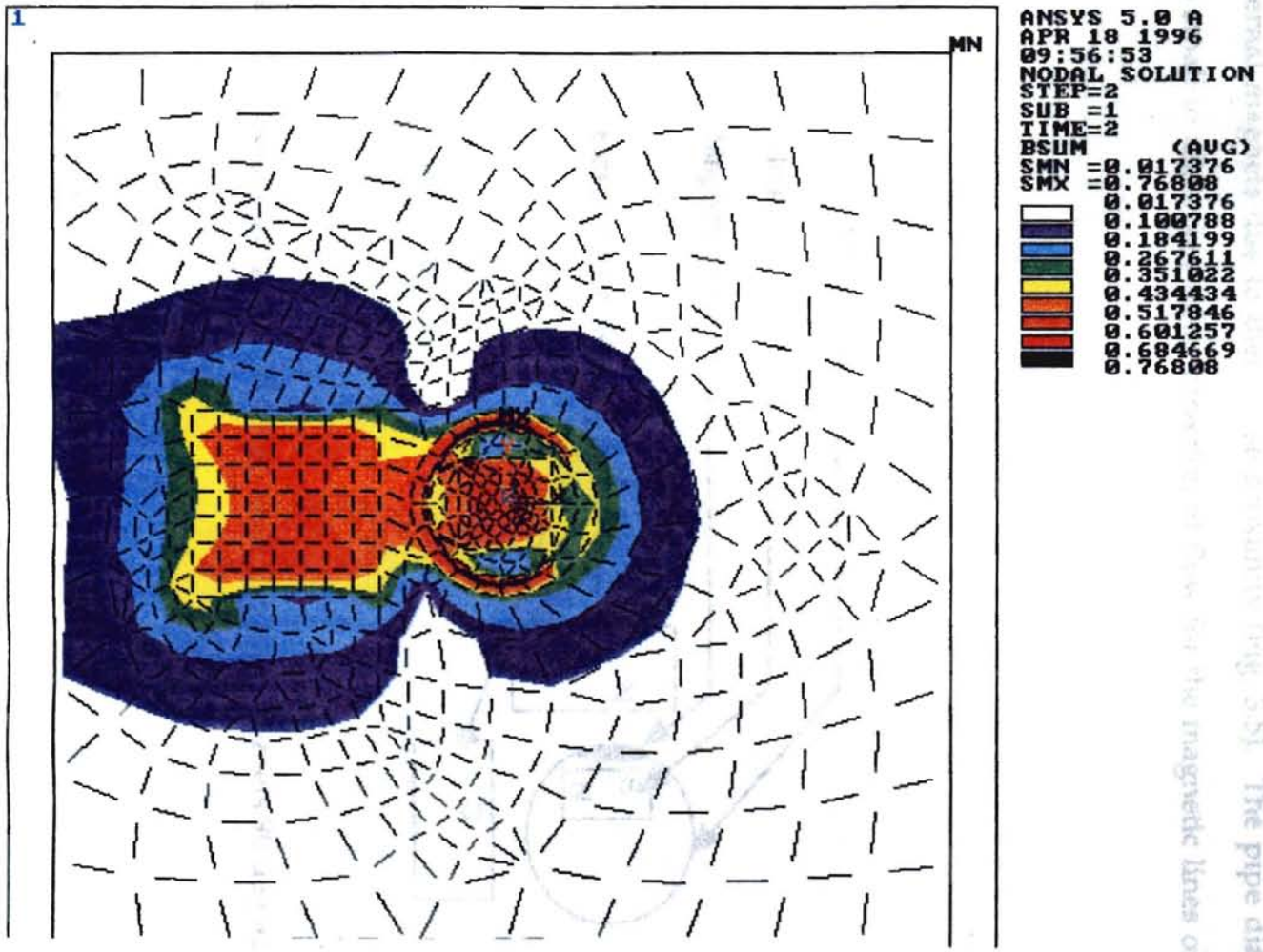

Figure 3.3 BH Plot of Setup with Internal Magnet

The use of another external magnet placed at right angles to the first was analyzed (Fig. 3.4). It is observed that the field shorts between the two external magnets due to their close proximity (Fig. 3.5). The pipe diameter is too small to allow any other direction of flow for the magnetic lines of force.

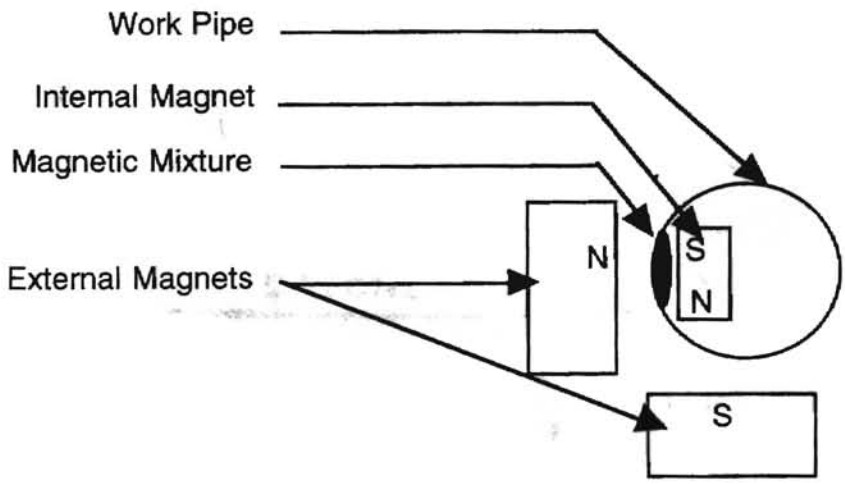

Figure 3.4 Geometric Model of Setup with External Magnets 90 deg apart

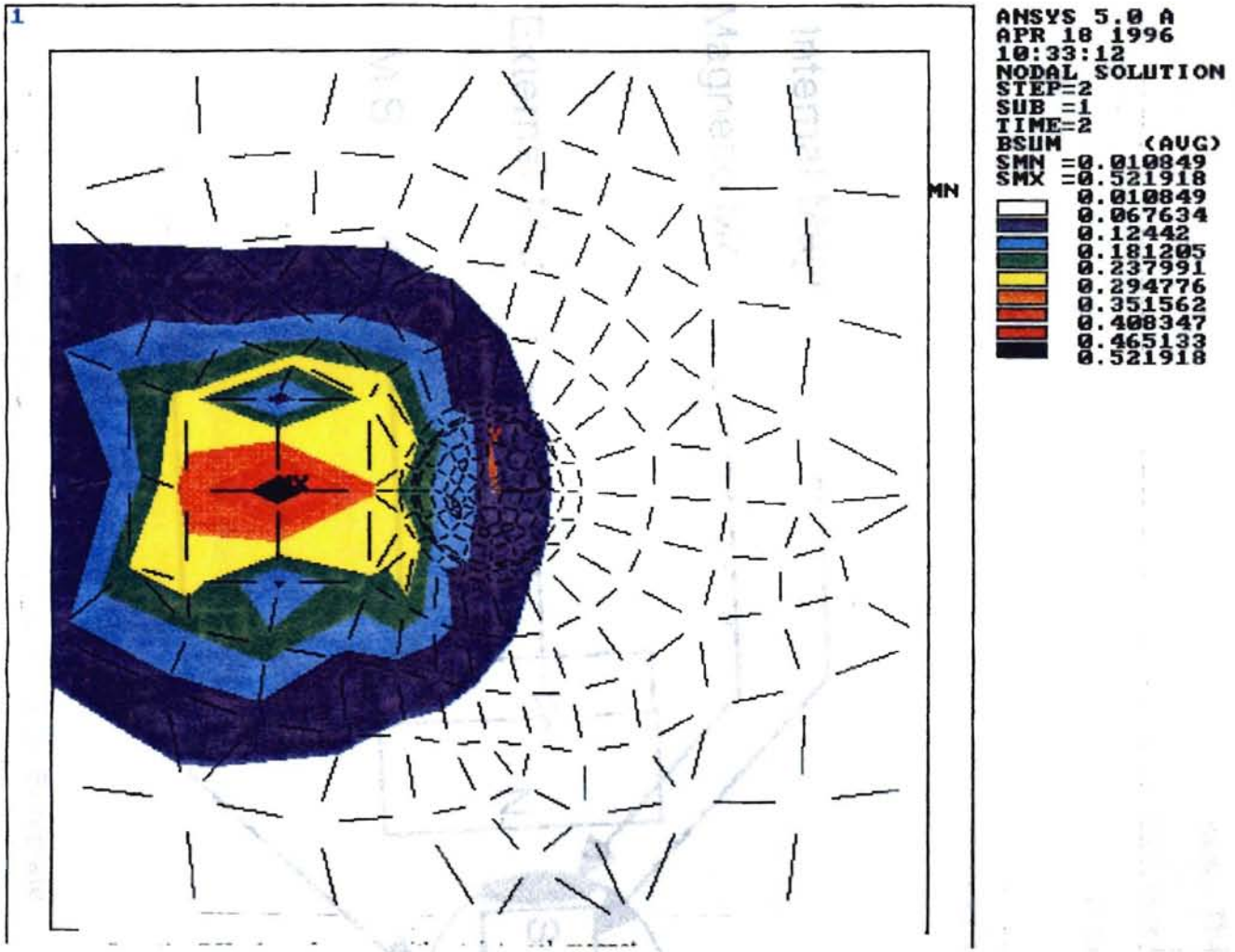

Figure 3.5 BH Plot of Setup without Internal Magnet

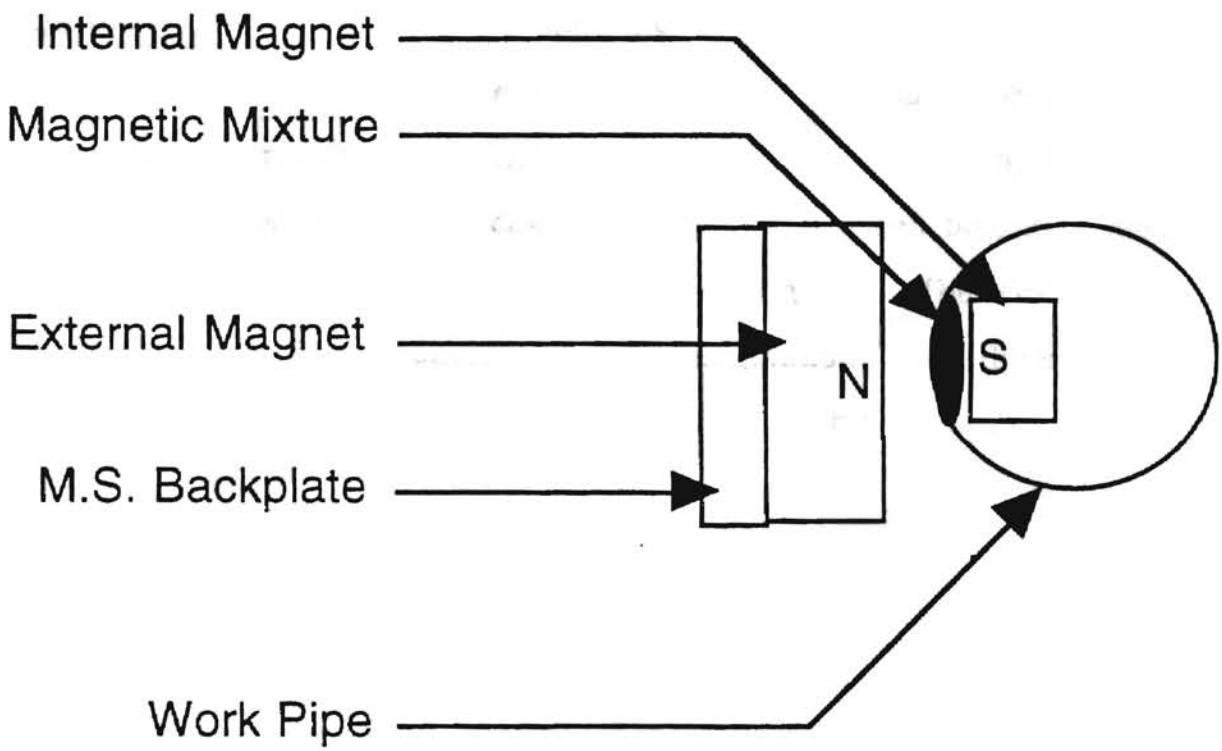

Figure 3.6 Geometric Model of Setup with Backplate

A method that was employed to direct the field more towards the polishing zone was the use a mild steel back plate on the external magnet (Fig. 3.6). The thickness of the plate was chosen to be 5 mm. The results of magnetic flux density in the polishing zone show a marked increase due to the presence of the back plate (Fig. 3.7). In consideration of the fact that adding back plates to the external magnet helps in better control of the field, two more plates were added on the top and bottom surface of the external magnet (Fig. 3.8). It was hypothesized that this would further help in directing the field in towards the polishing zone. But the actual effect of those two plates was to distort the field orientation due to the back plate. The field produced is symmetrically aligned (Fig. 3.9). As a further investigation in the use of mild steel plates, the effect of individual top and bottom plates in conjunction with the back plate was conducted (Fig. 3.10). The actual effect of these plates was only to distort the field configuration due to the back plate. The magnetic flux density in practice decreases with the use of these extra plates (Fig. 3.11).

The use of two magnets external to the pipe separated by magnetically permeable or nonpermeable materials (mild steel and aluminum) was analyzed to observe the effect on the magnetic flux density. The orientations of the external magnets was also varied such as in Figs. 3.12-3.15. It was observed that the case where the opposite/similar poles of the external magnets are in close proximity and they are separated by a mild steel plate, the field converges at the intersection of the two mild steel plates (Figs. 3.16-3.17).

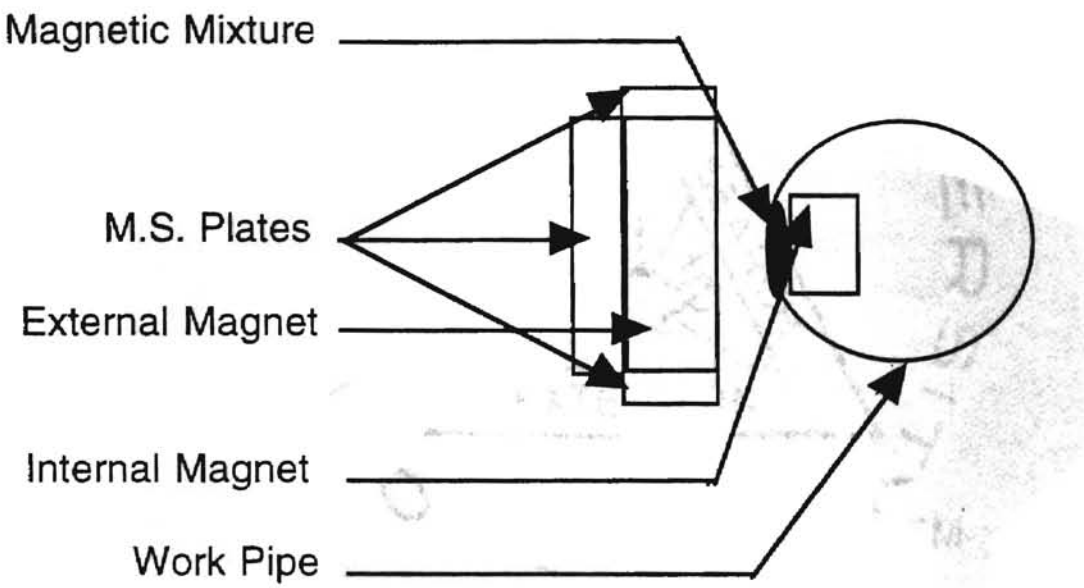

Figure 3.7 Geometric Model of Setup with Top and Bottom Plates

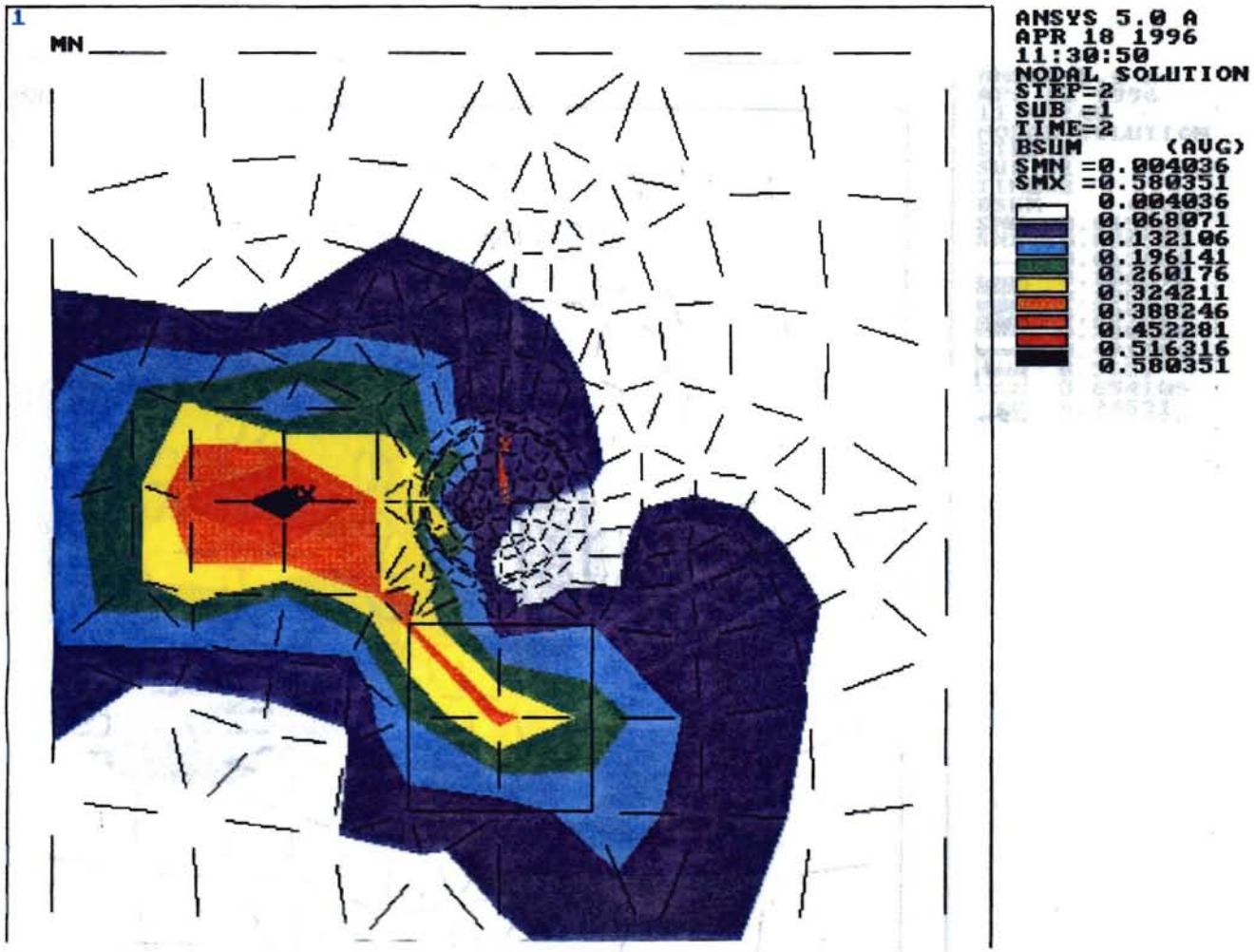

Figure 3.8 BH Plot of Setup with External Magnets 90 deg apart

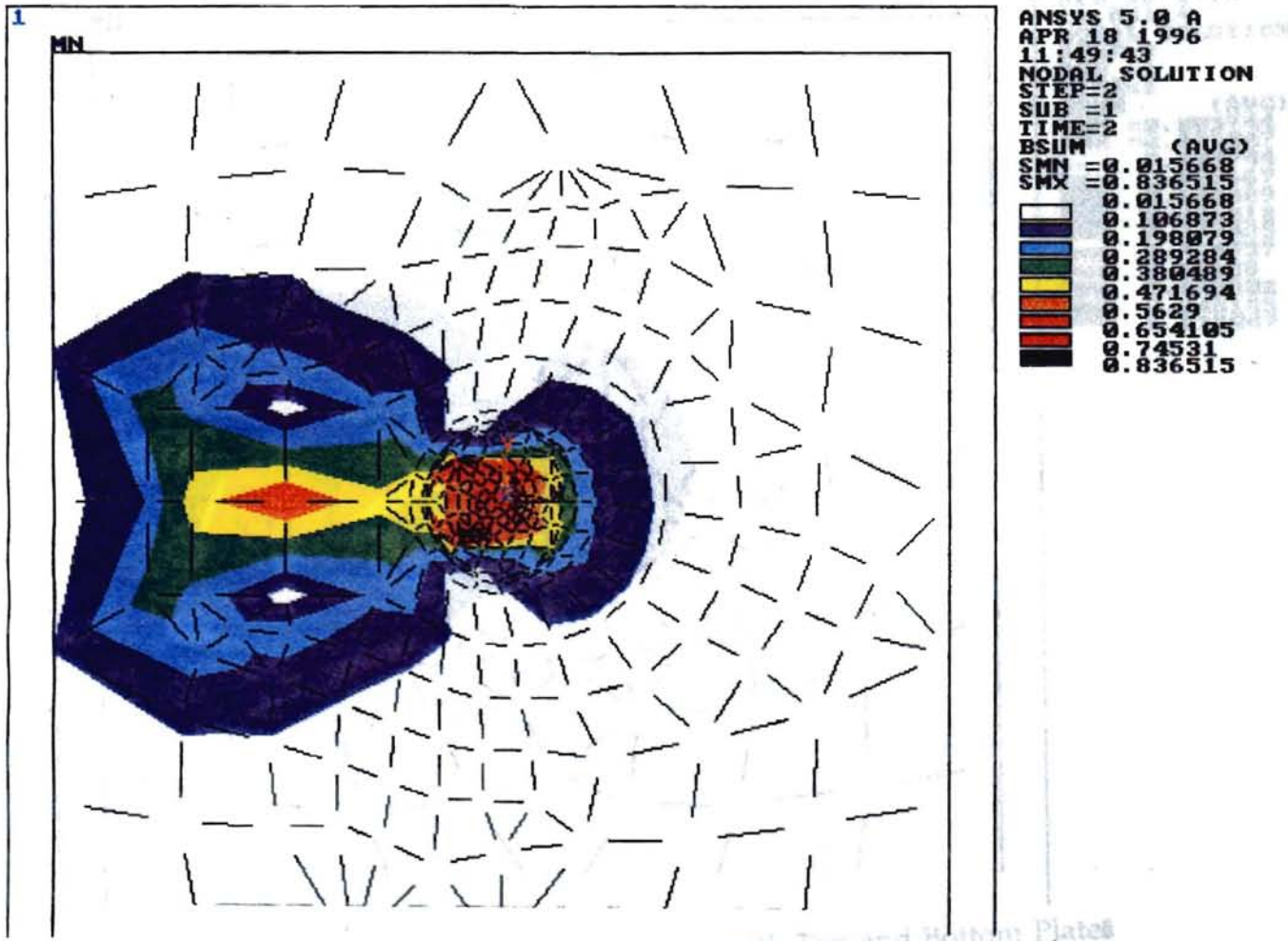

Figure 3.9 BH Plot of Setup with Backplate

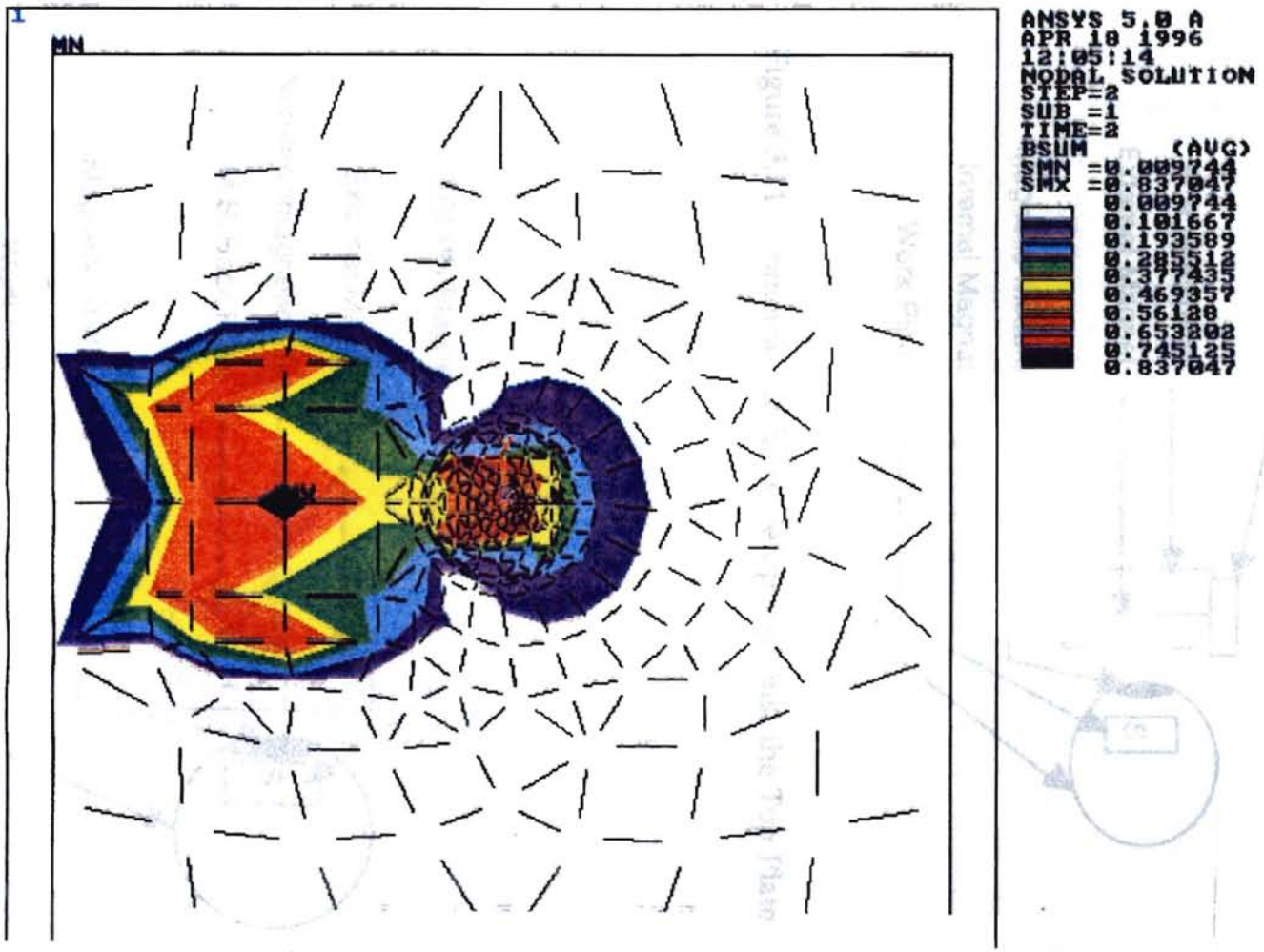

Figure 3.10 BH Plot of Setup with Top and Bottom Plates

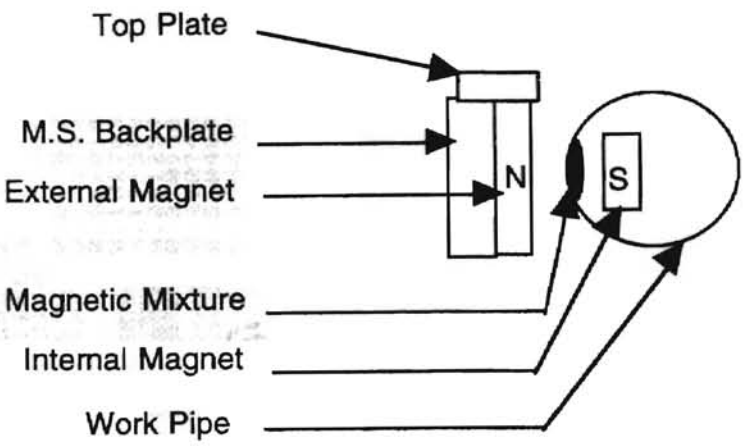

Figure 3.11 Geometric Model of Setup with just the Top Plate

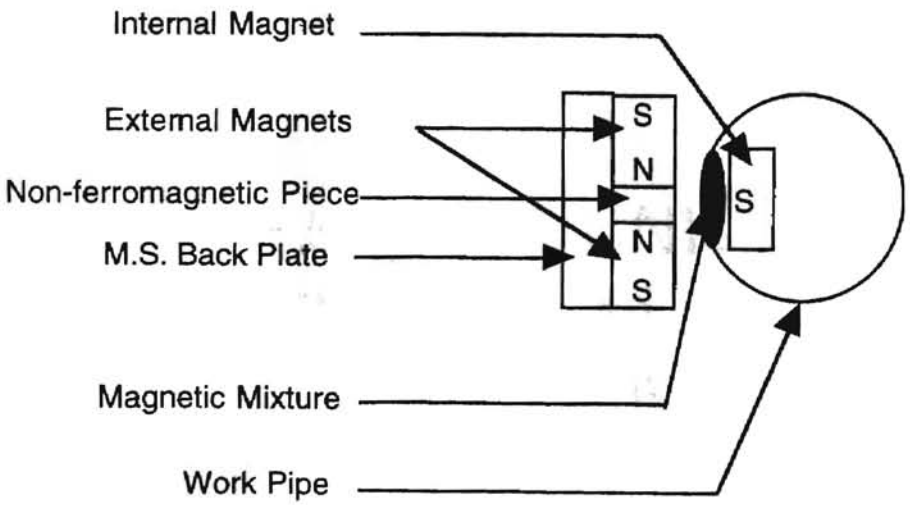

Figure 3.12 Geometric Model of Setup with 2 External Magnets (same poles facing) seperated by Non-Ferrous Piece

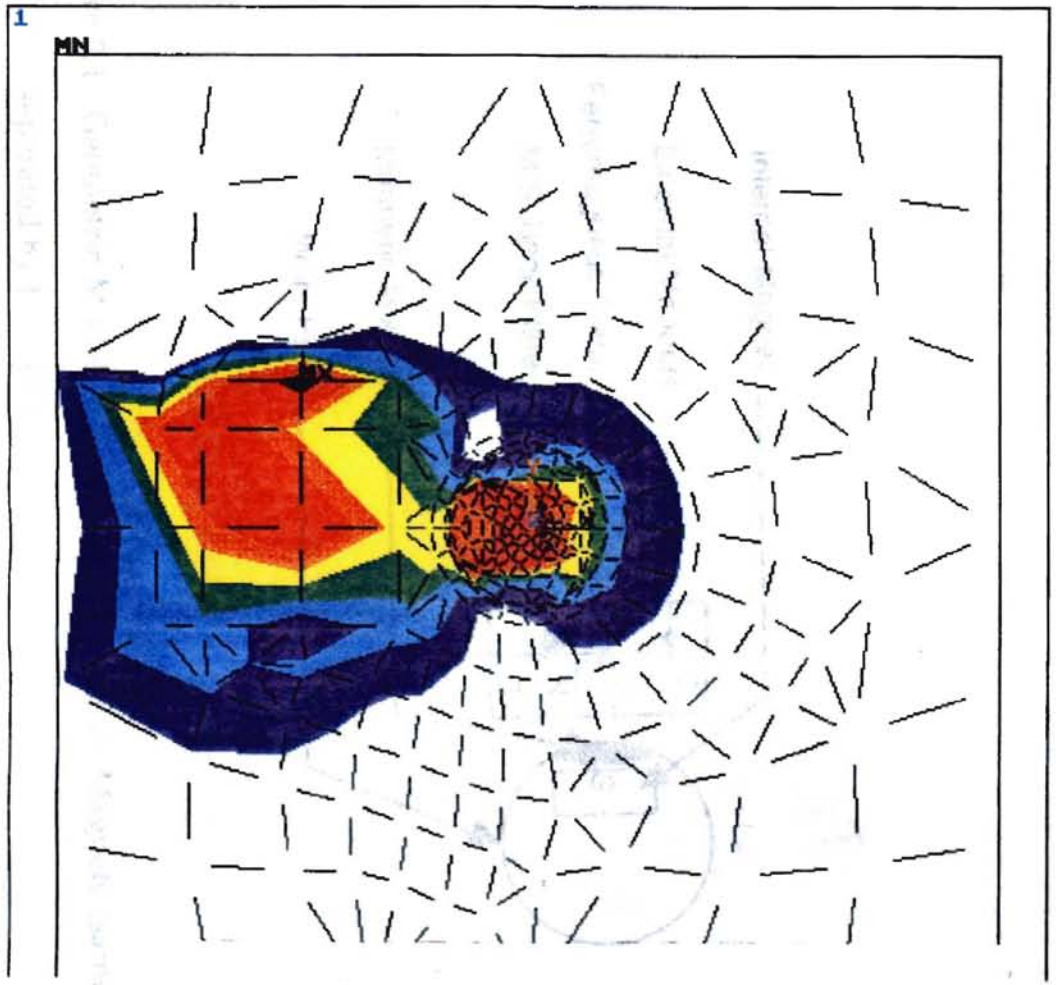

Figure 3.13 BH Plot of Setup with just the Top Plate

This is not desired as it pulls the field further from the polishing zone. In the case of being separated by a nonmagnetic material, the field is very low and almost nonexistent at the polishing zone (Figs. 3.18-3.19).

The uniformity of the field was the objective in the analysis where a curved external magnet was employed (Fig. 3.20). It was observed that the flux density did not improve in the polishing region, nor did it aid in improving the uniformity of the field (Fig. 3.21).

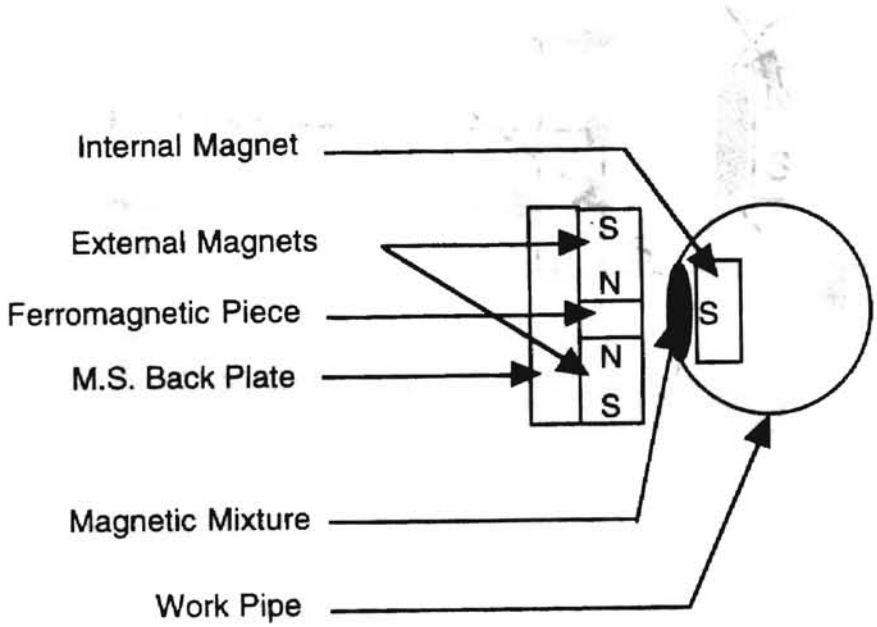

Figure 3.14 Geometric Model of Setup with 2 External Magnets (same poles facing) seperated by Ferrous Piece

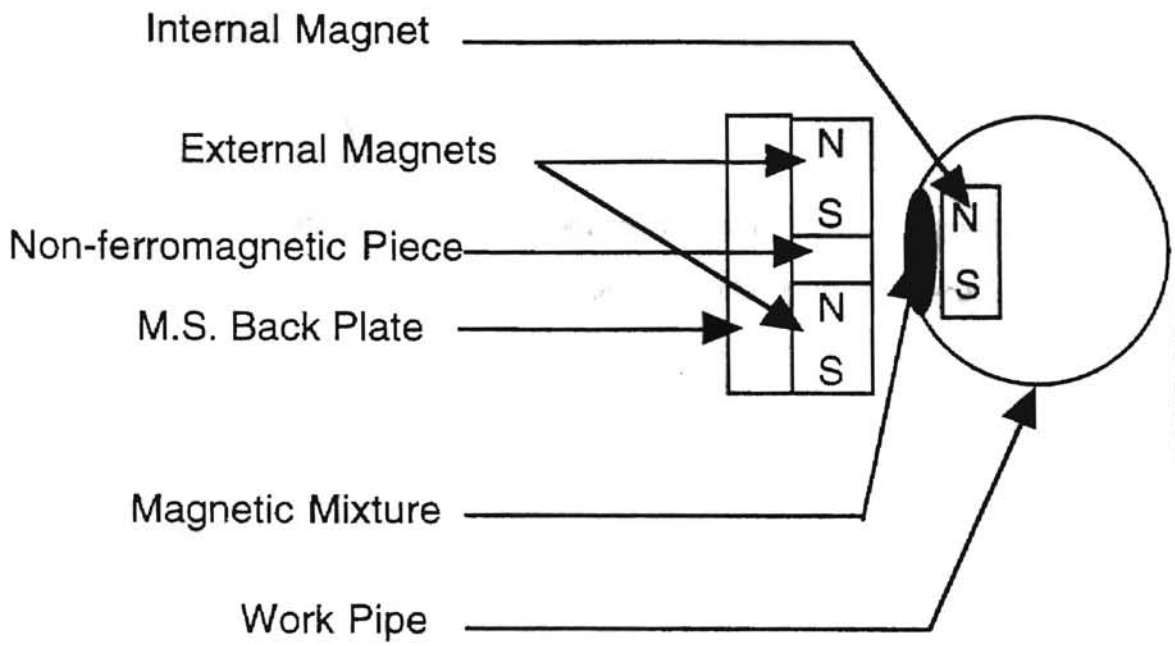

Figure 3.15 Geometric Model of Setup with 2 External Magnets (opposite poles facing) seperated by Non-Ferrous Piece

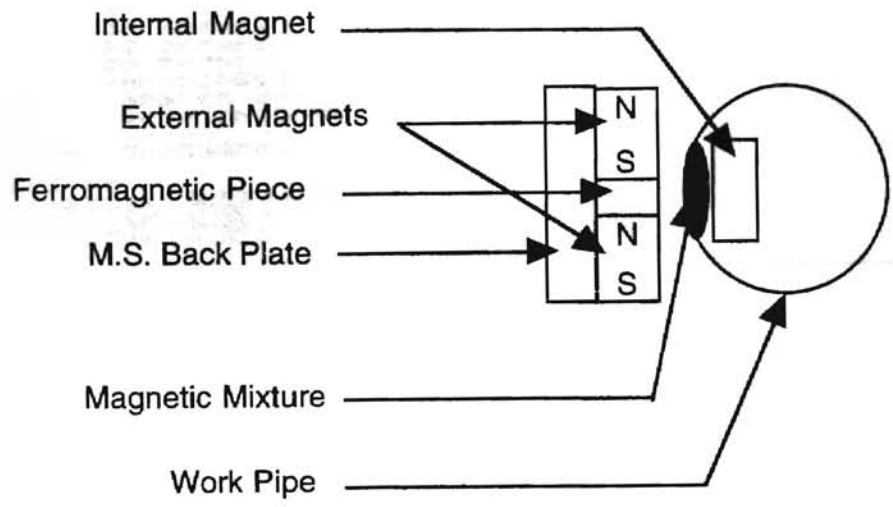

Figure 3.16 Geometric Model of Setup with 2 External Magnets (opposite poles facing) seperated by Ferrous Piece

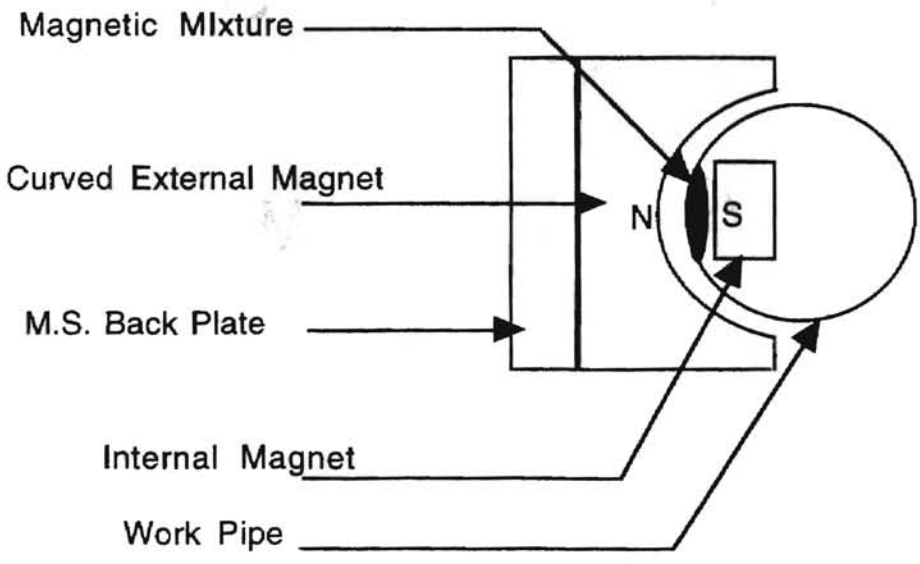

Figure 3.17 Geometric Model of Setup with Curved External Magnet

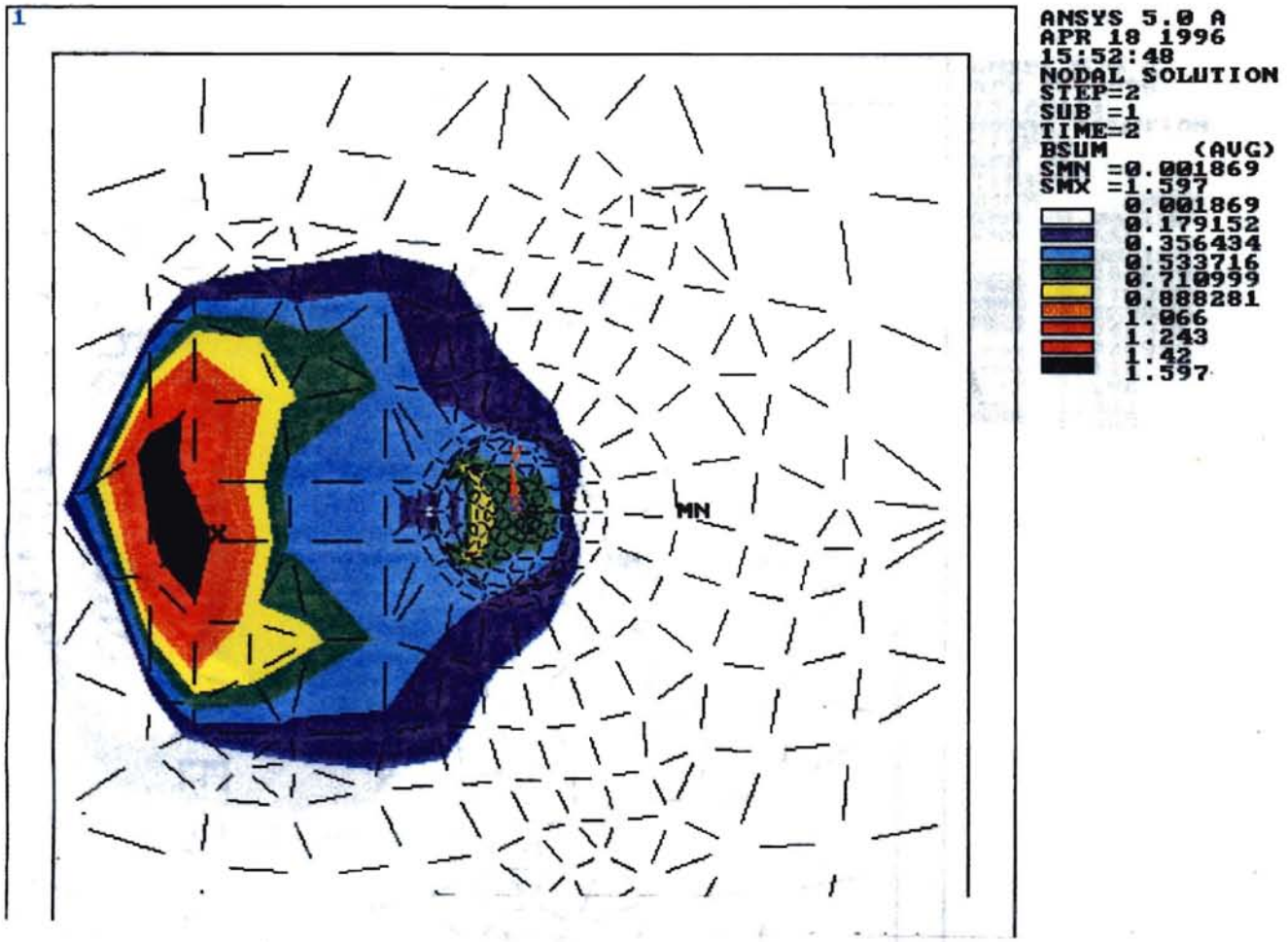

Figure 3.18 BH Plot of Setup with 2 External Magnets (same poles facing) seperated by Non-Ferrous Piece

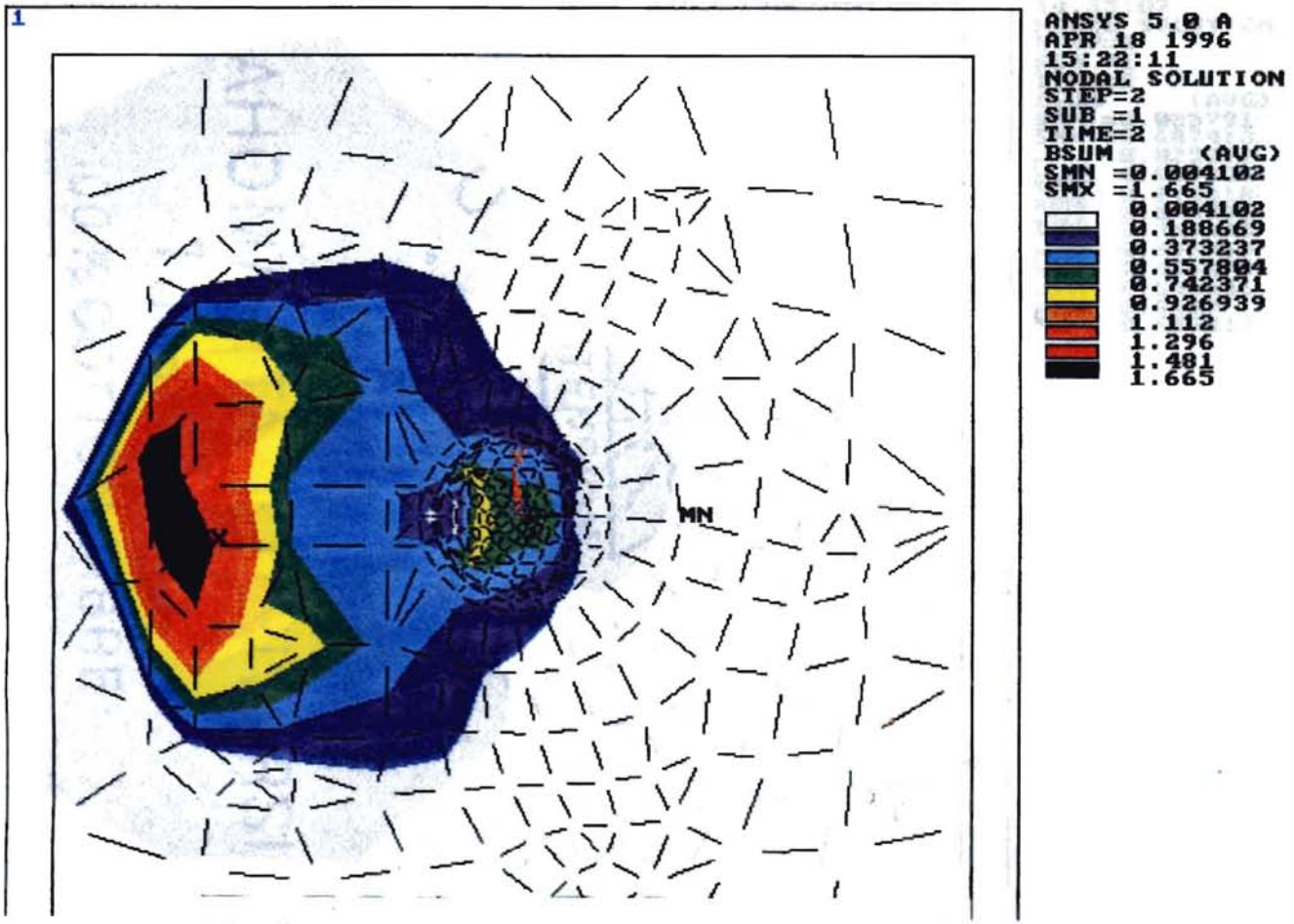

Figure 3.19 BH Plot of Setup with 2 External Magnets (same poles facing) seperated by Ferrous Piece

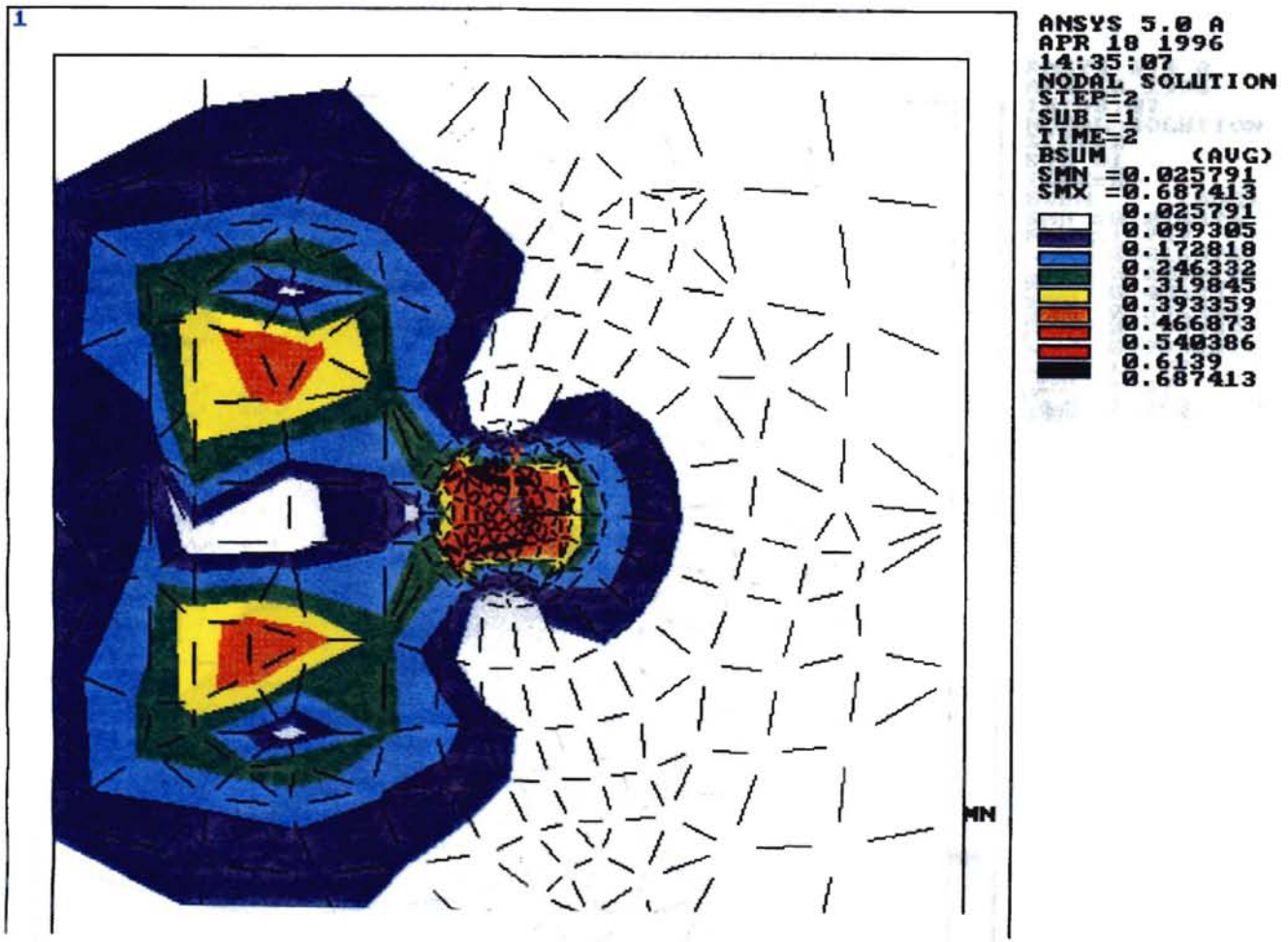

Figure 3.20 BH Plot of Setup with 2 External Magnets (opposite poles facing) seperated by Non-Ferrous Piece

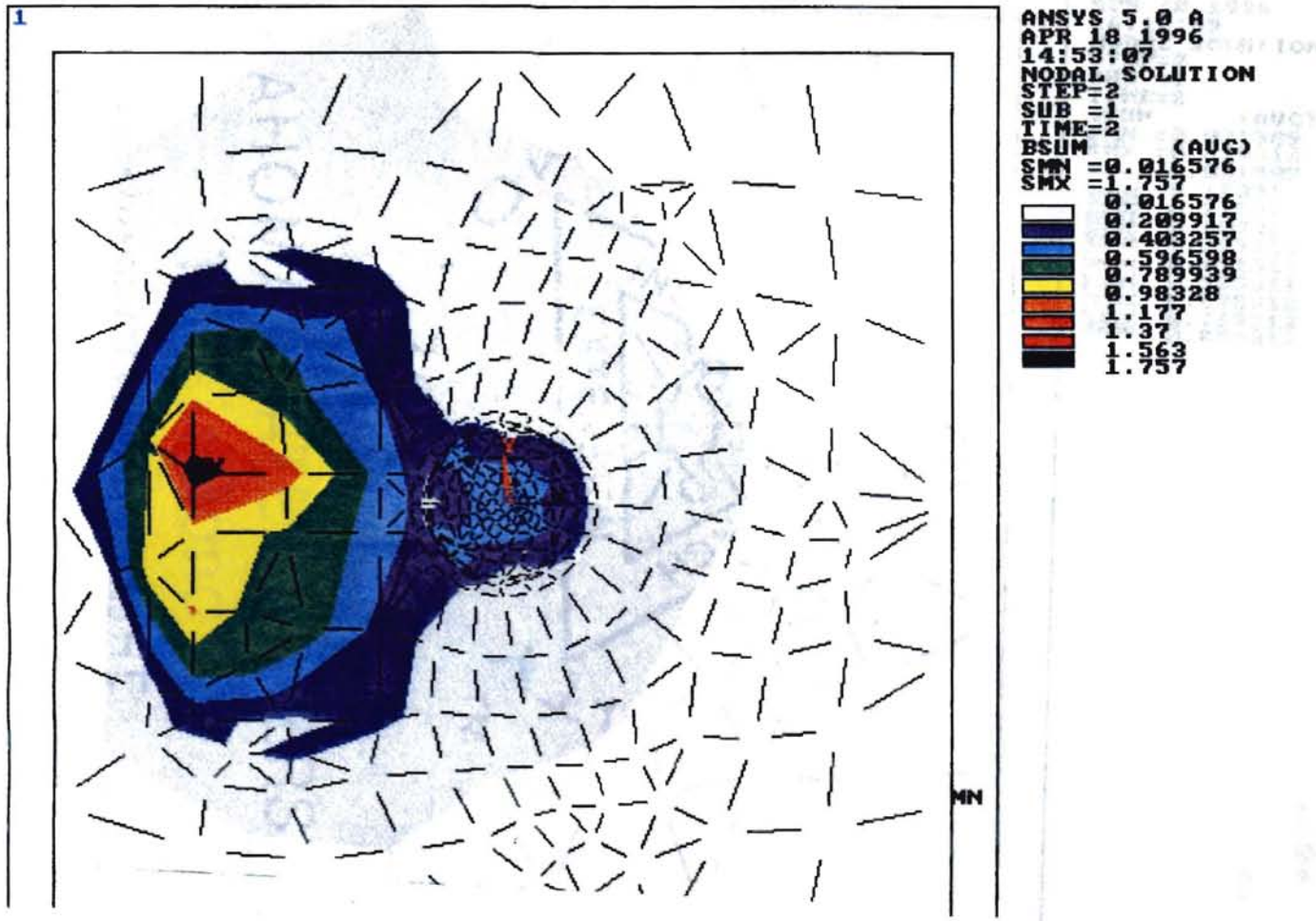

Figure 3.21 BH Plot of Setup with 2 External Magnets (opposite poles facing) seperated by Ferrous Piece

Figure 3.22 BH Plot of Setup with Curved External Magnet

3.2 Simulation of Forces

Another aspect to be considered was the variation of forces as a result of the air gap variation and amplitude of reciprocation. Assuming the magnetic circuit to be composed of the external and internal magnet, the energy product was defined as:

1/2 BH per unit volume

where B= Magnetic field intensity

H= Pole strength

But $B= f/A_g$

where f= Magnetic flux

A_g= Normal area across air gap

and $H= B/m_0$

where m_0= Relative permeability of free space

Therefore it implies that energy product E can be expressed as;

$$E= 1/2(f/A_g \sin q/A_g \sin q m_0)$$

where q= angle due to lead of external magnet

The equivalent reluctance of the circuit can be expressed as composed of the reluctances of the internal, external magnets and air gap.

$$R_{eq}= l_1/m_1A_1 + l_g/A_g m_0 \sin q + l_2/m_2A_2$$

where $l_{1,2,g}$= Length of magnets and gap

$A_{1,2,g}$= Cross-sectional areas of magnets and gap

$m_{1,2,0}$= relative permeabilities of magnetic materials and air

Considering F as the magnetomotive force, it is known that

$$f= F/R_{eq}$$

The forces in any direction would be the derivative of this energy, and hence

$$dE/dy=F_y= -F^2/R_{eq}{}^2A_g{}^2m_0y[(x^2+y^2)^{1/2}/R_{eq}+x^2/y^2]$$

Similarly it is observed that the force in the X direction would be

$$Fx= -F^2x(x^2+y^2)^{1/2}/R_{eq}{}^3A_g{}^3y^2m_0{}^2 + F^2x/R_{eq}{}^2m_0y$$

The dimensions and magnetic pole strengths were input as described.

$l_1= 0.0127$ m

$l_2= 0.00635$ m

$A_1= 0.000161\ m^2$

$A_2= 0.00004\ m^2$

$m_1= m_2= 4p \times 10^{-3}$

$m_0= 4p \times 10^{-7}$

F= 2.6 Oe

The normal force is observed to decrease as the air gap is increased. The drag force in the X direction increases at first but after a certain value of distance slid it decreases (Fig. 3.22). The point where the F_x curve starts dropping changes as the air gap is varied. The actual force of dragging the internal magnet over the surface of the workpiece is not F_x, but the resultant force in X direction.

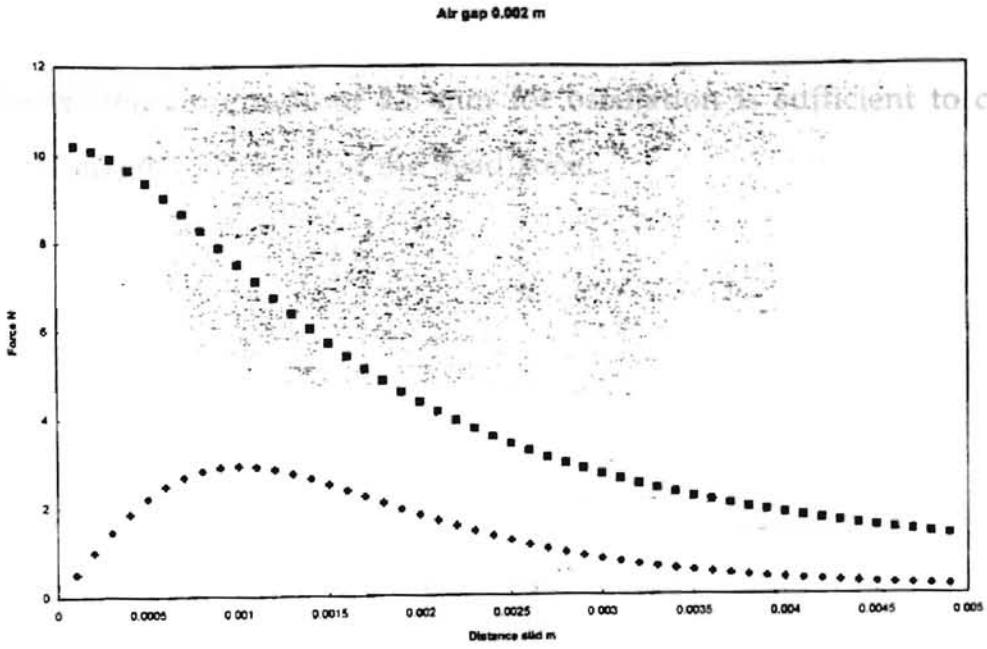

Figure 3.23 Force Variation with Distance Slid

That is due to the friction force which acts in the opposite direction to the F_x force. It can be mathematically expressed as;

$$F = F_x - mF_y$$

where m= the coefficient of friction

If the value is negative, then efficient polishing cannot occur. There is no movement of the internal magnet in the X direction. For any practical coefficient of friction and pole strength of magnets, there exists a dead zone wherein the drag force is negative. If the amplitude of vibration is less than this zone, there is no reciprocation of the internal magnet. This force F is observed to increase (Fig. 3.23) as the coefficient of friction is lower. Also the force F increases for a given m, but then decreases as the distance slid is increased further. This imposes a limit on the maximum amplitude which the internal magnet can effectively have for a specified magnetic field strength and assumed coefficient of friction. For the operating magnetic field

intensity, the amplitude of 2.5 mm for oscillation is sufficient to cause the internal magnet to be out of the dead zone.

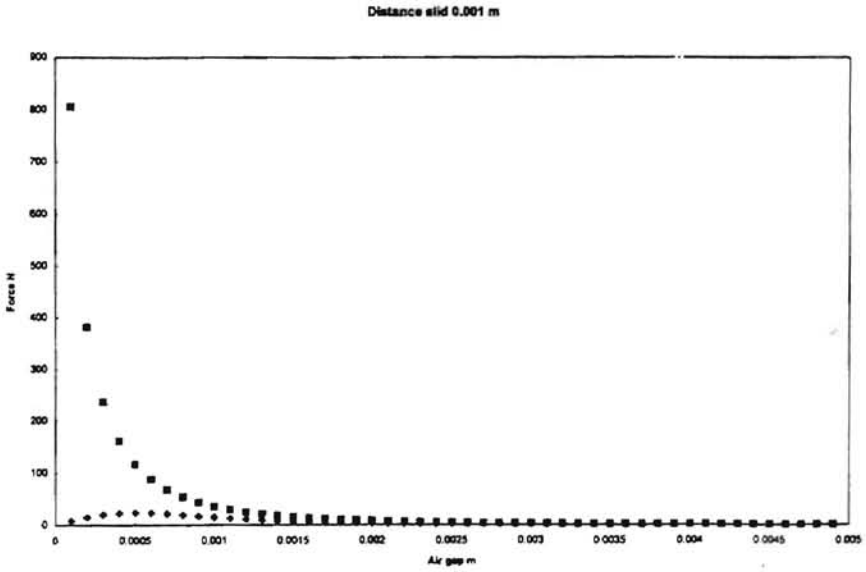

Figure 3.24 Force Variation with Air Gap

This can be explained by the fact that at very low distances of sliding, the F_y is large and thus the second term is larger than F_x. But as the sliding distance is increased further, the F_x increases and F_y decreases drastically as evinced by the graphs. This inverse relation between F_x and F_y does not last for very long, and they both decrease after a certain sliding distance. This is reflected in the decrease of the resultant force F after a certain sliding distance.

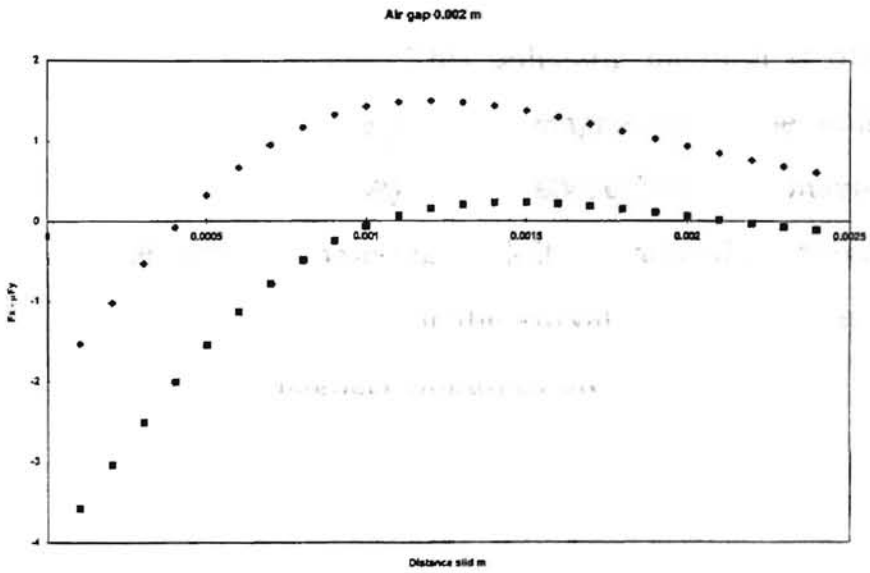

Figure 3.25 F-F_x with Different μ

CHAPTER 4

EQUIPMENT SETUP AND METHODOLOGY OF EXPERIMENTS

The setup of polishing employed in this instance consists of a permanent magnet external to the pipe and a permanent magnet internal to the pipe. The polishing medium is either a coated abrasive paper or a mixture of iron, abrasive, and solid lubricant. This polishing medium is placed in such a manner that it is between the internal magnet and pipe wall, the pressure being supplied by the magnetic force between the two magnets. Since the internal magnet itself is a hard material, it is wrapped in teflon and the edges of the magnet are rounded to fit the curvature of the pipe. The nominal dimensions of the two magnets employed are:

External 1x1x1/2 inches

Internal 1x0.3x.1 inches

The magnets are so aligned that the 1x1 face of the external faces the 1x0.3 face of the internal.

The pipe is held by a collet and rotated, with flexibility to change the rpm, the maximum rpm being 1500. In order to avoid the formation of circumferential grooves during polishing, a reciprocation is provided to the external magnet. This has been achieved by use of a reciprocating air cylinder which drives a linear slide on which the external magnet rests. The frequency of reciprocation can be varied by adjusting the air pressure to the cylinder. A linear relationship exists between the air pressure and frequency of reiprocation. Amplitude variations are possible by manipulating the

weight at the end of the cylinder piston. The external magnet is attached to the slide by means of magnetic attraction to a MS spacer plate on the face of the slide. The MS plate has been used with the purpose of increasing the magnetic field in the polishing region (as evinced by a finite element study of magnetic field). Also, any changes in the air gap between the pipe and external magnet can be achieved by changing the thickness of this plate. Figure 4.1 provides a detailed view of the setup.

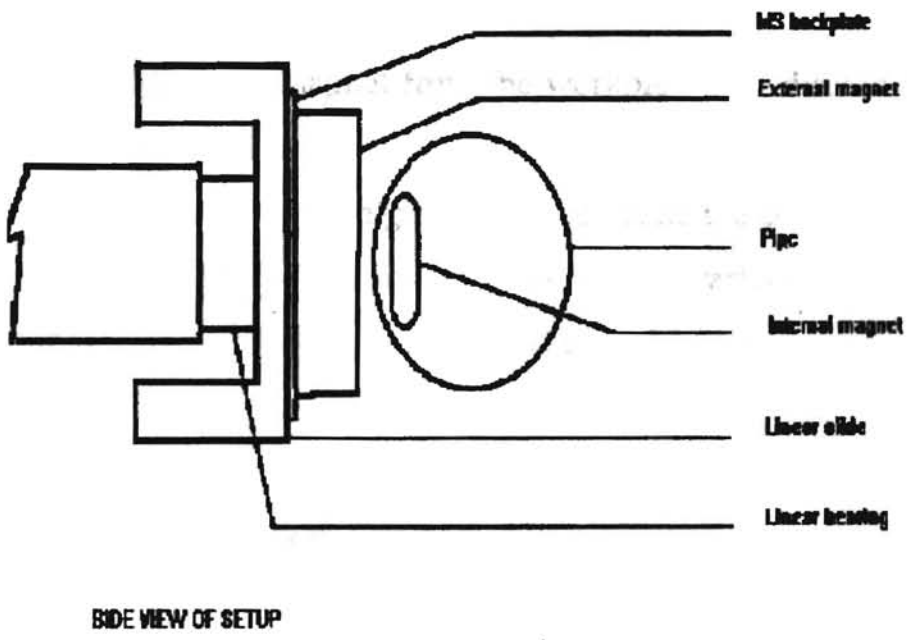

Figure 4.1 Experimental Setup

The steps involved in the polishing process can be described as follows

1] Prepare the mixture of abrasives, iron, and zinc stearate in the proper proportion.

2] Weigh the workpiece after thorough cleaning. Take 3 readings and note the average. Place the workpiece in the collet.

3] Cover the internal magnet completely with teflon tape. This is to prevent the edges of the internal magnet from scratching the workpiece surface.

4] Cover the surface of internal magnet with the abrasive mixture or coated paper (stuck with super glue) and place it inside the workpiece.

5] Rotate the workpiece and reciprocate the external magnet assembly for the set time.

6] Remove the internal magnet from the workpiece and discard the mixture and teflon tape on it.

7] Clean the workpiece and weigh it as before. Note the change in the weight.

8] Repeat steps 2-7 for the various grit sizes of the abrasives as planned.

9] Cut the workpiece axially with a vertical blade bandsaw, and deburr the cut edges.

10] Clean the polished surface thoroughly with methanol and measure the surface finish parameters on Talysurf.

CHAPTER 5

RESULTS

In this chapter, the results from experimental work is presented to study the effect of some of the parameters on material removal rate and finish. In order to logically approach the best results on the setup, a sequence of experiments was executed. The polished length in all cases was one inch. The summary of all the experiments conducted can be visualized in the form of a table as shown below:

Table 5.1 Set of experiments conducted

Exp No.	Objective	Parameters Varied
1	Decide on means of applying abrasive	Coated paper, loose mix
2	Decide type of abrasive	SiC, Al_2O_3
3	Decide polishing time per grit	1, 2, 3, 4, and 5 mins
4	Decide cross angle	28-38 Hz 450, 825, 1200 Rpm
5	Decide size of iron particles	40, 325 mesh
6	Decide weight percentage of iron in mix	20, 40, 60, 80, and 90
7	Decide weight percentage of solid lubricant in mix	5, 9, 13, 17, and 20

A more detailed study was conducted on AS304. Brass (A272) and Aluminum (A6061) were also polished.

5.1 Results on Stainless Steel AS304

The results of the experiments conducted on stainless steel have been detailed below.

5.1.1 Method of Applying Abrasive

In the first instance, it was tested whether it was advantageous to use a loose mix or a coated paper. The results for such an experiment showed that the material removal rates were higher, but the finish obtained for the same size of abrasive was rougher in the case of coated paper (Figs. 5.1 and 5.2).

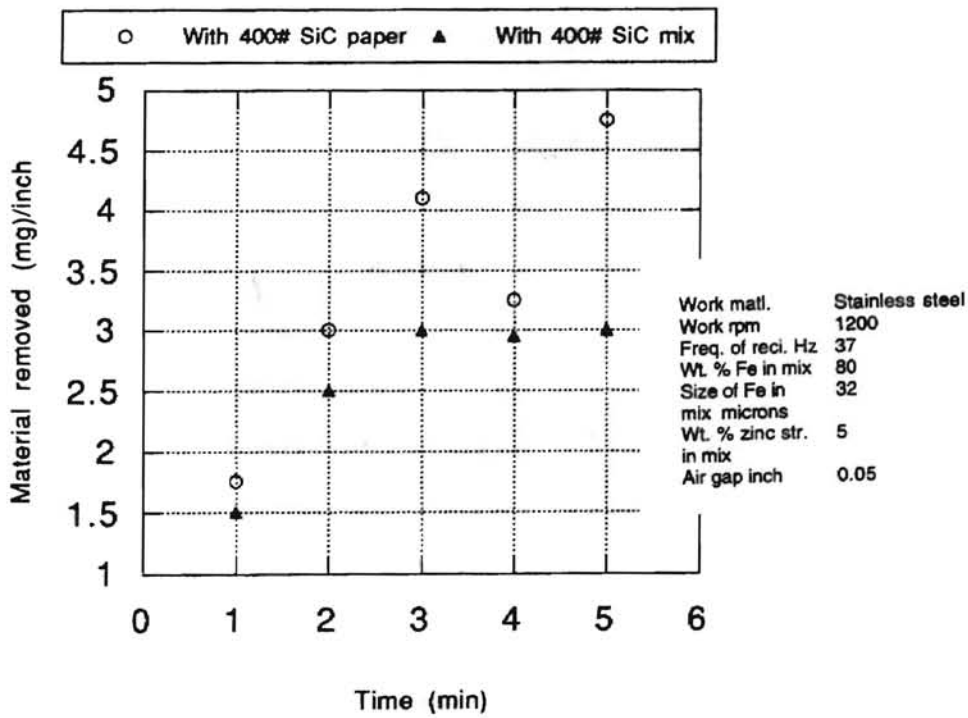

Figure 5.1 Material Removal Rates for Coated and Loose Abrasive Mixes

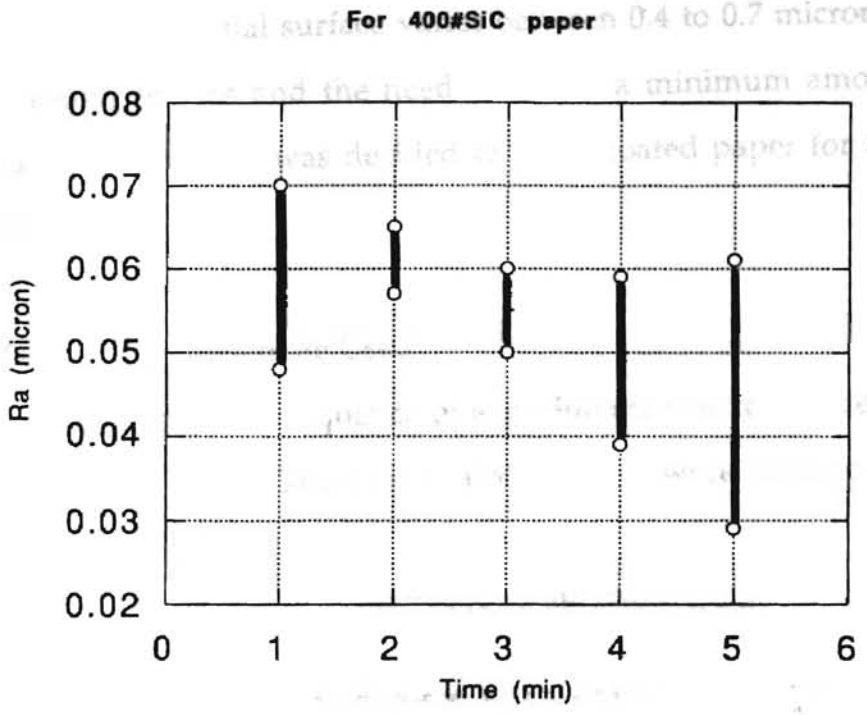

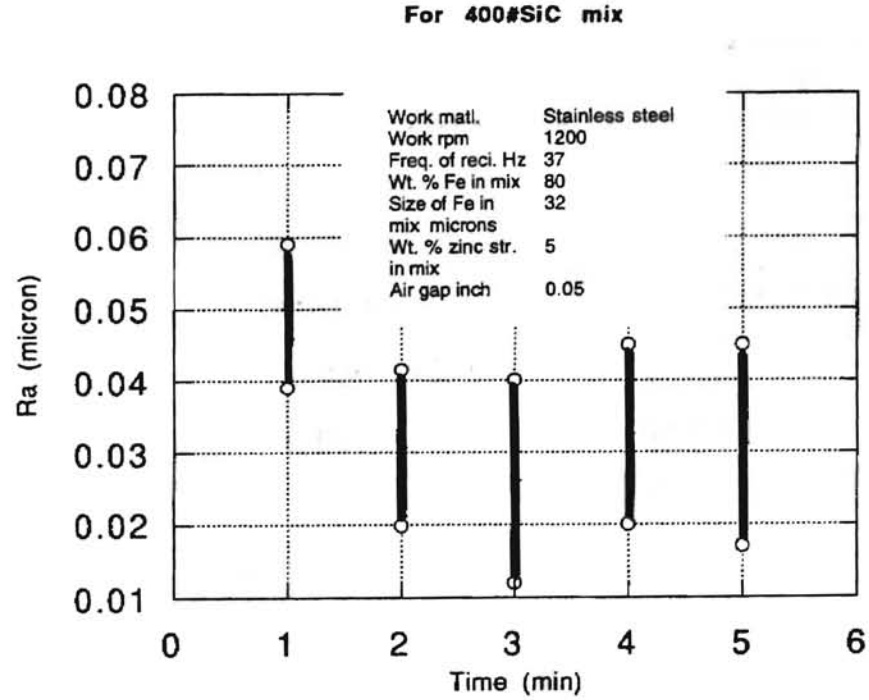

Figure 5.2 Surface Finish Results for Coated and Loose Abrasive Mixes

The finish of the initial surface varies between 0.4 to 0.7 microns Ra. In view of this rough surface and the need to spend a minimum amount of time in the roughing passes, it was decided to use a coated paper for the rough pass (grit 220).

5.1.2 Type of Abrasive to be Used

The next step in the sequence of experiments was to decide on the type of abrasive to be used. The two options which were studied were SiC and Al_2O_3.

Table 5.2 Types of abrasives used

Abrasive	Grit	Time	Mix/Paper
Al_2O_3 and SiC	220	2 min	P
	400	1 min	M
	1000	1 min	M

The initial finish for the finer grits were the corresponding coarser grits of the same type. A comparison was made of the material removal rates and finishes obtained. It is apparent that for 220 grit the material removal rates and finish obtained are not considerably different for both types of abrasive (Figs. 5.3 and 5.8). The spread of values of finish in the case of Al_2O_3 was lesser than SiC. This would indicate a much uniform surface. For the finer grits, it is observed that SiC is better than Al_2O_3 in terms of material removal rates and finish. Also a larger extent of loading was visually observed for Al_2O_3.

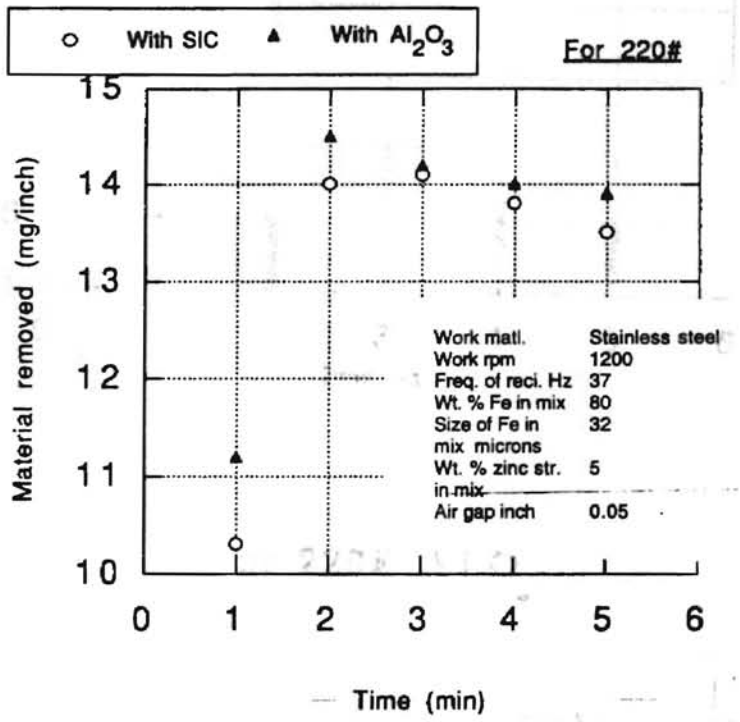

Figure 5.3 Material Removal Rate for 220 Grit Al_2O_3 and SiC

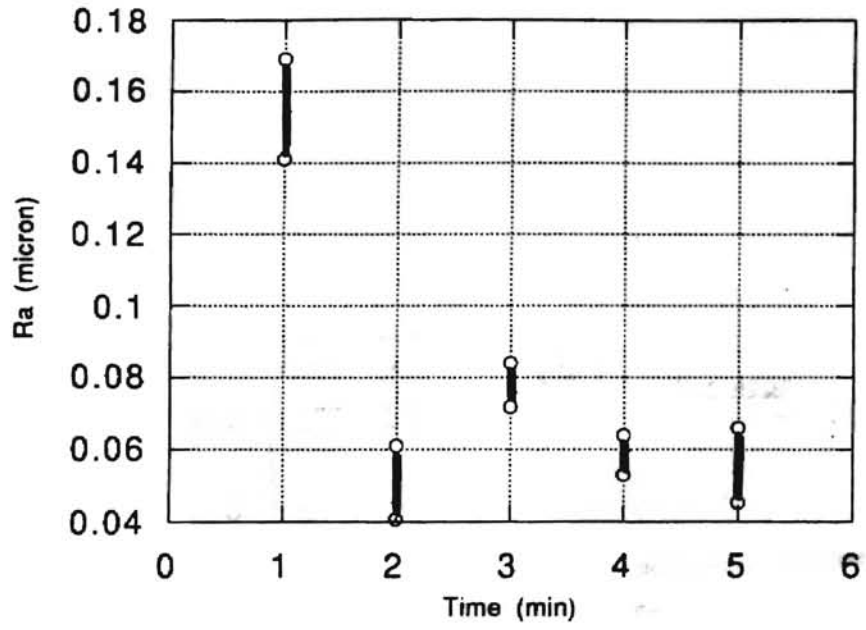

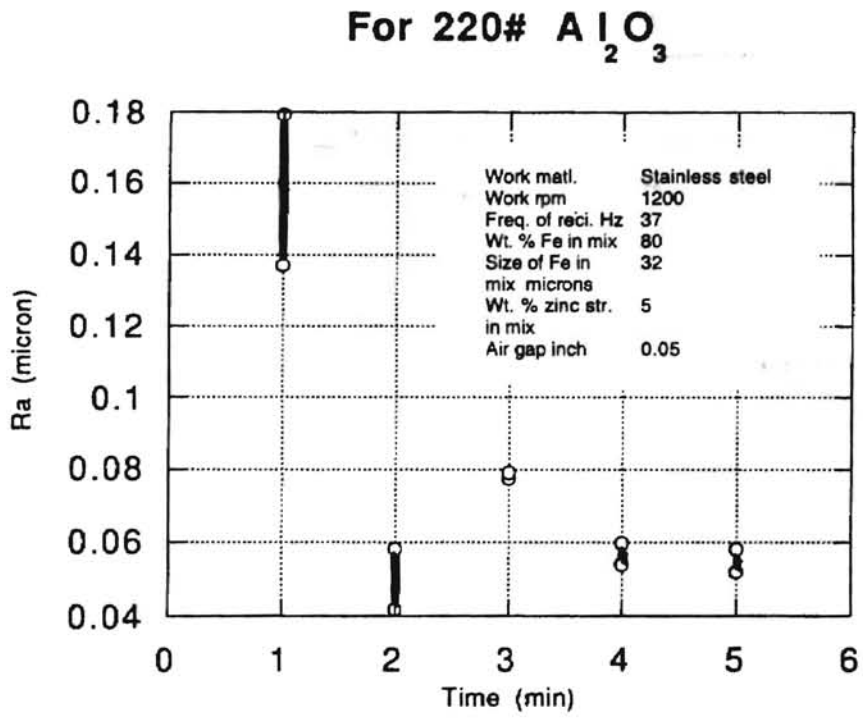

Figure 5.4 Surface Finish Obtained on Work for 220 Grit Al_2O_3 and SiC

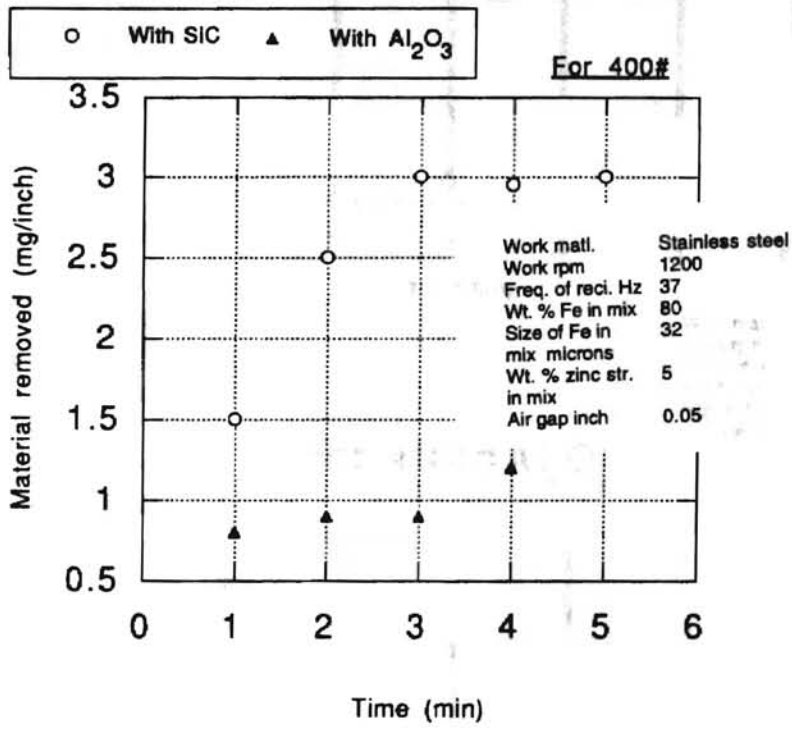

Figure 5.5 Material Removal Rate Obtained for 400 Grit Al_2O_3 and SiC

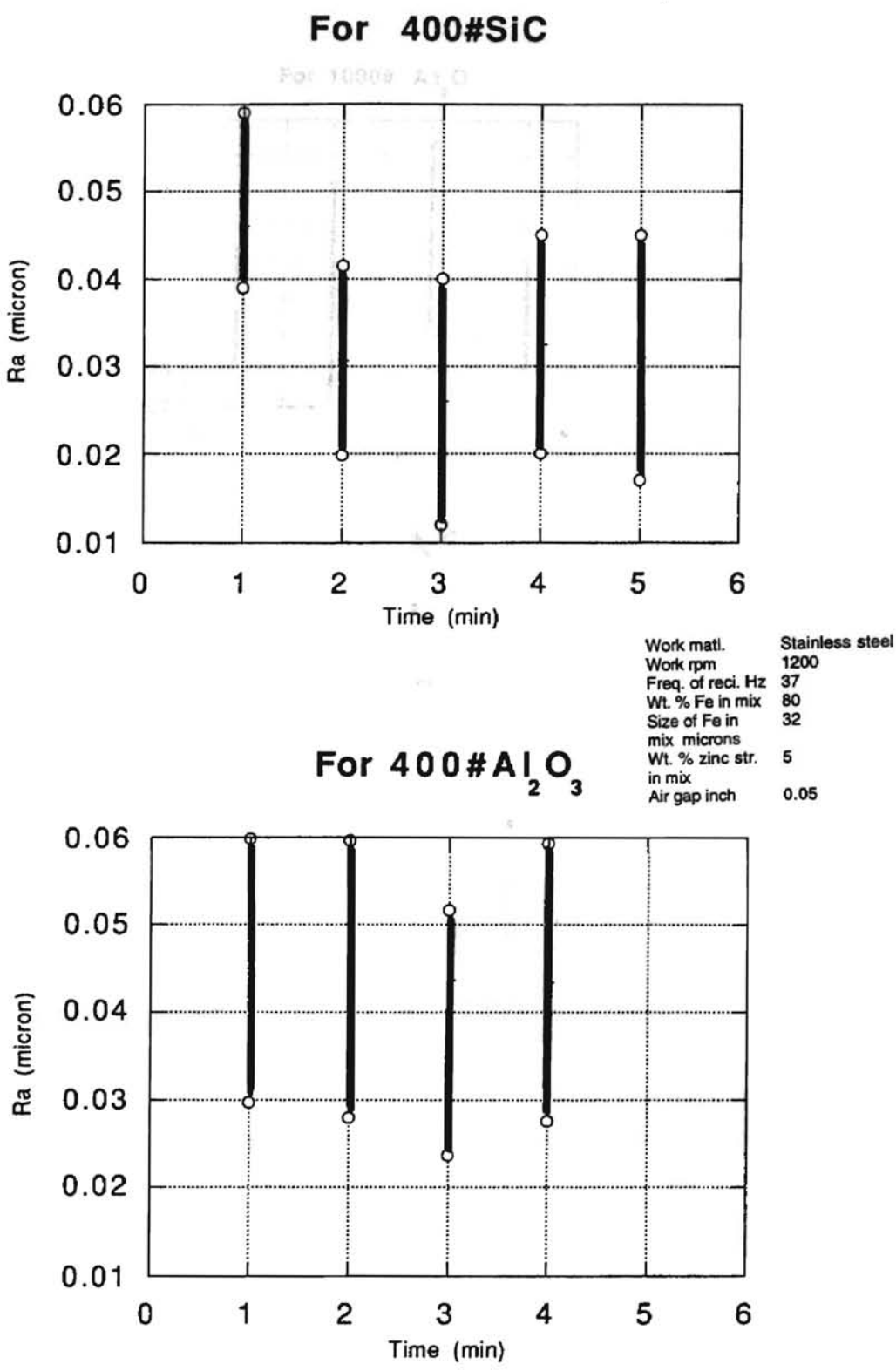

Figure 5.6 Surface Finish Obtained on Work for 400 Grit Al_2O_3 and SiC

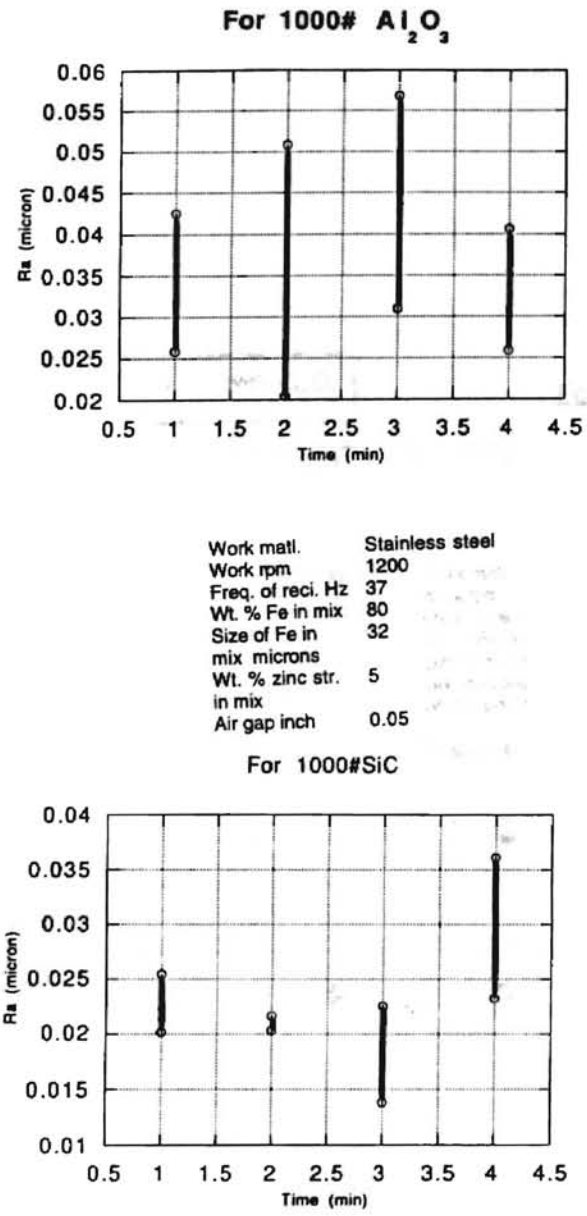

Figure 5.7 Surface Finish Obtained on Work for 1000 Grit Al_2O_3 and SiC

Hence it was decided to use SiC for the finer grits, but for the coarse grit, Al_2O_3 was prefered.

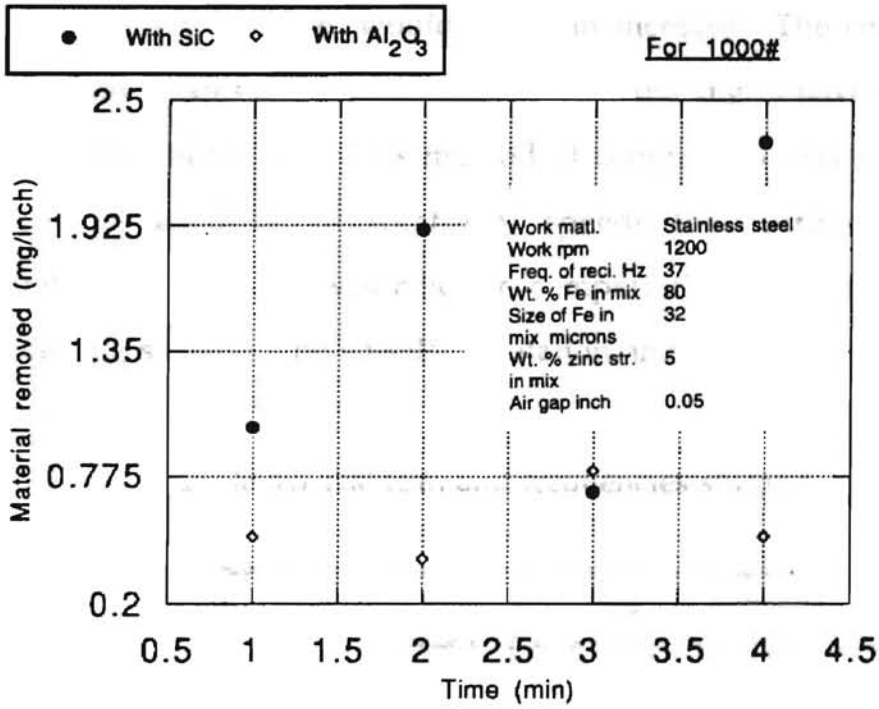

Figure 5.8 Material Removal Rate Obtained for 1000 Grit Al_2O_3 and SiC

5.1.3 Effect of Cross Angle

The rotation of the pipe and reciprocation of the external magnet induce a relative velocity to the abrasive particle. The actual motion of the particle is at an angle to the axis of the pipe. This angle has been defined as cross angle. It can be mathematically defined as $\sin^{-1}$ (rotation speed/reciprocation speed). The variation of angle with rotational speed, maintaining the same frequencies of reciprocation, would show an increase. The comparisons of material removal rates and finish for different cross angles have been made at different rotational speeds. This method of comparison was made with the rationale that at different rotational speeds the cutting speeds vary considerably. An attempt was made to compare the effect of cross angle at similar cutting speeds. The speeds of rotation and reciprocation were varied as shown below:

Table 5.3 The rpm and frequencies studied

Rpm		**450**	**825**	**1200**
Frequency (Hz)	**34**	-X-	-X-	-X-
	33.25	-X-	-X-	-X-
	37	-X-	-X-	-X-
	28.75		-X-	-X-
	28.28		-X-	-X-

The comparisons show that the results obtained are best at a rotational speed of 1200 rpm and cross angle varying between 30-40 degrees (Figs. 5.9-5.11). This was the reason for a higher number of observations in that region. The

results obtained by Fox and Komanduri (1993) in their similar studies of MFP of external surfaces for the same work material, agree in this respect.

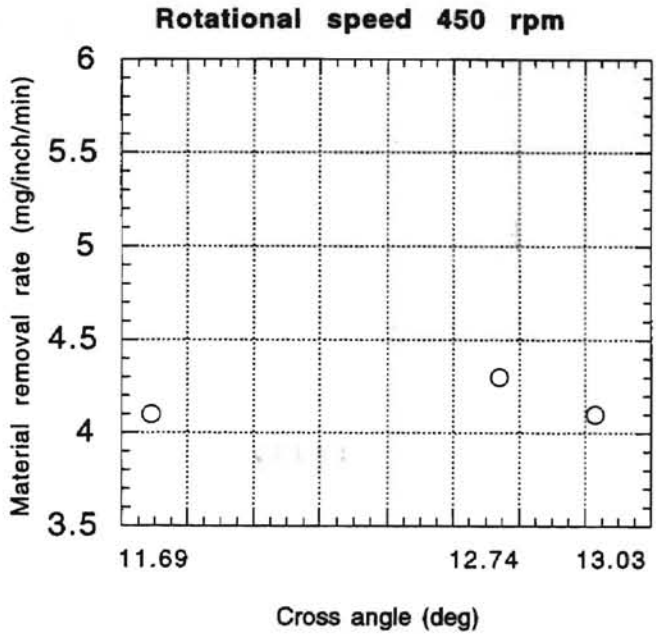

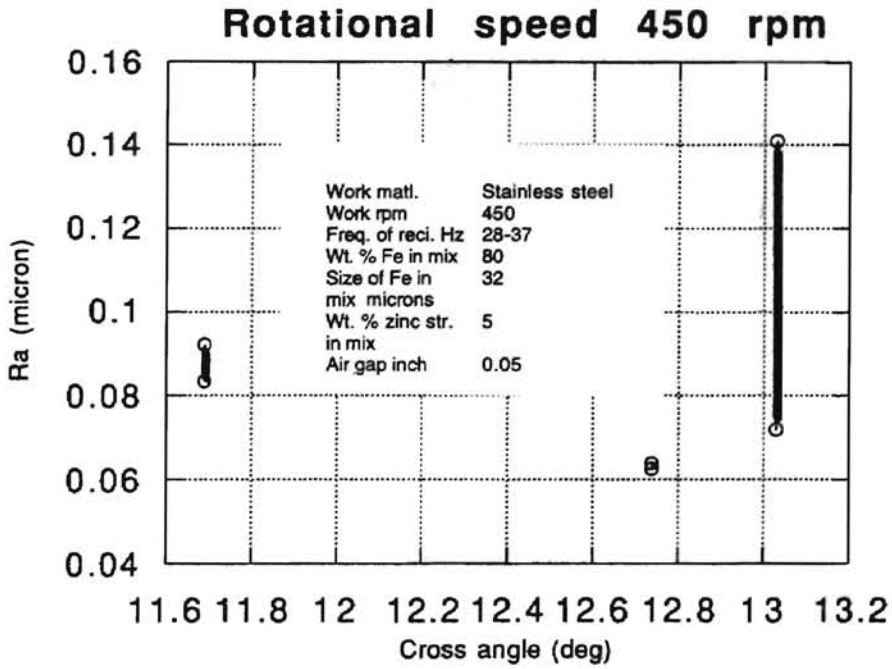

Figure 5.9 Material Removal Rate and Surface Finish Obtained for Work Speed of 425 Rpm

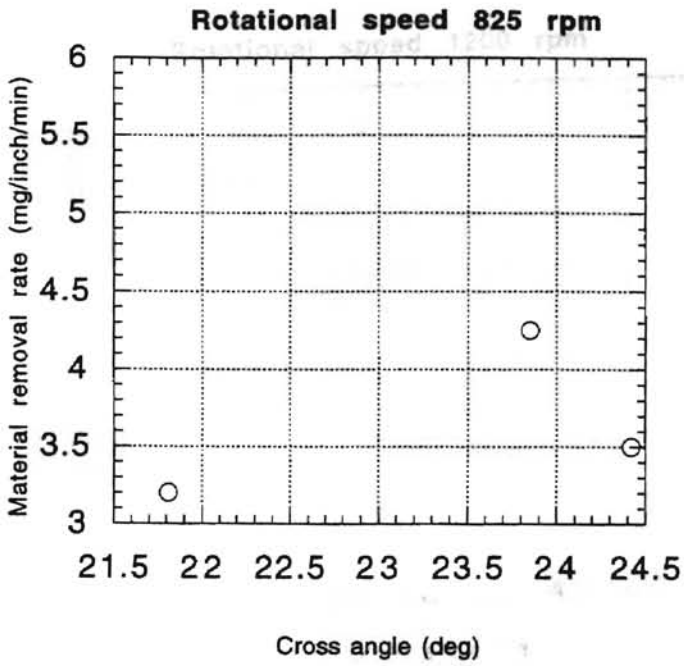

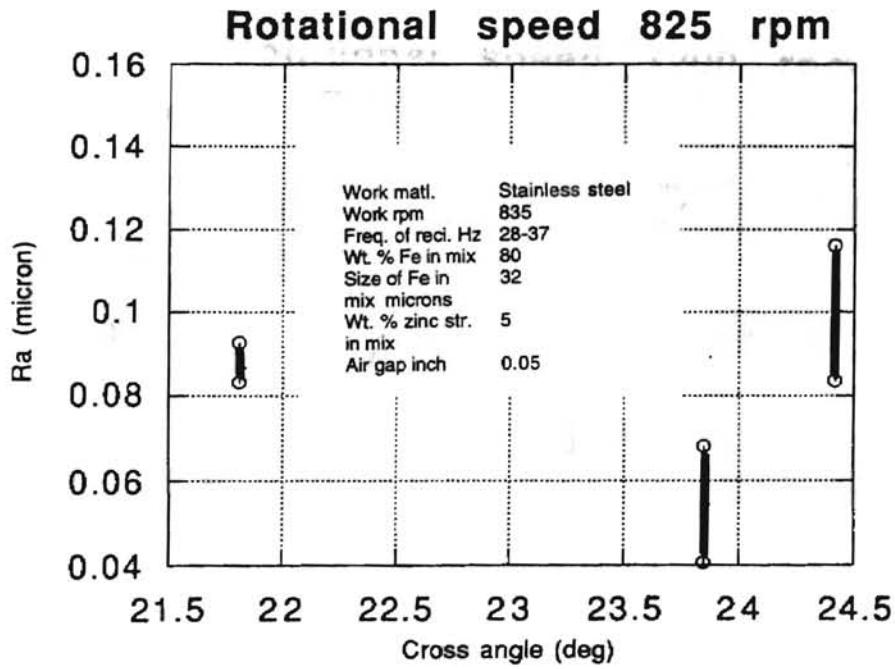

Figure 5.10 Material Removal Rate and Surface Finish Obtained for Work Speed of 850 Rpm

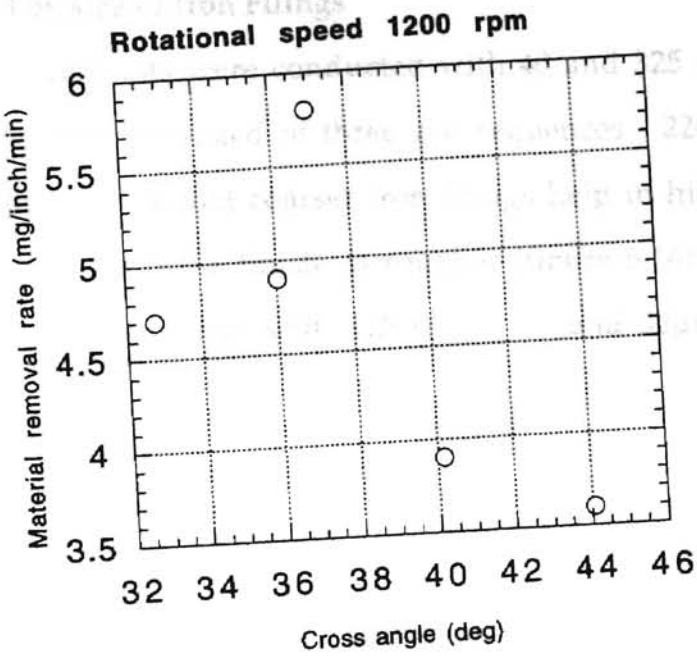

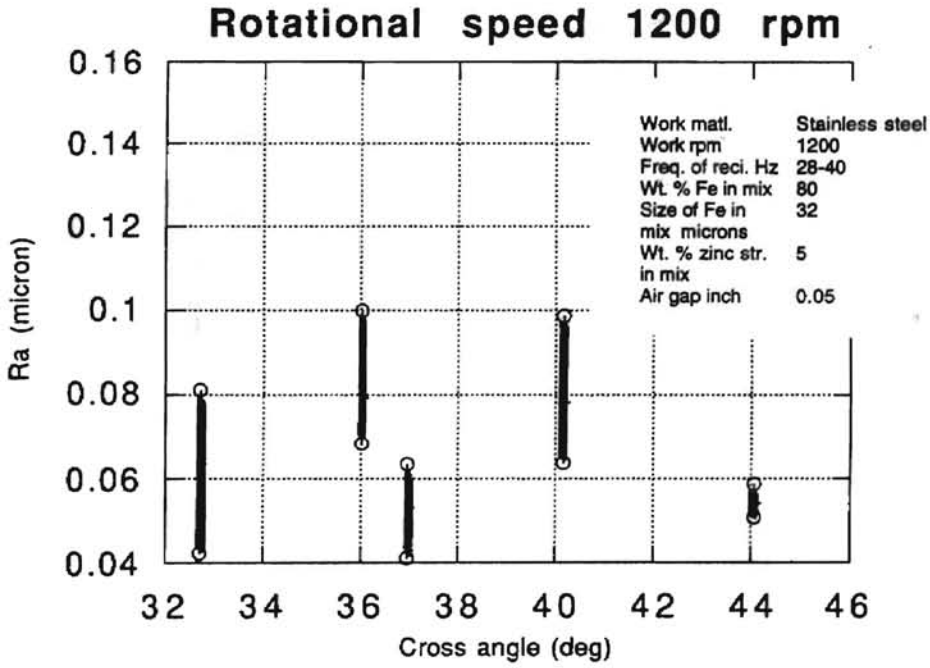

Figure 5.11 Material Removal Rate and Surface Finish Obtained for

5.1.4 Effect of Size of Iron Filings

The experiments were conducted with 40 and 325 mesh size iron filings. Each experiment consisted of three grit sequences - 220, 400, and 1000. The results clearly show that coarser iron filings help in higher material removal rates (Fig. 5.15), but the finish is rougher (figure 5.16). The surface finish is also much more uniform with 325 mesh (around 32μm) than with 40 mesh (around 600 μm).

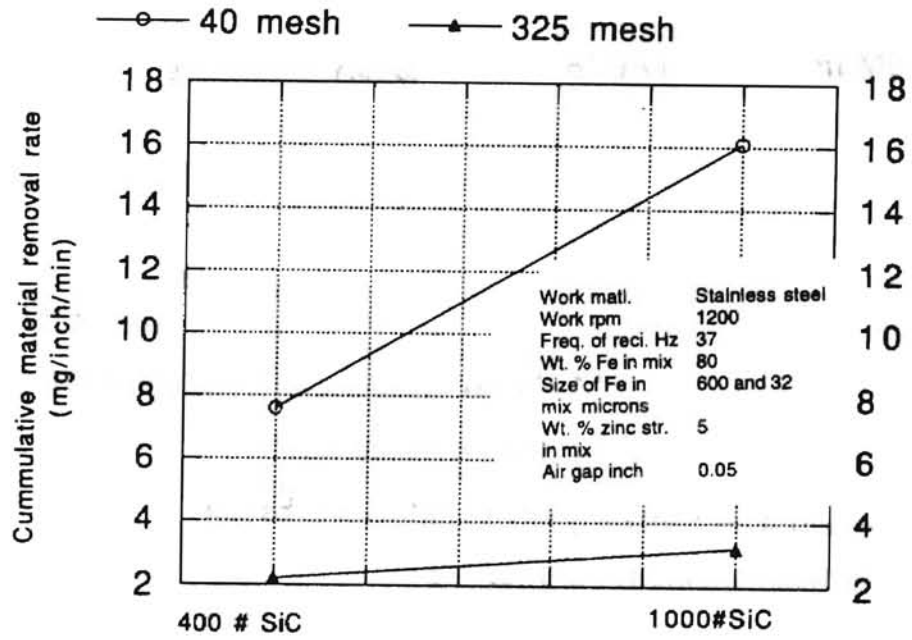

Figure 5.12 Material Removal Rate Obtained for Size of Iron Particles in Mix

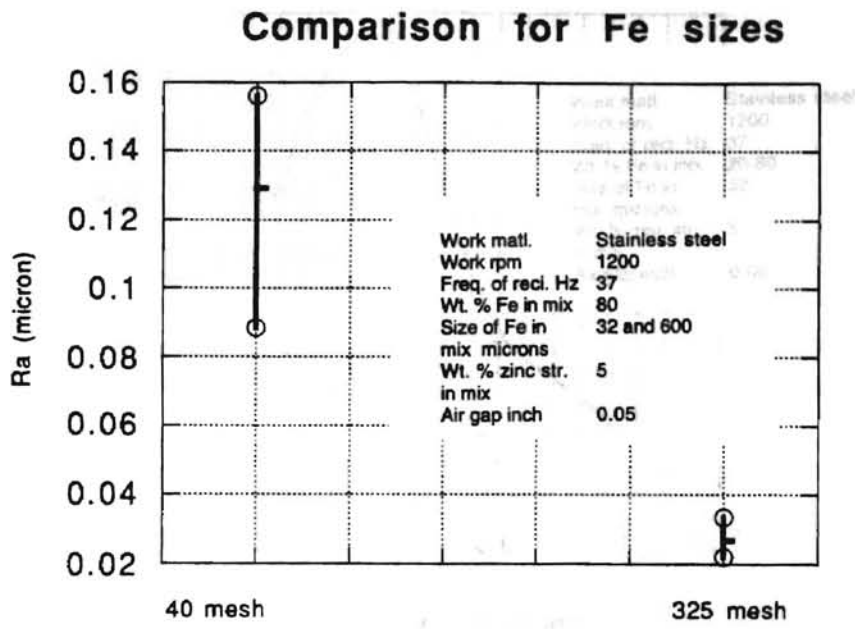

Figure 5.13 Surface Finish Variation for Size of Iron Particles in Mix

5.1.5 Effect of Weight Percentage of Iron in Mix

The results show a high material removal rate at a low percentage of iron, which can be explained by realizing the presence of more abrasives in the polishing area (Fig. 5.19). In this case, the dominant factor seems to be the presence of more abrasives. The finish also reflects the agressive material removal, since the polished surface is rougher and nonuniform. It improves in terms of values and spread of Ra as the percentage of iron in the mix is increased (Fig. 5.20). But as the percentage is increased further, that is beyond 80%, the finish deteriorates.

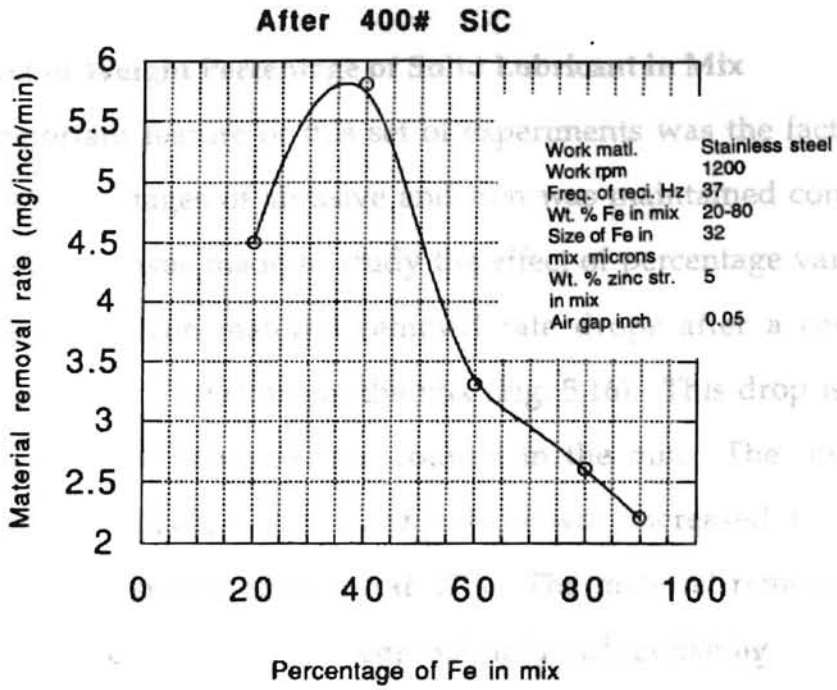

Figure 5.14 Material Removal Rate Obtained for Percentage of Iron Particles in Mix

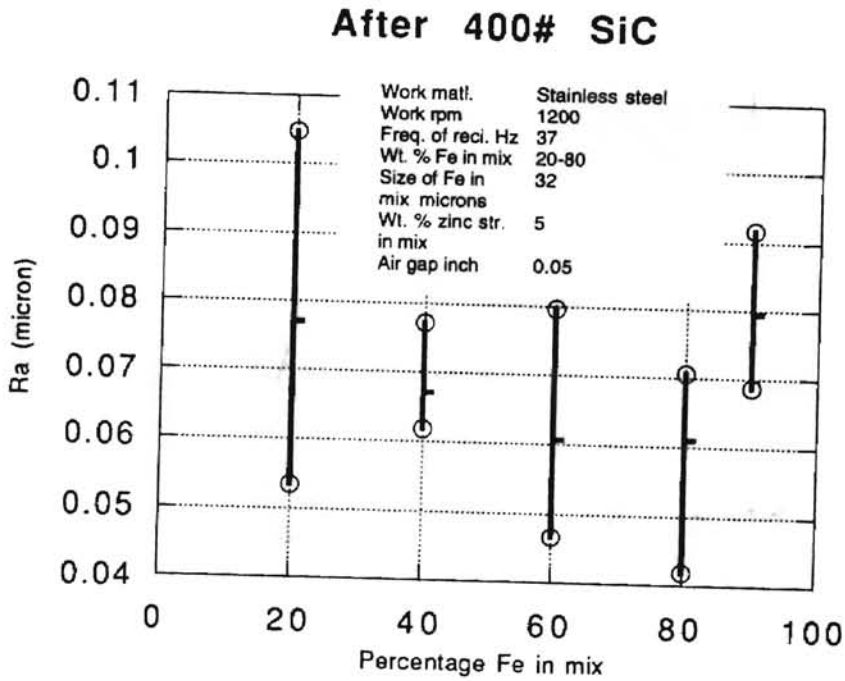

Figure 5.15 Surface Finish Variation for Percentage of Iron Particles in Mix

5.1.6 Effect of Weight Percentage of Solid Lubricant in Mix

An important feature of this set of experiments was the fact that the ratio of weight percentages of abrasive and iron was maintained constant (0.1875). Thus an attempt was made to study the effect of percentage variation of solid lubricant only. The material removal rate drops after a certain value of percentage of solid lubricant in the mix (Fig. 5.16). This drop is not as severe as it was for the increased iron content in the mix. The finish improved, almost monotonically, as the percentage was increased (Fig. 5.17). The limiting condition was obtained at 27%. The material removal rate is quite low at this stage, and it is apparent that not much polishing takes place.

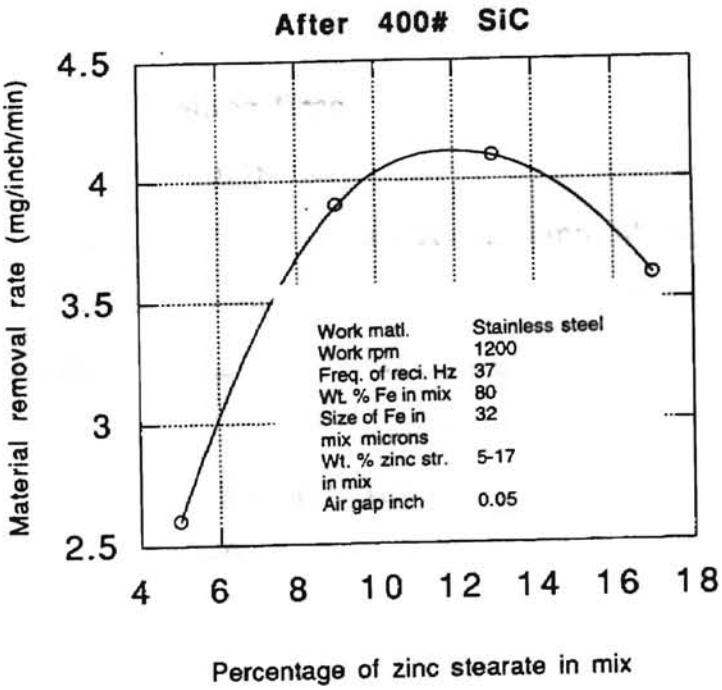

Figure 5.16 Material Removal Rate Obtained for Percentage of Zinc Stearate in Mix

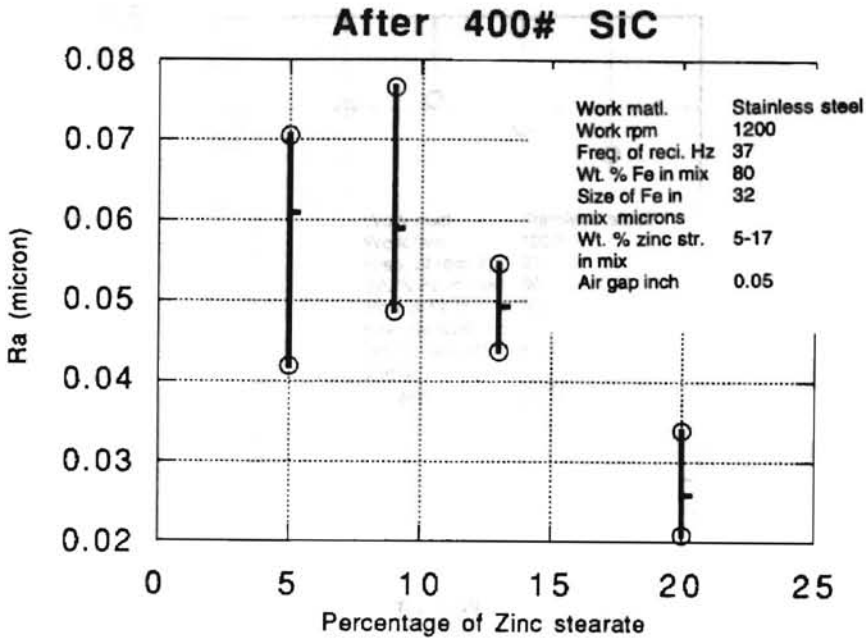

Figure 5.17 Surface Finish Variation for Percentage of Zinc Stearate in Mix

5.1.7 Effect of Polishing Time

The operating parameters in the process involve conditions which result in polishing the surface in a specific amount of time. It is essential to determine the optimum time for polishing with each grit. The experiments were conducted for 220, 400, and 1000 grits. As expected the material removal rate and finish saturate after some time for each grit. The results are graphed in Figs. 5.18-5.20. The selected values of time in minutes for each grit has been tabulated as follows:

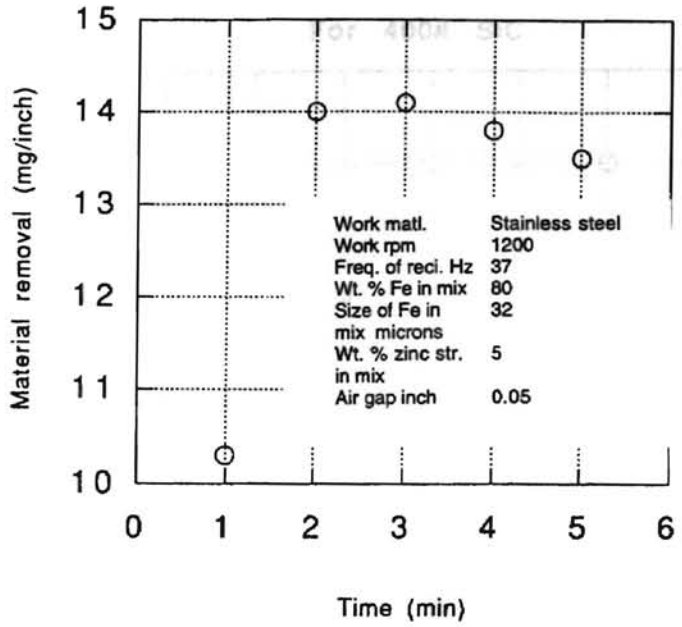

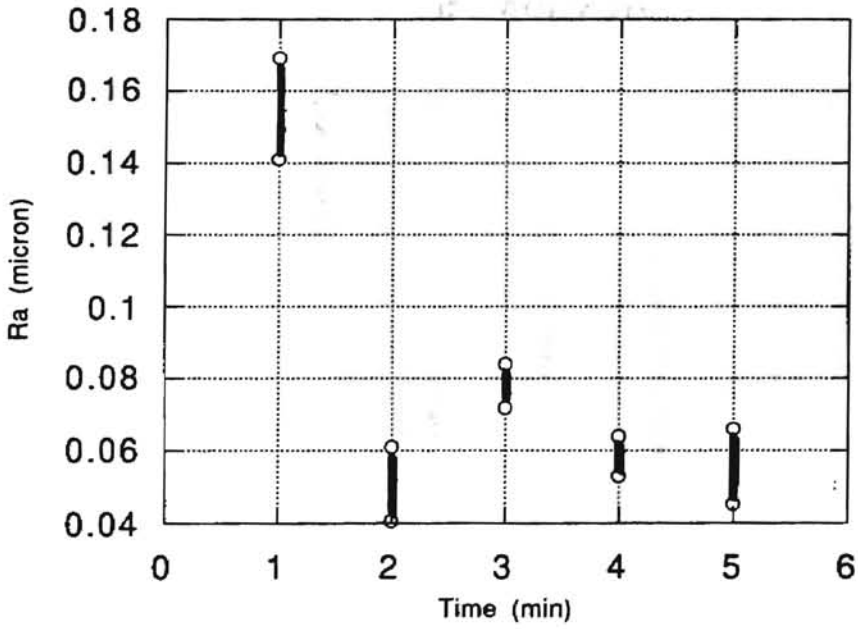

Figure 5.18 Material Removal Rate and Surface Finish Obtained for 220 Grit Al_2O_3 for Various Polishing Times

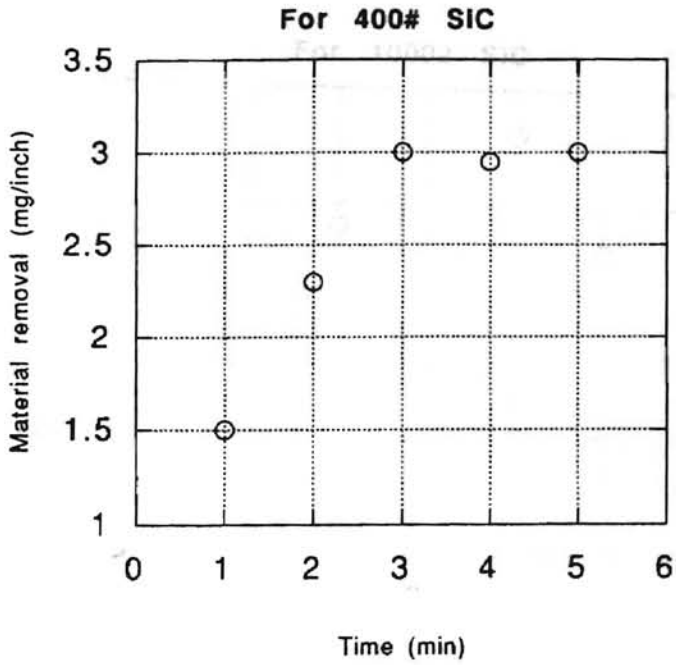

Work matl.	Stainless steel
Work rpm	1200
Freq. of reci. Hz	37
Wt. % Fe in mix	80
Size of Fe in mix microns	32
Wt. % zinc str. in mix	5
Air gap inch	0.05

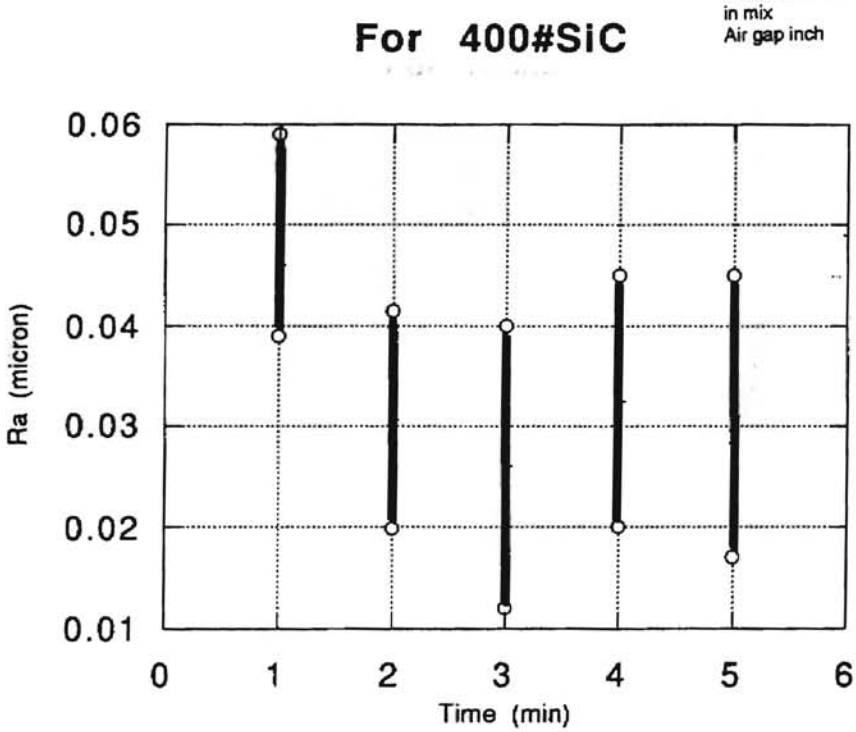

Figure 5.19 Material Removal Rate and Surface Finish Obtained for 400 Grit SiC for Various Polishing Times

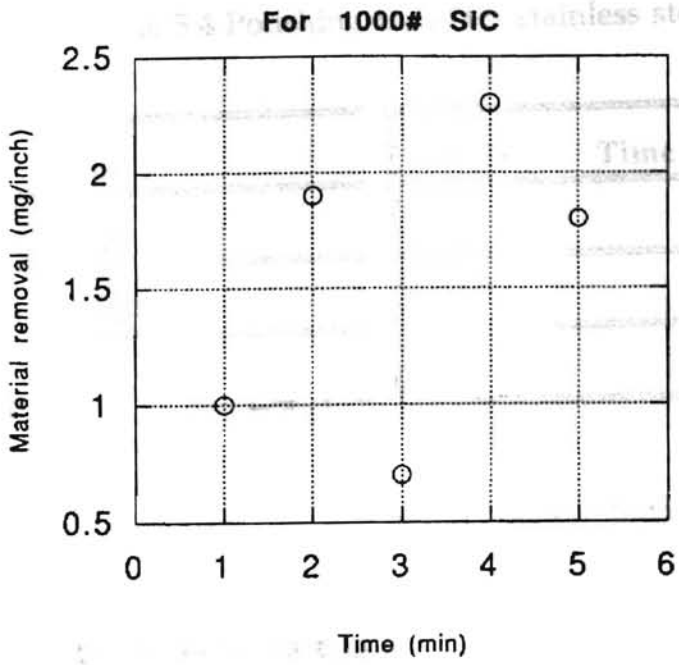

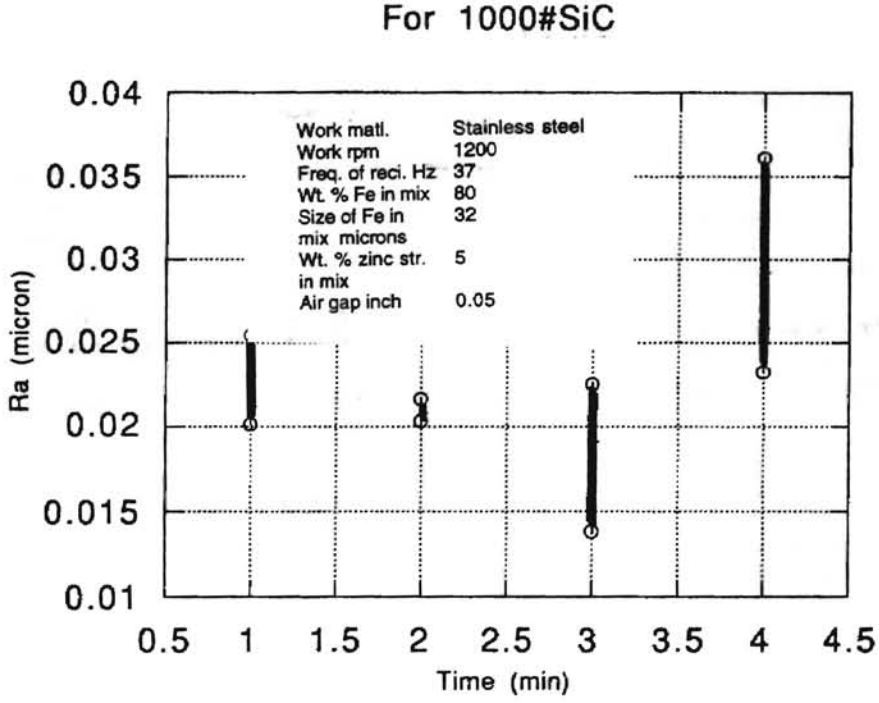

Figure 5.20 Material Removal Rate and Surface Finish Obtained for 1000 Grit SiC for Various Polishing Times

Table 5.4 Polishing times for stainless steel

Grit	Time (min)
220	2
400	1
1000	1

The final parameters for the process was determined after the sequence of experiments as:

Table 5.5 Final parameters for stainless steel AS304

Parameter	Value
Rotational speed of pipe	1200 Rpm
Frequency of oscillation	37 Hz
Amplitude of oscillation	2.5 mm
Magnetic flux density	0.83 Tesla
Pipe internal diameter	9.9 mm
Initial finish of pipe	0.3-0.7 mm Ra
Size of iron particles in mix	32 mm
Weight percentage of iron in mix	80
Weight percentage of solid lubricant in mix	5
Total time	4 mins
Grit sequence	220 (Al_2O_3), 400 (SiC), and 1000 (SiC)

5.2 Results on Brass A272 and Aluminum A6061

The experiments on brass and aluminum were conducted in the same manner as for stainless steel. The set of experiments for stainless steel were conducted prior to those for brass/aluminum in the project. This foreknowledge has caused a more biased approach in the selection of optimum conditions for the case of brass/aluminum. It is interesting to note that the optimum machine parameters remained the same for all three work materials.

The major difference between the polishing of brass/aluminum and stainless steel is in the low hardness of brass. The polishing pressures used for stainless steel would not be necessary for brass. There are two contradictory effects of increased polishing pressure exerted by the internal magnet.

- Increased pressure on the contacting grain causes it to dig deeper into the work producing deeper scratches
- The increased pressure causes more even spreading of the polishing mixture across the face of the internal magnet, bringing more grains into contact. This reduces the force/grain and depth of scratch produced.

The machine parameters for all the experiments were kept at the optimum conditions as obtained earlier, unless one of them was being changed. The effect of the parameters on the material removal was not considered, since the material removal rates are much higher in these cases compared to stainless steel.

5.2.1 Effect of Gap Width on Finish

When experiments were done with varying gaps of internal and external magnets the following results were obtained as in Fig. 5.21. The force was calculated as in the design procedure. The operating gap was fixed at 0.05 inch. As the gap is increased, the finish is better; but as it is increased beyond 0.05 inch, it deteriorates.

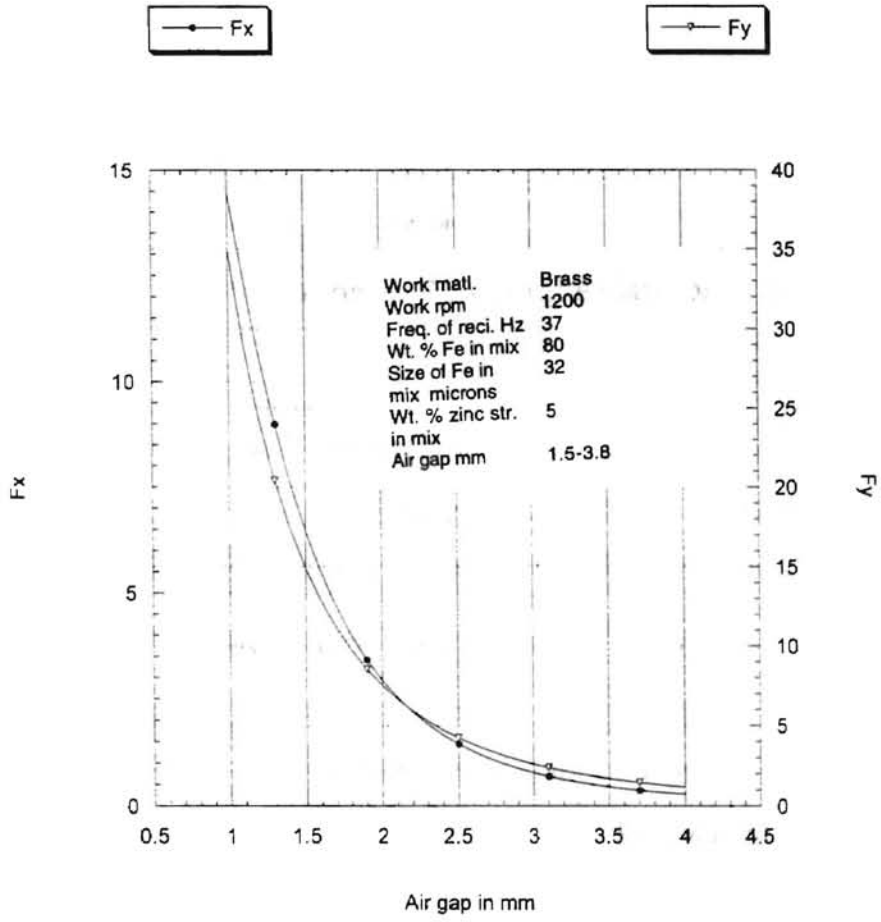

Figure 5.21 The Variation of Forces with the Gap for Brass

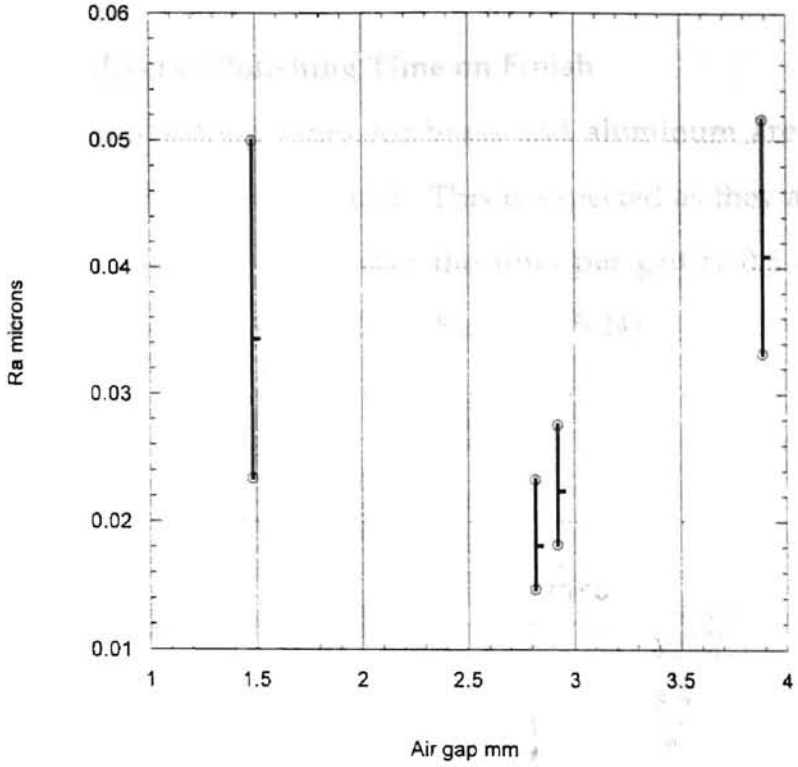

Figure 5.22 The Variation of Ra with the Gap for Brass

5.2.2 Effect of Abrasive Type on Finish

The abrasives tried were aluminum oxide and silicon carbide. It was found that SiC worked best on brass, but on aluminum, Al_2O_3 worked best. On trying SiC on aluminum, there were deep grooves on the surface of the pipe. Considering the initial extruded surface of the brass pipes, it was not necessary to have a stage using coated paper. The initial grit used was 1000 (5 micron). The final grit was 1 micron. In the case of aluminum, the initial surface was rougher. Hence it was decided that the grit sequence would be 400 grit paper, 400 grit loose mix and 1000 grit loose mix.

5.2.3 Effect of Polishing Time on Finish

The polishing times for brass and aluminum are considerably reduced as compared to stainless steel. This is expected as they are softer and less tougher materials. It is found that the time per grit is 0.5 minute for brass and 1.0 minute for aluminum (Figs. 5.23 and 5.24).

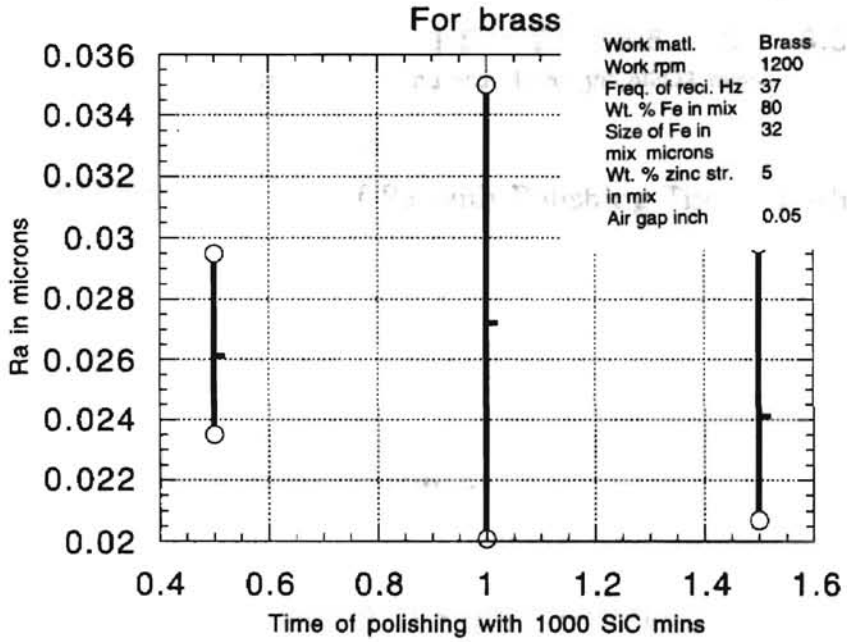

Figure 5.23 The Variation of Ra with Polishing Time for Brass

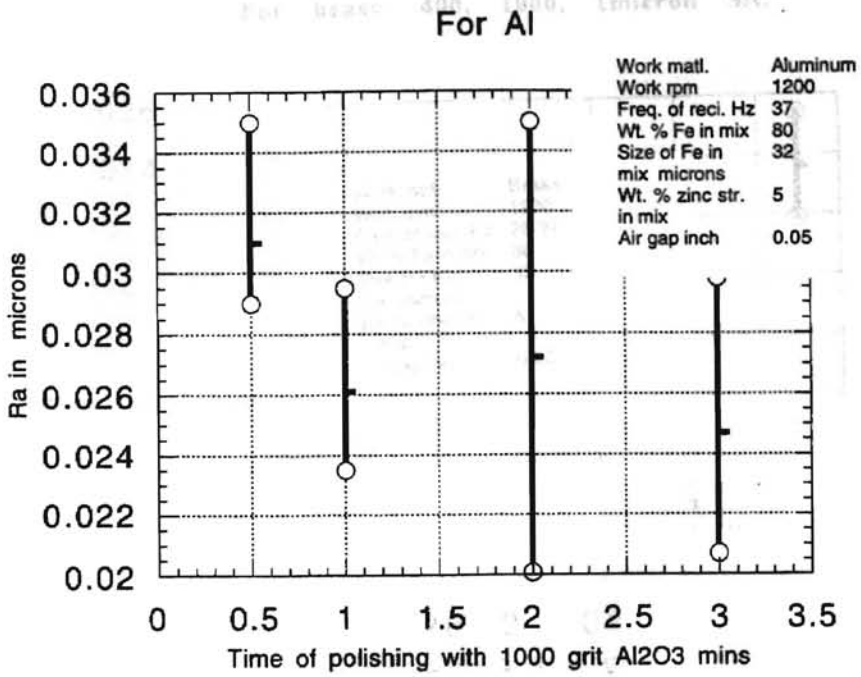

Figure 5.24 The Variation of Ra with Polishing Time for Aluminum

5.2.4 Effect of Cross Angle on Finish

The effect of cross angle for both brass and aluminum were same as that for stainless steel. The tests were done at 1200 rpm (Figs. 5.25 and 5.26).

5.2.5 Effect of Percentage of Iron in Mix on Finish

The optimum percentage of iron in the mix was found to be 80% as obtained previously. This was true for brass and aluminum (Figs. 5.27 and 5.28).

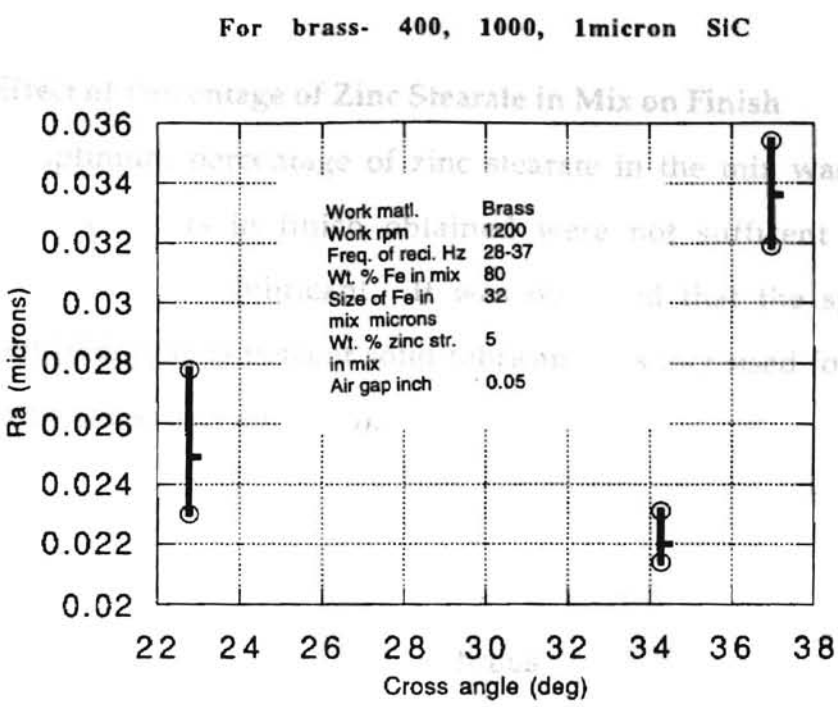

Figure 5.25 The Variation of Ra with Cross Angle for Brass

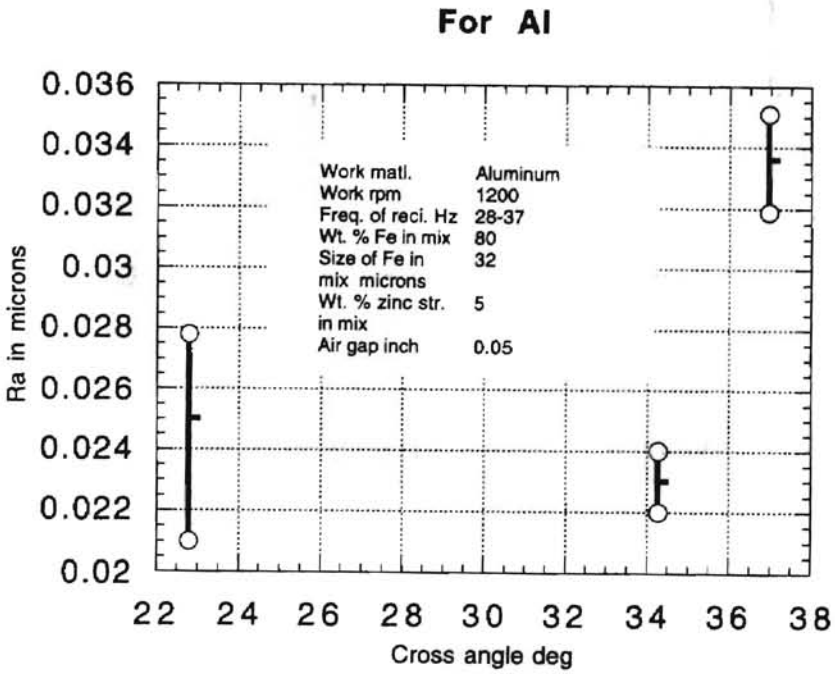

Figure 5.26 The Variation of Ra with Cross Angle for Aluminum

5.2.6 Effect of Percentage of Zinc Stearate in Mix on Finish

The optimum percentage of zinc stearate in the mix was found to be 5. The improvements in finish obtained were not sufficent to increase the percentage of solid lubricant. It was observed that the spread of values obtained increased as percent solid lubricant was increased for both brass and aluminum (Figs. 5.29 and 5.30)..

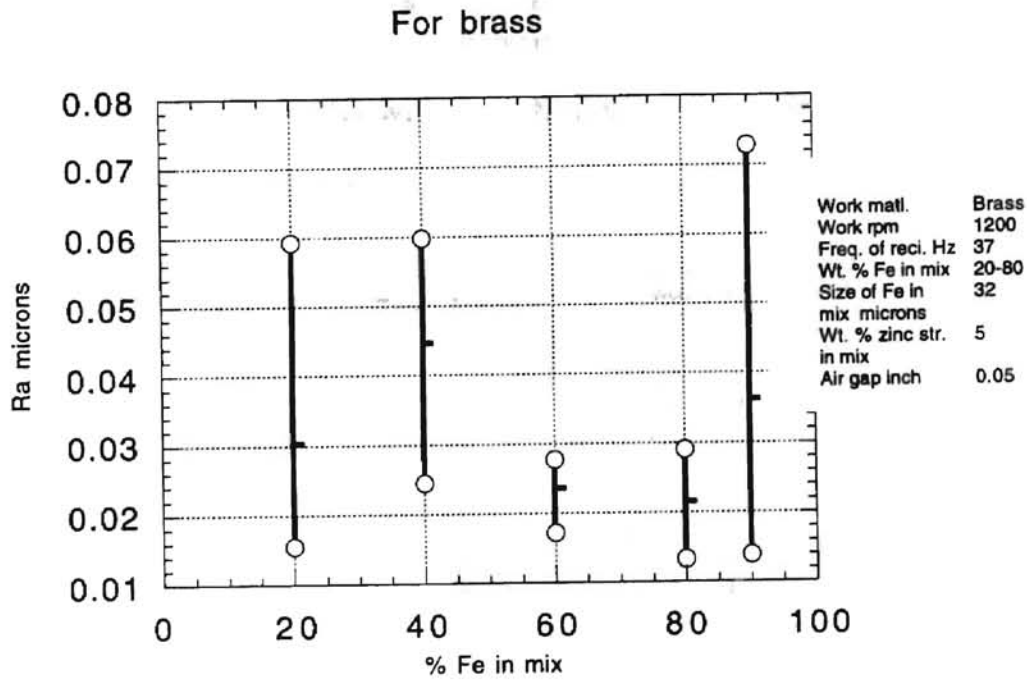

Figure 5.27 The Variation of Ra with Weight Percentage of Iron in Mix for Brass

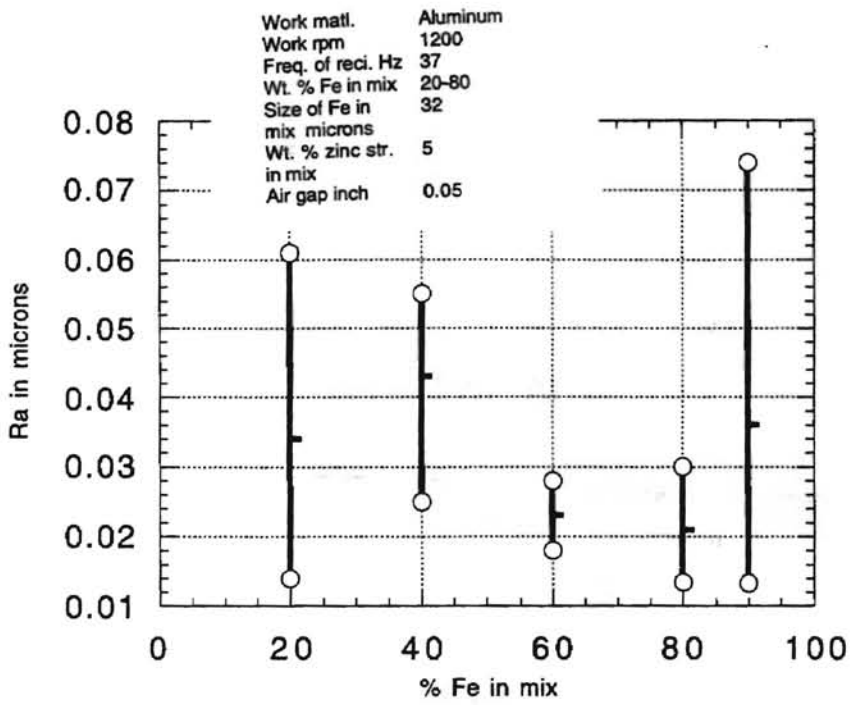

Figure 5.28 The Variation of Ra with Weight Percentage of Iron in Mix for Aluminum

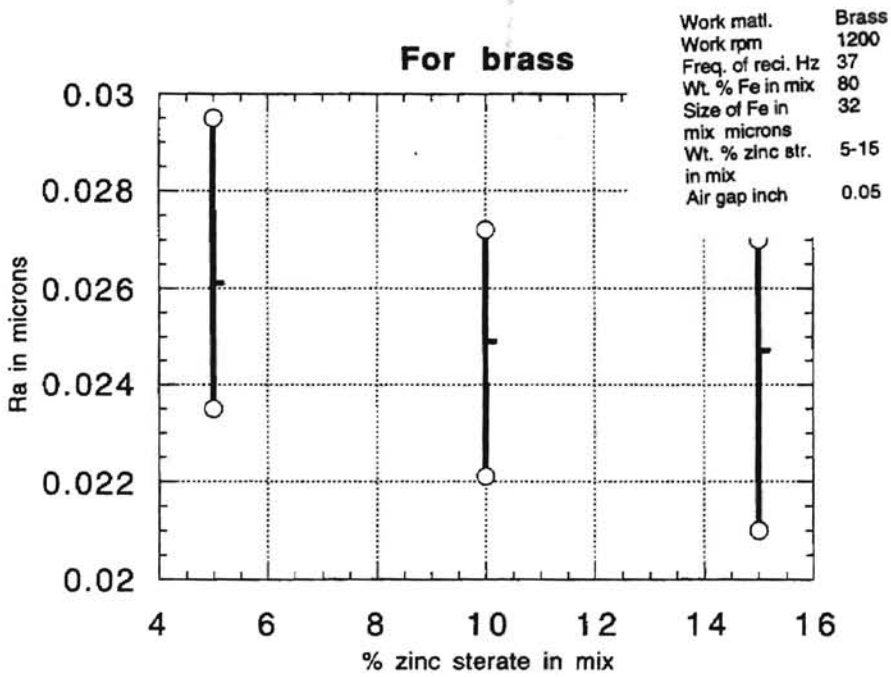

Figure 5.29 The Variation of Ra with Weight Percentage of Zinc Stearate in Mix for Brass

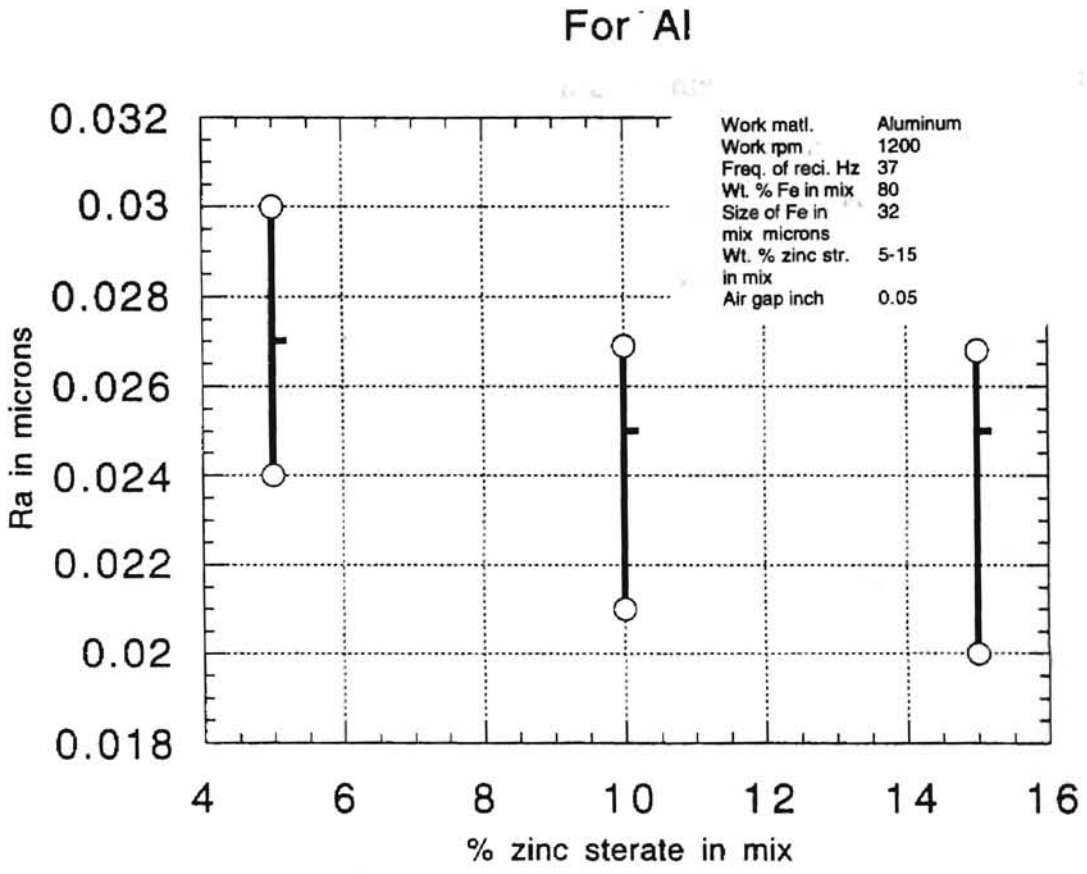

Figure 5.30 The Variation of Ra with Weight Percentage of Zinc Stearate in Mix for Aluminum

CHAPTER 6

DISCUSSION

The results obtained for polishing stainless steel, brass and aluminum can be discussed collectively for most parameters studied. The type of applying abrasive was the initial experiment in the project. The SEM pictures clearly show the deeper grooves in the case of coated paper (figures 6.1 and 6.3). The initial surface of the pipe shows evidence of asperities which have been knocked down due to the rolling process. The abrasives are better anchored in the case of coated paper and so cut more agressively. The material removal rates are clearly higher.

The use of Al_2O_3 abrasive for polishing of stainless steel proved to be improper. A similar observation was made by Komanduri (1976) in his study of grinding Co based superalloys with Al_2O_3. He proposed a rationale for the mechanism of build-up edge on aluminum oxide abrasive. The mechanism is based on initial oxidation. The reference is relevant in this instance due to the similar chromium contents of austenitic stainless steels and cobalt based superalloys.

The purpose of trying to use larger size iron filings was to increase the field in the region of polishing. It would intuitively seem that the size of the iron filings affect the finish and material removal rates. The larger the particle the higher the field induced. This increased magnetic field manifests itself as increased polishing force. The material removal rates would be high, but the finish obtained would be rough as the abrasives leave deeper grooves.

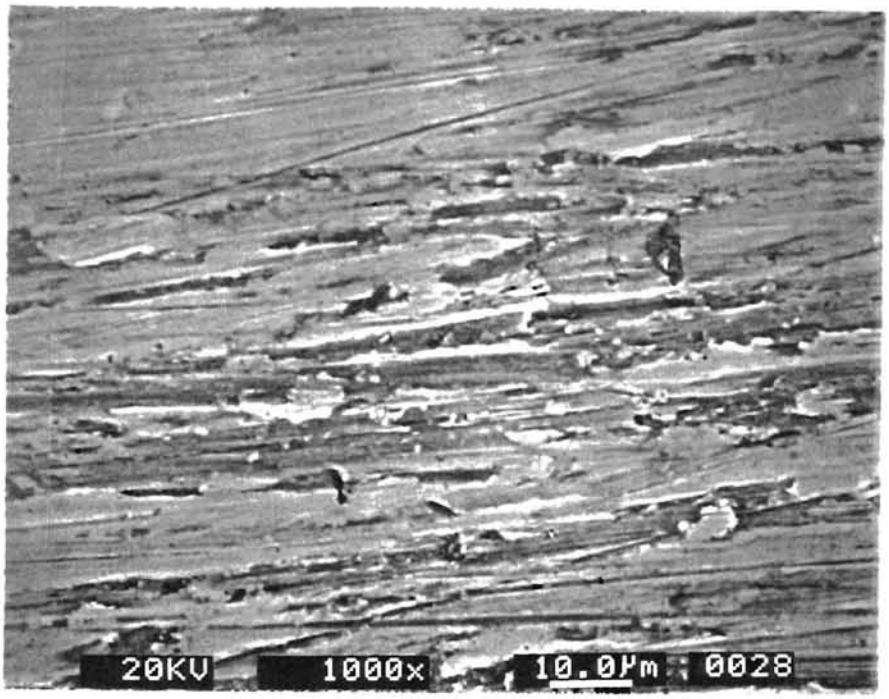

Figure 6.1 SEM Picture of Work Finished by 400 Grit Coated Paper

A similar option in an attempt to increase magnetic field in the polishing zone is to increase the sheer number of iron particles. The percentage of iron in the mixture was varied maintaining the total mass of the mix the same. This was done as only a fixed mass can be supplied to the polishing zone. The percentage of abrasive therefore varies inversely with the percentage of iron. The two factors which come into play in variation of percentage of iron in the mix are:

- Change in the number of actual cutting abrasives
- Change in the magnetic field in polishing zone

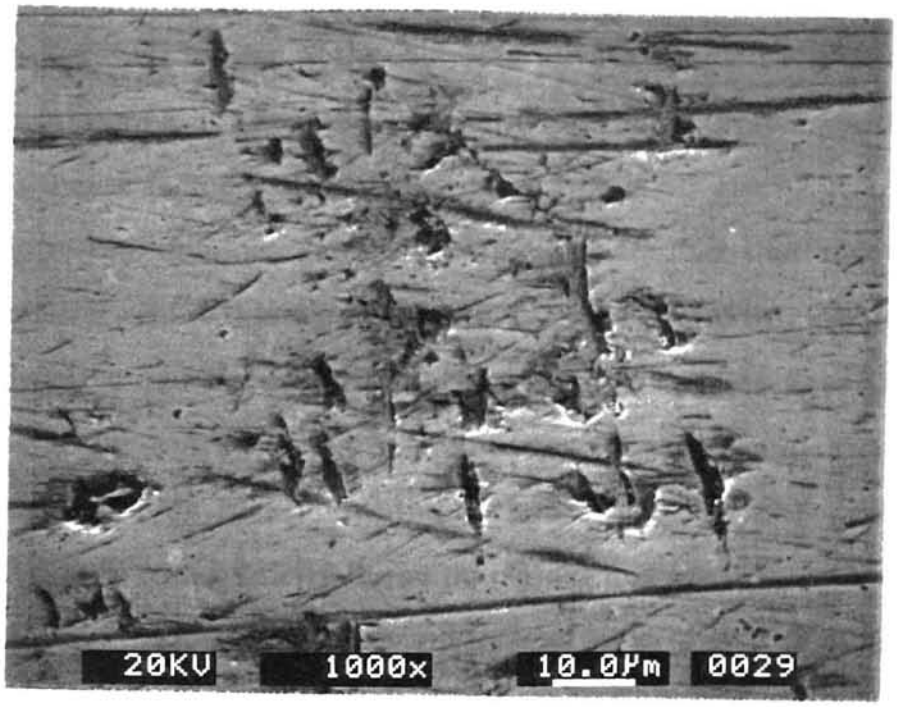

Figure 6.2 SEM Picture of Work Finished by 400 Grit Loose Mix

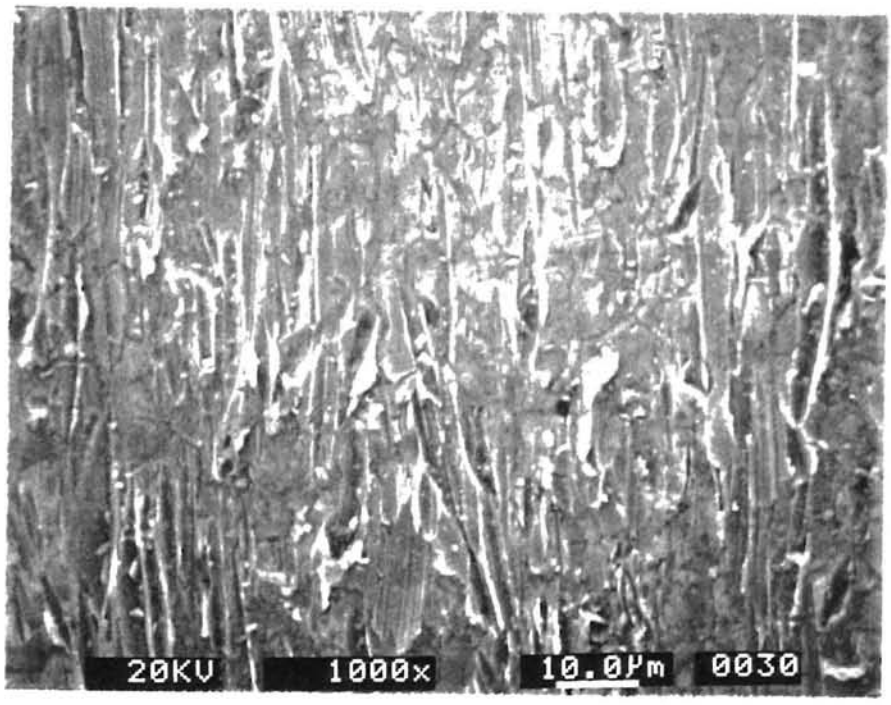

Figure 6.3 SEM Picture of Initial Surface of Work Before Polishing

A positive effect by one of the factors is always coupled with a negative effect by the other one. The net effect in terms of removal rates and finish is based on whichever factor is dominant.

The results obtained can be explained by the fact that at low percentages the material removal is very low and the polishing does not aid in removing the initial roughness in the surface. At higher percentages there is lack of cutting edges to effect material removal. Shinmura and Yamaguchi (1995) observed similar results in their experiments on the optimum weight percentage of iron particles in the polishing mixture.

Another important component of the mix is the solid lubricant- zinc stearate. The functions of the lubricant can be broadly stated as:

- To avoid the conglomeration of abrasives and thus aid in free cutting
- To reduce the friction between the iron particles and stainless steel work material

In theory as the percentage of solid lubricant is increased in the mix, the material removal rates should increase. But as a fixed quantity of mix is supplied to the polishing zone, beyond a certain percentage the actual number of abrasives decreases considerably and no cutting action occurs. Also, the magnetic field decreases as an result of decreased presence of iron particles. Both these factors affect the removal rate negatively.

The "optimum" cross angle which was obtained has to be correctly interpreted. It is known that the Al_2O_3 and SiC abrasives are capable of cutting at speeds of 30 m/s. In the present project, the speeds are in the range of 20-45 m/min. Hence, the "optimum" rotational speeds obtained here cannot be taken as absolute, but optimum for the current setup. The same cross angle could be obtained at different speeds by changing the frequencies

of reciprocation. The reason higher frequencies were not experimented was that the setup became unstable above a frequency of 40 Hz.

Another issue which has to be addressed is the application of this process to tubes of different inner diameter. The rotational speeds for the optimum conditions would logically change to maintain the same surface speed. Also the amount of mix supplied to the polishing region will change. For smaller diameter pipes a smaller internal magnet will have to be selected and so on. If the same internal magnet as used in the present study were to be used for larger diameter pipes (say 50.8 mm), then the abrasive mix will be loaded faster and cease to cut material. For a range of diameters the same internal magnet can be used as decided by the user.

The literature review conducted shows the work done by Shinmura et al. in this area. He has experimented with a permanent magnet setup. The major differences between his setup and the present setup can be stated as follows:

The use of the M.S. backplate has not been made to achieve better field configuration and strength.

Shinmura et al. have finished pipes of inner diameter 50.8 mm as compared to 9.9 mm in this project.

Shinmura et al. use magnetic abrasives, while in this project conventional abrasives are used.

Shinmura et al. have used two external magnets placed 90 deg apart.

CHAPTER 7

CONCLUSIONS

- MAF of internal surfaces which is capable of finishing surfaces to a roughness of 20 nanometers has been developed. Using this process pipes (12.7 mm O.D. and 9.9 mm I.D.) of AS304, A272, and A6061 were finished. over a length of 25.4 mm. Polishing times were 4, 2, and 3 minutes respectively.
- The design methodology established the configuration of magnets and the necessary reciprocation amplitude. Magnetic analyses were done using FEM. Use of an internal magnet and a M.S. backplate on the external magnet gave rise to stronger field in the polishing zone.
- The force analysis conducted established the presence of a dead zone in the reiprocatory amplitude of the internal magnet when the desired polishing does not occur. Accordingly, the amplitude was chosen to be 2.5 mm.
- Parametric tests were conducted to determine the effects of cross angle, polishing time, abrasive type, percentage Fe in mix, and percentage zinc stearate in mix on material removal rate (MRR) and Ra. The main results are as follows. The best results in terms of MRR and Ra are obtained at a cross angle between 30-40 degrees. Al_2O_3 was found to be suitable for finishing A6061 and SiC was suitable for finishing AS304 and A272. The optimum weight percentages of iron and zinc stearate in the mix are 80 and 5 respectively.

Future work

- The average Ra over the length of the surface was 20 nm, but there were certain visible scratch marks on the polished surface for all 3 work materials. These could not be eliminated. It was tried to determine the reason for these scratch marks, but the attempts proved to be futile. The possible problem areas could be vibration in the system and nonuniform loading of the abrasive mixture.
- The cylindricity of the polished lengths was not studied. This was because the raw stock itself had a out of roundness of 0.014 inch. In addition to a good surface finish, a good cylindricity would be required in most practical applications. In order to study the cylindricity, it is important that the stock be controlled in terms of cylindricity. It would be advisable to use raw tubes previously ground on the internal surface and having tolerable cylindricity.
- Using the process, longer lengths of surfaces could be polished. The external magnet assembly is on a slide which can be moved over 300 mm. Necessary supports for the slender workpiece can be designed for stiffness of the setup.
- Extending the process to smaller diameter pipes can be attempted. The reccomended size would be 5 mm inner diameter.
- While fairly short polishing times are required, total cycle times are longer since workpiece needs to be cleaned, weighed and the polishing mix needs to be replaced after every polish. It should be possible to reduce these times by automating and successful monitoring of the process.

REFERENCES

Konovalov, E. G., and Sulev, G. S., "Finishing Machining of Part by Ferromagnetic Powder in Magnetics Field," Naukaitechnika, Minsk, (Russian), 1967.

Mekedonski, B. G., "Schliefen in Magnetfeld," Kotschemidov, A. D., Fertigungstechnik Und Betrieb, 24, H 6, pp. 230-235, 1974.

Konovalov, E. G., and Sakulevich, F. J., "Principles of Electro-Ferromagnetic Machining," Naukaitechnika, Minsk, (Russian), 1974.

Baron, J. M., "Technology of Abrasive Machining in Magnetics Field," Masino-strjenije, Leningrad, (Russian), 1975.

Komanduri, R., "The Mechanism of Metal Built-up on Aluminum Oxide Abrasive," Annals of CIRP, Vol 25, no.1, pp.191-196, 1976.

Komanduri, R., Shaw, M. C., "Attritious Wear of Silicon Carbide," Journal of Engineering for Industry, pp. 1125-1134, Nov 1976.

Moskowitz, L. R., "Permanent Magnet Design and Application Handbook," Cahners Books International, 1976.

Sakulevich, F. J., Kozuro, L. M., "Magneto-Abrasive Machining of Fine Parts," Vyssaja Skola, Minsk, (Russian), 1977.

Sakulevich, F. J., and Kozuro, L. M., "Magneto-Abrasive Machining," Naukaitechnika, Minsk, (Russian), 1978.

Shinmura, T., Takazawa, K., and Hatano, E., "Advanced Development of Magnetic-Abrasive Finishing and its Application," SME: Deburring and Surface Conditioning '85 Conference Proceedings (held in Chicago), 1985.

Wang, Y. L., and Wang, Z. S., "An Analysis of the Influence of Plastic Indentation on Three-Body Abrasive Wear of Materials," Wear, 122, pp. 123-133, 1988.

Shinmura, T., "Study on Internal Finishing of a Non-Ferromagnetic Tubing by Magnetic Abrasive Machining Process," Prepr. of JSPE at Spring Conference, (Japanese), 1991.

Shinmura, T., Yamaguchi, H., and Aizawa, T., "A New Internal Finishing Process of Non-Ferromagnetic Tubing by the Application of a Magnetic Field-The Development of a Unit Type Finishing Appartus Using Permanent Magnets," 1992.

Shinmura, T., Iizuka, T., and Shinbo, Y., "A New Process for Internal Finishing of Non-Ferromagnetic Tubing using Rotating Magnetic Field," Transactions of NAMRI/SME, Vol XXI, 1993.

Shinmura, T., and Yamaguchi, H., "Study on a New Internal Finishing Process by the Application of Magnetic Abrasive Machining (Internal

Finishing of Stainless Steel Tube and Clean Gas Bomb)," JSME International Journal, Series C, Vol 38, no. 4, pp. 798-804, 1995.

Umehara, N., Kobayashi, T., and Kato, K., "Internal Polishing of Tube with Magnetic Fluid Grinding Part1, Fundamental Polishing Properties with Taper Type Tools," Journal of Magnetism and Magnetic Materials, Vol no. 149, pp. 185-187, 1995.

Umehara, N., Kobayashi, T., and Kato, K., "Internal Polishing of Tube with Magnetic Fluid Grinding Part2, Fundamental Polishing Properties with Rotating Balls and with Oscillating Balls," Journal of Magnetism and Magnetic Materials, Vol no. 149, pp. 188-191, 1995.

Kim, J. D., and Choi, M. S., "Simulation for the Prediction of Surface-Accuracy in Magnetic Abrasive Machining," Journal of Materials Processing Technology, Vol 53, pp. 630-642, 1995.

Kim, J. D., and Choi, M. S., "Simulation of an Internal Finishing Process of Rectangular Tube Using a Magnetic Field," Wear, Vol 184, pp. 67-71, 1995.

Kim, J. D., and Choi, M. S., "Development and Finite Element Analysis of the Finishing System Using Rotating Magnetic Field," International Journal of Machine Tools and Manufacturing, Vol 36, no. 2, pp. 245-253, 1996.

APPENDIX

Stylus type instrument

A stylus type instrument (Form Talysurf 120L) was used in the project for measuring the surface finish of the work surfaces. The instrument is capable of measuring waviness and roughness. The instrument consists of an epoxy granite base mounted on a tubular steel frame. The base is supported on anti-vibration pads. The base supports the workpieces and column. The column supports the traversing unit and provides the drive to move the traversal unit in the vertical direction. Further, the traversing unit can also be tilted about an axis perpendicular to both column and traversing direction. The traverse unit consists of a drive unit to move the stylus over the work. The stylus moves in the vertical direction, conforming to the surface.

The vertical motion of the stylus is transduced by the laser interferometer. A straightness datum is incorporated into the traverse unit, which enables scans up to 120 mm to be made without loss in accuracy. A digital computer is interfaced with the instrument, so that slope and curvature of the surface can be compensated. Various parameters such as Ra, amplitude distributin, bearing area, etc. can be obtained. One of the newer features is the calculation of form factors such as slope and curvature and surface waviness.

The table below gives the parameter settings on the Talysurf

Instrument:	**Talysurf 120L**
Stylus	Diamond tip radius =1.5-2.5mic
	stylus force = 0.7-1.0 mN
Vertical resolution	10.0 nm

Horizontal resolution	0.25 mic
Filter type	ISO 2CR
Cut-off	0.8 mm
Bandwidth	300:1
Smallest wavelength	2.5 mic
Total measurement length	4.8 mm
Form compensation	Least square arc

VITA

Vinoo Thomas

Candidate for the Degree of

Master of Science

Thesis: MAGNETIC ABRASIVE FINISHING OF INTERNAL SURFACES

Major Field: Mechanical Engineering

Biographical:

Personal Data: Born in Bombay, India on September 8, 1972.

Education: Graduated from Holy Family High School, Bombay, India in May 1988; received Bachelor of Science degree in Mechanical Engineering from Bombay University, Bombay, India in May 1994. Completed the requirements for the Master of Science degree with a major in Mechanical Engineering at Oklahoma State University in (July, 1997).

Experience: Employed by Grindwell Norton Ltd. as a product engineer Bombay, India 1994 to 1995; employed by Oklahoma State University, Department of Mechanical and Aerospace Engineering as a graduate research assistant; Oklahoma State University, Department of Mechanical and Aerospace Engineering, 1996 to present.